TÉCNICO LISBOA

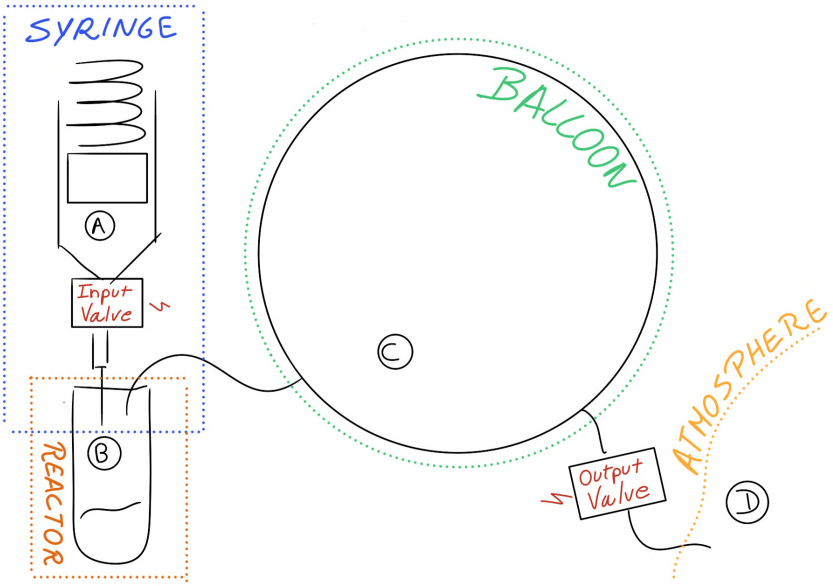

Simulation of a latex balloon with a hydrogen generation system

Vasco Miguel Campos da Gama Teles Cepêda

Thesis to obtain the Master of Science Degree in

Mechanical Engineering

Supervisors: Prof. Alexandra Bento Moutinho
Prof. Rui Pedro da Costa Neto

Examination Committee

Chairperson: Prof. Paulo Jorge Coelho Ramalho Oliveira
Supervisor: Prof. Rui Pedro da Costa Neto
Member of the Committee: Prof. José Maria Campos da Silva André

October 2020

Dedicated to my esteemed friend Micael Coelho

Acknowledgments

During the development of this thesis, I was able to count on a large number of people, who have always shown great sympathy and willingness to help me reach my goals. First, I would like to thank my two supervisors, Prof. Dra. Alexandra Bento Moutinho and Prof. Dr. Rui Pedro da Costa Neto. Professor Alexandra Moutinho is a very kind and available person and it has always been a pleasure to work with her during my last years on the course. Professor Costa Neto is a highly motivated and resourceful person, always ready to think outside of the box and give practical solutions for helping me to solve my problems. It was the first time I have worked with the professor and also a pleasure to share this experience with him.

Secondly, I would like to thank Prof. Dr. Aires José dos Santos, Prof. Dr. José Manuel Da Silva Chaves Ribeiro Pereira, Prof. Dr. José Maria André and Prof. Dr. Viriato Sérgio de Almeida Semião for helping me to make valid assumptions and simplify the theoretical equations corresponding to each one of their areas of speciality. Within these, I would like to highlight professor Maria André and professor Viriato. During my graduation, I never had classes with professor Maria André but right after our first meeting, I can now say I could not be more impressed. He is an extremely kind person, who was always interested in my work and always ready to help me. Finally, Professor Viriato helped me a few times during the pandemic, and his inputs were crucial for a considerable part of my work.

Third, I would like to thank Sr. Eng. Luis Raposeiro and Sr. Eng. Camilo Christo for helping during the development of the chemical reactor's prototype. I'm very grateful to them for their practical support.

Fourth, I would like to thank all of my friends, always there to motivate me and give me opinions regarding most of my hypothesis. I would like to thank my roommate Micael Melo Coelho, an extremely kind and intellectual person. His inputs were crucial for the development of this thesis. Furthermore, I would like to thank Pedro Manuel Serro Messias, Miguel Dias dos Santos, Miguel Marques Carreira, Carolina Gonçalves Guerra, Sofia Gonçalves Carreira, and Yang Jia Jia. All of these people are extremely important for me.

Finally, I would like to thank my loving mother and sister. They were always there to motivate me and to help me overcoming difficult times.

Resumo

Atualmente, devido às suas propriedades físicas e tecnologias mais baratas, os balões estratosféricos são amplamente utilizados em monitorização ambiental. Contudo, controlar a altitude desses balões é desafiante, principalmente quando estes se movem numa estratosfera onde os ventos podem atingir os 100 Km/h e as temperaturas os -90^{o}C. Encontrar uma maneira de o fazer torna-se essencial. O objetivo consiste em controlar o volume do balão e a sua massa total, obrigando-o a procurar correntes de vento favoráveis, de forma a garantir que este ficará sempre dentro de uma determinada região. As soluções mais recentes distinguem-se não só pelo método de controlo, mas também pelo tipo de gás e balão que são utilizados. Num ambiente acadêmico, onde o custo e tempo são fatores a considerar, o laboratório serve de partida para o desenvolvimento de um pequeno protótipo: um balão de látex equipado com um sistema de produção de hidrogênio, gerado através da hidrólise do hidreto de cálcio. Para desenvolver este protótipo, um certo pré-conhecimento sobre o comportamento do sistema torna-se essencial, a fim de reduzir custos e economizar tempo para as futuras fases do projeto. Posto isto, um simulador para o sistema total é proposto. Para estudar a reação, um reator químico foi desenvolvido e testado antes do aparecimento da pandemia. Relativamente aos outros sistemas, foram aplicados princípios de mecânica dos fluidos e termodinâmica, e encontrados conjuntos adequados de equações para descrever o seu comportamento. O modelo final foi desenvolvido em *Matlab/Simulink* R2018a.

Palavras-chave: balões estratosféricos, hidreto de cálcio, latex, hidrogénio, hidrólise

Abstract

Nowadays, given their physical properties and cheaper technologies, stratospheric balloons are widely used in most of the environmental monitoring missions. Nevertheless, controlling their altitude is challenging, especially when dealing with a stratosphere where winds can reach 100 Km/h and temperatures may achieve -90^{o}C. Finding a way to control their movement becomes essential. The main objective is to control the volume and the total mass of the balloon, and force it to find favorable wind streams in order to ensure it will always remain within a certain region. The most recent solutions are distinguished not only by the control method but also by the type of gas and balloons that are used. Moving towards a more academic environment, where cost and time are factors to consider, the laboratory is a valid starting point for the development of a prototype: a latex balloon equipped with a hydrogen production system, generated through the hydrolysis reaction of calcium hydride. Nonetheless, to develop such prototype, pre-knowledge about the system's behaviour is crucial, in order to reduce costs and save time for the future project generations. Given this, a simulator for the total system is proposed. To study the hydrolysis reaction, a chemical reactor prototype was developed and tested before the appearance of the virus COVID-19. For the other subsystems, fluid mechanics and thermodynamic principles were applied, and a suitable group of equations was used to describe their behaviour. The final model was developed in *Matlab/Simulink* R2018a.

Keywords: stratospheric balloons, hydrogen, latex, calcium hydride, hydrolysis

Contents

List of Tables

List of Figures

Nomenclature

A_s	Circular area for any section of the syringe's subsystem, [m^2]
A_b	Balloon's circular area, [m^2]
$A_{plunger}$	Plunger's area, [m^2]
C_D	Atmospheric drag coefficient
Cp_{H_2}	Hydrogen's heat capacity, ≈ 14.5 [J/(Kg.K)] [1]
F_{spring}	Spring's elastic force, [N]
$G(s)$	Transfer function to relate the volume of hydrogen produced with the water mass flow rate
H_R	Enthalpy of reaction, [KJ/mol$_{[CaH_2]}$]
L_R	Reactor's length, [m]
L_{needle}	Syringe subsystem needle's length, [m]
L_{spring}	Spring's natural length, [m]
$L_{syringe}$	Syringe's length, [m]
L_s	Length of a syringe's subsystem streamline gathering points A and B, [m]
M_{H_2}	Hydrogen's molecular mass, $\approx$ 2.02 [Kg/kmol]
M_{air}	Air's approximated molecular mass, $\approx$ 28.97 [Kg/kmol]
M_a	Mach number
Q_ω	Syringe's subsystem water volumetric flow rate, [m^3/s]
R_b	Balloon's radius [m]
R_g	Ideal gas constant, ≈ 8314.5 [J/(mol.K)]
R_{g,H_2}	Hydrogen's relative universal gas constant, $\approx$ 4157 [J/(Kg.K)]
$R_{g,air}$	Air's relative universal gas constant, $\approx$ 287 [J/(Kg.K)]
Re_ϕ	Reynolds number (for a circular section with diameter ϕ)

T_b	Balloon's internal temperature [K]
T_R	Reactor's internal temperature, [K]
T_{atm}	Atmospheric temperature, [K]
T_{out}	Forced temperature in the surroundings of the reactor, $= 288.19$ [K]
V_R	Reactor's internal volume, [m^3]
V_b	Balloon's spherical volume, [m^3]
$V_{H_2,gen}$	Volume of hydrogen generated, [L]
$V_{b,design}$	Design volume (zero-pressure balloons), [m^3]
$[p]$	Difference between the balloon's internal and external pressures, [bar]
Δt	Period of time, [s]
$\Delta t_{in,v}$	Input valve's actuation time, [s]
$\Delta t_{out,v}$	Output valve's actuation time, [s]
Ω_T	Total thermal reactor equivalent resistance, [m.K/W]
δ_t	Sampling time, [s]
$\dot{E}_{gen}$	Reactor's generated power, [W]
$\dot{E}_{lost}$	Reactor's released power, [W]
$\dot{m}_{H_2,R\rightarrow b}$	Hydrogen input mass flow rate, [Kg/s]
$\dot{m}_{H_2,b\rightarrow atm}$	Hydrogen output mass flow rate, [Kg/s]
$\dot{m}_{H_2,gen}$	Hydrogen generated mass flow rate, [Kg/s]
$\dot{m}_{\omega}$	Water mass flow rate [Kg/s]
$\dot{z}_b$	Balloon's vertical velocity, [m/s]
γ	Rate at which hydrogen is being generated, [mol/s]
μ_{ω}	Water's dynamic viscosity, [Pa.s]
ν_{ω}	Water's kinematic viscosity, [m^2/s]
ϕ_i	Diameter of tube connecting the reactor to the balloon, [m]
ϕ_o	Diameter of the tube connecting the balloon to the atmosphere, [m]
ϕ_s	Syringe's subsystem diameter for a specified circular section located at x, [m]
$\rho_{H_2,R}$	Hydrogen's density inside the reactor, [Kg/m^3]

$\rho_{H_2,b}$	Hydrogen's density inside the balloon, [Kg/m^3]
ρ_ω	Water's density, ≈ 1000 [Kg/m^3]
ρ_{atm}	Atmospheric density, [Kg/m^3]
f	Darcy coefficient
g	Acceleration of gravity ≈ 9.81 [m/s^2]
h	Convection coefficient [W/(m^2.K)]
k	Spring stiffness constant, [N/m]
k_{glass}	Thermal conductivity for the reactor walls, [W/(m.K)]
$m_{H_2,R\rightarrow b}$	Hydrogen released mass , [Kg]
$m_{H_2,b\rightarrow atm}$	Lost hydrogen mass, [Kg]
$m_{H_2,gen}$	Hydrogen mass generated, [Kg]
$m_{[CaH_2]}$	Mass of hydride left inside the reactor, [Kg]
m_ω	Mass of water left inside the syringe, [Kg]
m_e	Envelope's mass, [Kg]
m_{pch}	Parachute's mass, [Kg]
m_{pl}	System's payload mass, [Kg]
m_{rest}	Unknown components mass (tubes. batteries, reactor, syringe, etc...), [Kg]
m_{total}	System's total mass, [Kg]
p	Fluid's pressure, [Pa]
p_R	Reactor's internal pressure, [Pa]
p_b	Balloon's internal pressure, [Pa]
p_{atm}	Atmospheric pressure, [Pa]
r_b^0	Balloon's barely inflated radius, [m]
r_i	Reactor's internal radius, [m]
r_o	Reactor's external radius, [m]
s_+, s_-	Elastic balloon coefficients, $\approx 3, -0.3$ [Bar] [2]
t_e^0	Balloon's envelope thickness, [m]
t_{glass}	Reactor's wall thickness, [m]

u	Water velocity along a syringe subsystem's streamline gathering points A and B, [m/s]
v	Water velocity along a reactor subsystem's streamline gathering points B and C, [m/s]
v_i	Hydrogen's velocity through the connection tube located between the reactor and the balloon, [m/s]
v_o	Hydrogen's velocity through the connection tube located between the balloon and the atmosphere, [m/s]
x, y, z	Syringe's subsystem cartesian coordinates, [m]
z_b	Balloon's altitude, [m]

Chapter 1

Introduction

1.1 Motivation

Global warming is the issue of our time. The three greatest forest areas are constantly being deforested, which can lead to forest fires and ecosystems damage. Polar caps are melting, the water level is rising, pollution is increasing, temperatures are collapsing and despite all of this, some of the greatest international economies are not aware about severity of these problems. Technology is forced to interfere. Within a slow but very emergent transition to act, it is imperative to invest and to improve our methods for predicting fire occurrences and preventing pollution levels to increase.

High altitude monitoring systems have become one of the most common to serve this kind of missions, especially the ones regarding high altitude balloons. These systems are normally made of a very elastic material, which allows them to expand by many times in volume and carry with them great amounts of low-density gas. Due to this, they are capable of reaching the most elevated layers of our atmosphere and carry with them considerable payload masses, thus making them suitable to serve this kind of applications. Until now, drones were widely used for this purpose. The problem is that they are very limited in what concerns their flight autonomy, as most of their battery is lost during the ascension phase. The current idea is to use high altitude balloons to transport the drones to a specific altitude and release them when the target area is located. Nevertheless, the duration of these missions is highly dependent on the atmospheric conditions. In stratosphere, for example, temperatures reach below -90^{o}C and wind speeds can be greater than 100 Km/h. These conditions challenge the application of stratospheric balloons for this kind of missions, as normally, they do not have actuation mechanisms and they are highly difficult to control. Finding a way to control the altitude of such balloons becomes one of the most important tasks and quite complex to achieve. Given the harsh conditions presented in stratosphere, instead of designing a horizontal motion controller for the balloon, the approach is different: the balloon is forced to move vertically in order to find a favourable wind stream. This control technique is known as *Station-Keeping Control Method* [3].

The balloon's district used for this method is shown in figure 1.1. The idea is to try to maintain the balloon inside the cylindrical district, by reversing its cruise direction every time it attempts to leave it.

By knowing the vertical wind profile throughout the different layers of stratosphere, one is able to force the balloon to move upwards or downwards to an altitude where the wind forces it to stay inside the represented cylindrical volume. In order to do this, a control action must be taken before the balloon reaches the outside radius of the cylinder R. This is where innovation starts, as there are multiple ways for controlling the altitude of a balloon, multiple types of high altitude balloon architectural structures and quite a few options regarding the lift gas that might be used to provide lift, which is the main focus of the next section.

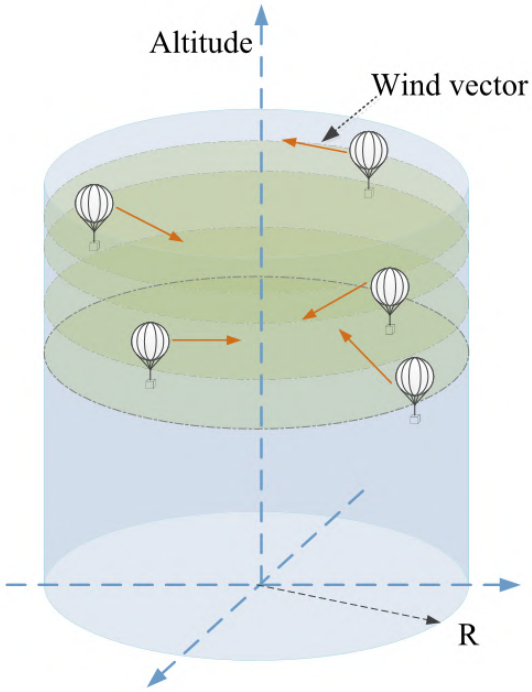

Figure 1.1: Balloon's cylindrical district (with a radius R) [3]

1.2 An opportunity for hydrogen

During the last decades, helium has been used as the principal low-density gas to provide lift for high altitude balloon applications. Until the well-known *Hindenburg* disaster, which happened in the year of 1937, hydrogen was used to provide lift for balloons and airships, but as most of the investigations identified hydrogen as the main responsible for the occurrence of the disaster [4], helium has started to be used instead. However, unlike hydrogen, helium may hardly be identified as a renewable resource and the world is running out of it. In August 2018, *National Geographic* published on its website an article regarding the international helium market crisis [5]. Despite being the second most abundant element in the universe, being hydrogen the first, it is one of the most difficult elements to capture and produce inside the earth's horizon. In addition to that, the supply chain of this resource is quite faulty, which results in a global helium market unable to meet all the industrial needs.

From 2011 to 2013, the helium industry faced shortfalls of 20 percent, leading to crippling shortages.

During hundreds of millions of years, the decay of radioactive elements near the earth's core has created helium, which managed its way to go up until getting caught in geological formations occurring near the earth's surface. The gas is constantly bubbling up, however it is so light that it can easily escape from the earth's gravitational pull. Practically, most of the helium that is sold today is a by-product of the natural gas industry. However, not every deposit of natural gas bears helium and it does not always make financial sense for companies to refine it, which leads to a financial helium market supply crisis.

Despite being one inert element that does not freeze for a wide range of temperature values, which makes it a truly non-replaceable element for multiple scientific and medical applications, companies have acknowledged the necessary need to develop substitute technologies that do not rely on helium, and when it comes to high altitude balloon applications, hydrogen technologies seem to appear as very promising and more advantageous alternatives. In addition to being the most abundant element on the universe, unlike helium, hydrogen may be obtained through renewable sources [6] and balloons that contain hydrogen instead of helium may benefit from a greater number of advantages:

- Since hydrogen is a lighter gas, helium has only 92% of its lifting capacity [7].
- Unlike helium, hydrogen has a high energy storage density and a fuel cell might be used to generate electricity. Fuel cells are chemical devices that combine hydrogen and oxygen in order to produce electricity through their chemical reaction. When compared to rechargeable batteries, these devices present a lot more advantages, especially when it comes to high altitude balloon applications:
  - **Lighter system**: Basically, the heavier the payload it has to carry, the more hydrogen the balloon will need to have, in order to carry its total mass. In addition to this, the lighter the secondary payload components (batteries, supports, etc...), the more space is left for primary payload components, like for example lift gas storage devices and ballast (which is normally used to reduce the total weight of the balloon and increase its altitude). In general, fuel cell systems are lighter than rechargeable batteries, even when taking into account the supporting systems that are required for hydrogen storage. When it comes to balloons, the balloon itself might work as its hydrogen container [8].
  - **Higher energy density:** Hydrogen has more or less 10 times more energy per weight than batteries. Generally, a fuel cell is able to give more bang per energy buck than a battery with a similar size [8].
  - **Increased lifetime:** Generally, fuel cells last longer than batteries. Batteries are limited in what concerns the number of times they can be recharged and normally they need to be quickly replaced [8].
  - **Environmentally friendly:** It is very expensive to properly dispose a rechargeable battery, as it normally contains hazardous materials and dangerous components. When it comes to this matter, fuel cells are harmless and their chemical reaction products are pollution-free: a) hydrogen molecules are used to produce the electrical current; b) when needed, water may

be used to cool down the electrical components and also to regenerate hydrogen by running a fuel cell in reverse (explained in the following topic) [9]; c) finally, heat can be used to warm up the balloon components, thus preventing icing and freezing problems, which may appear on the upper layers of the atmosphere.

- Contrary to helium, which may hardly be produced via a chemical reaction, hydrogen can be generated through renewable sources [10]. When the generation of electricity via solar, wind, or geothermal renewable sources is greater than its demand, the surplus current may be used to split water into hydrogen and oxygen through a process called electrolysis [6]. Furthermore, this process may also be used to run a fuel cell in reverse. Basically, hydrogen is used to generate electricity, which is then used to power the circuits and split the water to produce hydrogen and oxygen and revert the process once again. Of course that the efficiency of this process might not be as good as the one of a rechargeable battery, but it still offers some promising benefits.
- In the event of not using a fuel cell, hydrogen may be difficult to transport or to store, but many solutions have already overpass these disadvantages (see section 1.3).

As it can be seen, using hydrogen for higher altitude balloon applications brings a lot of advantages. One of the principal disadvantages of using this gas is related to its higher flammability. But even this risk may be controlled by setting the proper conditions when using this gas. Because the rate of diffusion of hydrogen in air is very rapid, when released, it quickly dilutes below dangerous concentrations, thus making it more viable to use under special conditions. Of course that these conditions must be studied before any experiment is taken. Some discuss the *Hindenburg* disaster has occurred because the airship was designed to operate on helium, which the production was mainly controlled by the U.S. at the time [4]. The main problem of using hydrogen is still associated to its storage, which is the main focus of the next chapter.

1.3 Hydrogen storage: an overview on metal hydrides

Hydrogen storage is a challenging task. Being the lightest element on earth, hydrogen has a really small density. At normal pressure and temperature conditions, one cubic meter of hydrogen weights only about 0.08375 Kg. For it to be economically viable, other methods are required to increase its storage density.

In the context of portable hydrogen applications, especially the ones regarding high altitude balloons, within all the possible ways for storing and generating hydrogen, the hydrolysis reaction of a metal hydride has started to appear as a really promising technique. Metal hydrides are chemical compounds that are formed when hydrogen reacts with a metal element or a group of elements containing a metal (a reaction that occurs normally at very high temperature and pressure conditions). Once formed, their hydrolysis reaction (in case water is used) represents a very promising alternative for producing great quantities of hydrogen gas in short time. But even within this world of unlimited possibilities, some of the hydrides are not suitable to achieve an easily controllable hydrogen production. When selecting the

proper one, multiple metal compounds are able to stand out thanks to their properties. For high altitude balloon applications, these are the main reaction and chemical properties of interest:

- **Hydrogen content:** Depending on the reaction, variable quantities of hydrogen are produced per unit mass of hydrogen source that is consumed. Most of these sources are quite easy to achieve for a similar cost (especially the ones regarding ionic metal hydrides (1.3.1)) and therefore, it would make sense to choose the one that maximizes the efficiency of the process.
- **Density:** For high altitude balloon applications, the density of the metal hydride is also an important factor that must be considered, as lighter hydrides will help to decrease the overall mass of the system, thus making it easier to elevate the balloon. Furthermore, the lighter the hydride, the less volume is required to store the same mass.
- **Reactivity:** Within the multiple hydrides, some of them are highly reactive with water, thus making it harder to control the amount of hydrogen that is being produced. When selecting a metal hydride for hydrogen generation, one should choose a compound that is able to react faster with water, however not too fast, as the controlling action becomes more challenging for reactants presenting a higher reactivity. As reactivity increases, trying to safely control the reaction might become an unfeasible task, especially under normal laboratory conditions. In order to deal with this type of reactants, one would require special conditions, thus increasing the cost of the installation and thus ruining the efficiency of the whole process. On the other hand, choosing a less reactive reactant may require the addition of a chemical catalyst, which will also increase the cost of the process and reactor's design.
- **Reaction products:** From the hydrolysis reaction of a metal hydride, the products are normally the respective metal's hydroxide and hydrogen. The rate of reaction will be greatly influenced by the metal hydroxide's solubility in water, as this may form a protective layer over the reactant, thus not allowing for the reaction to continue [11]. If the solubility of the hydroxide is too low, sometimes a catalyst needs to be added, in order to improve the reaction kinetics.
- **Enthalpy of reaction:** Finally, entalphy of reaction is also a factor to be considered. Hydrolysis reactions are highly exothermic, thus releasing great amounts of heat to the surroundings. This will influence the solubility of the hydroxide that is formed and therefore the consequent rate of hydrogen production.

Once formed, depending on the type of their chemical bonds, metal hydrides are divided into several classes (explanation goes beyond the scope of this master thesis) [12]. For the application of these compounds as promising hydrogen storage mediums, the most common and widely known are the ones designated by *ionic metal hydrides* (also called *saline hydrides*) and also the *complex light metal hydrides*:

- **Ionic metal hydrides** are formed when hydrogen reacts with an *alkali* or *alkali earth* metal at high temperature and pressure conditions. Examples of these are the lithium hydride LiH, the

sodium hydride NaH, the potassium hydride KH, the calcium hydride CaH_2 and the magnesium hydride MgH_2 [12, 13]. The majority of them, with the exception of MgH_2, are extremely violent and reactive around the presence of liquid water, which makes the production of hydrogen a more difficult and challenging task.

- **Complex light metal hydrides** are chemical compounds that are formed when hydrogen reacts with light metals from the periodic table groups IA, IIA and $IIIA$ to create chemical complexes like AlH_4^-, AlH_6^{3-}, BH_4^-, NH_2^- and NH^{2-} which are capable of forming ionic bonds with an *alkali* metal and produce stable hydrides like for example, $NaAlH_4$, Na_3AlH_6, $NaBH_4$, $LiNH_2$ and Li_2NH [12]. Within all of these, sodium borohydride $NaBH_4$ is one of the most common hydrides used for hydrogen storage in portable applications [13]. Nevertheless, complex light metal hydrides are less abundant and more expensive than the others. In the context of this master thesis, these were not consider, even tough their properties might bring huge benefits for future hydrogen portable applications.

1.3.1 Light weight ionic metal hydrides: an overview

In the context of this master thesis, ionic metal hydrides were chosen given their higher availability and relatively acceptable cost (for academic purposes). In this section, the advantages of using some of them for hydrogen generation are analysed and compared.

It is important to mention that, because of their level of reactivity, most of these hydrides are highly pyrophoric. After a few minutes, they may start to react spontaneously with air. This property challenges their application, as it will affect their level of purity, which will ruin the efficiency of the entire process.

1 - **Potassium hydride KH:** Within the ones that were previously mentioned, KH is the second heaviest and most reactive ionic metal hydride. Its hydrolysis reaction is so violent that it may be rapidly discarded against all of the other options.

2 - **Sodium hydride NaH:** Moving upwards in the periodic table, NaH is the second most reactive light weight ionic metal hydride. It reacts with water according to:

$$NaH(s) + H_2O(l) \rightarrow NaOH(aq) + H_2(g) \tag{1.1}$$

NaH can achieve a hydrogen storage density of 4.3 wt%. Stoichiometrically, 1 gram of NaH reacts with water in excess to produce 0.083 grams of H_2 and 1.62 grams of sodium hydroxide $NaOH$. The reaction is highly exothermic and the solubility of $NaOH$ decreases for an increase in temperature [14]. Despite seeming attractive, as it happens with KH, NaH is extremely dangerous, thus making it undesirable under certain operating conditions. Because of its level of reactivity, NaH is usually supplied in the form of a dry gray powder dispersed in mineral oil, which usually requires a complex process for them to be separated [15]. When settled, pure NaH requires a dry atmospheric environment in order to be handled. Sodium metal reacts vigorously with water, and when bonded to hydrogen its reactivity is even higher. When mixed with water, the heat of

reaction is usually enough for hydrogen to ignite. In addition, NaH pure powder is highly corrosive and irritant, which makes its application even more challenging.

3 - **Lithium hydride LiH:** LiH is the lightest within the metal hydrides. Its hydrolysis reaction is represented by:

$$LiH(s) + H_2O(l) \rightarrow LiOH(aq) + H_2(g) \tag{1.2}$$

Lithium hydride has the highest hydrogen content within the selected group of hydrides. Stoichiometrically, 1 gram of LiH produces 0.254 grams of H_2 and 3.01 grams of $LiOH$. The reaction is highly exothermic, releasing approximately 250 KJ for every mol of hydride consumed [16], and the solubility of $LiOH$ increases with an increase in temperature. At 20ºC, each cm^3 of water is able to dissolve 0.128 grams of $LiOH$ [17]. The presence of this chemical compound greatly influences the reaction rate. Studies reveal the necessary addition of excess water in order to be possible to remove it and proceed with the chemical reaction [16]. Furthermore, the presence of $LiOH$ requires more volume, thus ruining the compactness of the chemical reaction [16]. Regarding its safety, LiH is extremely irritant, highly toxic and highly corrosive, thus making it undesirable to use without having protective equipment [18]. Finally, despite being capable of producing great quantities of hydrogen, LiH is one of the most reactive with liquid water, being third most reactive within the selected *alkali* ionic metal hydrides.

4 - **Magnesium hydride MgH_2:** Moving towards the second column of the periodic table, MgH_2 is presented as a very promising alternative for producing hydrogen in portable applications, nevertheless, it also offers some challenging disadvantages. MgH_2 reacts with water to produce hydrogen according to:

$$MgH_2(s) + 2H_2O(l) \rightarrow Mg(OH)_2(aq) + 2H_2(g) \tag{1.3}$$

MgH_2 can achieve a hydrogen storage density of 7.6 wt%. From its hydrolysis, a stoichiometric quantity of 0.152 grams of H_2 is formed for each gram of MgH_2 that is consumed. Nonetheless, the hydrolysis of this hydride displays a huge drawback: the magnesium hydroxide that is formed presents a very low solubility in water. At 25ºC, the solubility is only 0.0000064 grams per each cubic centimeter of liquid water [19]. When the reaction starts, a magnesium hydroxide layer is rapidly formed on the surface of MgH_2, thus hindering the production of hydrogen [11]. Given the lower solubility of this hydroxide, using MgH_2 as a hydrogen storage medium requires the use of a catalyst to accelerate the rate of reaction [20]. Despite all of this, as shown in [20], when using citric acid to increase the rate of reaction, there is a clear improvement of this rate associated to an increase in temperature. Furthermore, the reaction is highly exothermic, releasing 270 KJ for each mol of hydride consumed, which means temperature will increase over time. As temperature increases, the solubility of the magnesium hydroxide will also increase, thus allowing for the reaction to be faster.

5 - **Calcium hydride CaH_2:** Moving downwards along the *alkaline earth* metals column, CaH_2

reacts with water according to:

$$CaH_2(s) + 2H_20(l) \rightarrow Ca(OH)_2(aq) + 2H_2(g) \tag{1.4}$$

Comparing to the hydrides that were mentioned in the previous sections, CaH_2 may be found more or less inside the same price range and it also presents some interesting chemical properties:

- Regarding hydrogen content, calcium hydride can achieve a hydrogen storage of 5 wt%. For each gram of hydride consumed, 0.095 grams of H_2 are formed (a little less compared to MgH_2).
- On what concerns its reactivity, with the exception of MgH_2, it is the least reactive when compared to the other light weight ionic metal hydrides. In addition, the reaction is also the least exothermic, releasing only 183 KJ for every mol of hydride that is consumed [21]. Given these properties, when compared to the others, it might be easier to control the rate of hydrogen production.
- Despite being the least exothermic, the reaction displays an interesting feature: calcium hydroxide, $Ca(OH)_2$, presents a higher solubility in water than $Mg(OH)_2$ (around 0.00173 grams in each cm^3 of water at 20ºC) but its solubility decreases with an increase in temperature [22]. This may be either an advantage, in the way that when temperature increases less hydroxide will be dissolved, thus slowing down the reaction (which might be a good thing), or a disadvantage, in case the amount of undissolved hydroxide is too high to allow for the reaction to continue.
- Regarding hazards, as well as the others, CaH_2 is also pyrophoric, and even though not so reactive, it should be stored and handled under dry conditions [23].

In a first attempt to control the production of hydrogen, CaH_2 was chosen from within the various ionic metal hydrides. Throughout research, very little information on the hydrolysis of this compound was found. The majority of studies focused on the advantages of using magnesium hydride, sodium borohydride or other more complex and expensive hydrides. In an initial phase, it was the main focus of this thesis to study the hydrolysis reaction of CaH_2.

1.4 An overview on different balloon architectural types and existing control solutions

In addition to the type of gas that might be used for lift promoting, the balloon's architecture has also a major influence on what concerns its flight duration. Nowadays, there are several types of balloons that may be used to serve this kind of missions. The most common are **Latex Balloons** (or weather balloons), which are *non-fixed volume* systems that can expand by many times in volume. They are often made of a rubber material, which is able to stretch until the balloon reaches its terminal volume, the burst volume.

Zero Pressure Balloons are *fixed volume* systems that are normally filled up with lift gas until a certain volume is reached, the designed volume [24]. Usually, they are made of a very thin plastic sheet unable to stand over-pressure additional forces, therefore, when the balloon reaches its designed specified volume, the extra lift gas is expelled to the atmosphere. To prevent pressure from building up and to allow for the gas to escape, these balloons have open ducts hanging from the sides. Usually, this type of balloons gains height by releasing small portions of ballast (loosing weight). A characteristic flight for this type of balloons is explained next:

- **Launching the balloon during daytime:**
  In the beginning, the balloon is only partially filled and this specific amount of lift gas must be supplied and calculated in a way to ensure the balloon will have an initial vertical resultant force high enough to overpass its weight.

- **Increasing the altitude:**
  As the sun rises, the amount of lift gas that held inside the balloon expands due to temperature increase, thus filling its complete shape. The excess amount of lift gas (which is determined by the zero over-pressure requirement) is exhausted through the opening located at the bottom of the plastic envelope. The balloon will hover at a constant altitude when the volume of the balloon times the difference of gas and air densities equals the balloon's total weight.

- **Maintaining the altitude during the night:**
  At night, the lift gas bubble shrinks and the lift force is reduced, causing the balloon to loose altitude. Facing this situation, in order to maintain the altitude, many ascending mechanisms may be adopted. Normally, a dropping ballast mechanism is actuated to decrease its total weight.

- **Maintaining the altitude during the next day:**
  During the next day, the whole assembly is slightly lighter given the necessity of dropping ballast. The sun will warm up the lift gas, causing it to expand, and given its reduced total weight, the balloon will achieve a higher altitude. As previously explained, the excess gas will be removed through the side openings. This way of controlling the altitude of the balloon will be maintained until the total amount of lift gas is fully exhausted.

Many experiments show latex-type balloons will burst after few hours of flight before they can even reach buoyancy equilibrium [25]. In what concerns zero-pressure balloons, these are quite limited in what concerns their flight duration, as the balloons, despite gaining altitude by using ballast dropping devices, will always loose great quantities of lift gas which are very difficult to recover.

Super-pressure Balloons are *fixed mass* and *fixed volume* systems and they are designed to fly at a specific pressure altitude. They are completely sealed, thus containing zero open ducts, which forces the gas to stay inside the balloon's envelope and maintain buoyancy for longer periods of time [24]. To achieve that, they are composed of a stronger envelope, made of a material which is able to always stand a positive differential pressure (the pressure inside the balloon will always be greater than the

pressure from the outside environment [26]). A usual flight for this type of balloons is characterized by the following phases:

- **Launching the balloon during daytime:**
  - Similarly to what happens with zero-pressure balloons, the lift gas will be warmed up and expand until the balloon reaches its designed maximum volume.
- **Reaching the desired altitude:**
  - As atmospheric pressure goes down, balance is achieved and the extra gas is not vented off. Instead, this extra amount of lift gas is used to pressurize the balloon [26].
- **Maintaining the altitude during daytime and during the night:**
  - During the day, the sun rays will warm up the gas, which will result in an increase of the pressure inside the balloon.
  - During the night, the balloon cools down and the differential pressure despite being still above zero, will be much lower when compared to the one during daytime.

These balloons are filled normally with a specific measure amount of lift gas, and since the gas is never lost (in theory), they are perfect to solve ultra-long distance trajectory problems. Nevertheless, despite providing higher flight duration, given the always positive differential pressure, this type of balloons is way more expensive than the others, as they are dependent on the strength of the envelope's material to handle the bigger pressure inside it.

Dual-type Balloons have recently been presented to increase lifetime and improve floating performance. They are *fixed mass* and *fixed volume* systems which are composed by a super-pressure balloon involved in a zero-pressure one. In this way, the balloon never looses lift gas (which is stored in the super-pressure balloon) and maintains a zero differential pressure between the inside and the outside environment. The super-pressure balloon works only as an auxiliary container to store the extra amount of lift gas [27]. A typical flight for this type of balloon is characterized by the following phases:

- **Launching the balloon during daytime:**
  - Once the sun rises, the lift gas that is held inside the balloon will expand and fill the balloon's inner region to its maximum specified volume. The extra lift gas is stored inside the super-pressure smaller balloon, in order to maintain a zero differential pressure inside the bigger one.
- **Maintaining the altitude during the night:**
  - At night, the lift gas bubble will shrink and the loss of altitude is compensated by releasing the stored lift gas that was kept inside the super-pressure balloon.

This new design overpasses most of the drawbacks encountered by the other solutions:

- First, it is composed by a lighter overall structure (especially in what regards the payload mass), since a dropping ballast mechanism is not required to adjust the altitude (the proper management of lift gas between the super-pressure and zero-pressure balloon does it automatically).

- Secondly, a super-pressure balloon that is only used to store the extra lift gas as a container does not require a special design like common super-pressure balloons, which normally suffer a complex process to improve the strength to weight ratio [27].
- Third, it provides longer lifetime and stability.
- Last but not least, at launching, the super-pressure balloon may store a little extra lift gas, in order to compensate for miscalculations of the necessary quantity at floating level [27].

Within all the types of balloons that can be used for this kind of monitoring missions, the way to control their movement can be achieved by a multiple number of possible approaches. In the following sections, some of them are presented.

Loon project solutions

Loon is a network of stratospheric balloons designed to bring Internet connectivity to rural and remote communities worldwide [28]. For developing this project, Google has presented a great variety of solutions and alternatives in what respects high altitude balloons controlling techniques. These are resumed next [29]:

- **Pumping/Exhausting system**
  One of the methods proposed by Google is based on a simple pumping/exhausting valve system. To decrease the altitude, lift gas is pumped out to a higher pressure storage chamber (like a super-pressure balloon). To increase the altitude, lift gas returns to the envelope. This actuation mechanism is usually used in dual-type balloon systems. The idea is to maintain the zero differential pressure between the balloon's internal pressure and the outside atmospheric pressure. Therefore, the parameters that are considered to trigger control actions are the volume and the value of the differential pressure. Based on the measured values, the control actions are the following:
  - During daytime:
    - If $[p] > 0$ (i.e. $V_b > V_{b,design}$) then turn on the compressor. The extra lift gas mass is pumped from the zero-pressure to the super-pressure balloon.
    - If $[p] = 0$ (i.e. $V_b = V_{b,design}$) stop the compressor.
  - During the night:
    - If $[p] < 0$ (i.e. $V_b < V_{b,design}$) then open the valve. The lift gas mass which is stored inside the super-pressure balloon returns to the zero-pressure balloon.
    - If $[p] = 0$ (i.e. $V_b = V_{b,design}$) close the valve.

  where $[p]$ is the difference between the internal and external pressures.
- **Insulation method**
  - This method is based on the advantages of solar radiation absorption by the balloon's envelope

material. Half of the balloon's envelope is painted black and the other half is painted white. In order to increase its altitude, the balloon is rotated about its vertical axis and its black part is faced towards the sun, which causes the lift gas to expand and create a consequent increase in the lift force. To decrease the altitude, the balloon turns its white painted part towards the sun, which will cause the gas bubble to shrink, resulting in a consequent reduction of the lift force and balloon's altitude.

- **Hydrogen balloon with a fuel cell integrated system**
  - In this system, the balloon runs a fuel cell in reverse to re-generate hydrogen, which is pumped back into the envelope to increase buoyancy. From the fuel-cell chemical reaction, hydrogen is used to produce electricity and feed the electrical circuits. This system brings the huge advantage of not using batteries and solar panels to generate the necessary electricity, which will probably result in a lighter system when compared to the other solutions.

Latex-type balloon solutions

Regarding lower cost alternatives, latex balloons-related techniques are also very promising for controlling the balloon's flight. For example, if one intends to make larger altitude adjustments to the balloon, which might be the case in consideration, when compared to most of the fixed-volume systems (zero-pressure and super-pressure), latex non-fixed volume systems may be more advantageous, as they allow for higher altitude variations. Recently, substancial research has been devoted to this type of balloons, which normally would rupture after 3 hours of flight [25]. In 2017, a group of researchers has proposed a new designed for a typical latex balloon, the *ValBal* system. They have shown that, by controlling the payload mass and lift gas volume, the duration of a typical latex balloon's flight could be extended from 3 hours to several days [25]. In addition to this, they have demonstrated that, with their system, the balloon's altitude could be repeatedly adjusted and varied within an altitude range that most fixed-volume structures would not be capable to achieve. Furthermore, latex balloon's associated low cost and easy assembly make them very suitable for most of the flying missions, as normally, they do not require expensive equipment and qualified personnel like other type of alternatives do. As for the *ValBal* system, most of the latex solutions have adopted a ballast mechanism, where the balloon's altitude is usually adjusted by releasing small portions of ballast. This master thesis suggests a different solution. It is presented in the next section.

1.5 Objectives and contributions

This thesis intends to explore the advantages of using calcium hydride CaH_2 for hydrogen generation and its respective application for controlling the altitude of a normal latex balloon. The main objective is to design a physical prototype, in which the balloon has to carry its own chemical reactor in order for the hydrolysis reaction to occur. A simplified sketch of the total system and its proposed actuation mechanisms is represented in figure 1.2.

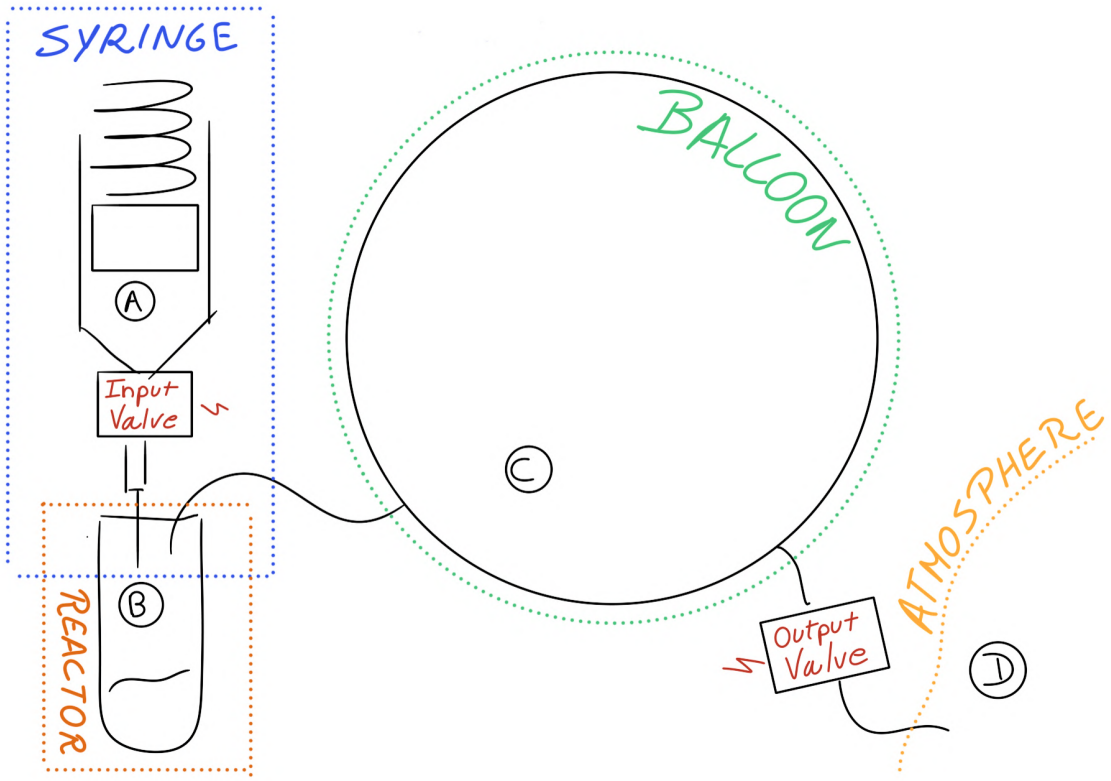

Figure 1.2: Final prototype proposed solution

The total system is composed by 4 main subsystems:

- **Syringe subsystem** 🔵

  The syringe subsystem is responsible for injecting the necessary amount of water inside the chemical reactor. It is composed by a spring element, a syringe and its respective needle, and the input valve, used to control the hydrogen production. In a simple way, every time the **input valve** is actuated, the spring element is released and a certain quantity of liquid water exits through the needle. Regarding the physical elements that were chosen for this system, when moving through the earth's atmosphere and even inside normal laboratory conditions, the balloon will experience considerable changes in its vertical velocity while trying to be controlled. In addition to this, the mass of all the elements that the balloon will carry with him will affect its resultant force and vertical velocity. Having this in mind, for injecting the water inside the chemical reactor, a spring elastic element was chosen, as this type of system would probably be the most suitable for this kind of task.

- **Reactor subsystem** 🟠

  This subsystem is where the hydrolysis reaction occurs. Depending on the injected amount of water, a certain amount of hydrogen will be generated and forced to enter the next subsystem, due to pressure and temperature increase. For its practical part, a glass test-tube was selected, as this type of system would allow one to directly observe the chemical reaction through its walls. Ideally, a metal-made reactor should be used instead, in order to maximize energy losses and

stand higher differential pressures.

- **Balloon subsystem** 🟢

  This subsystem represents the latex balloon. It expands or contracts depending on the amount of hydrogen that is being produced or released and depending on the surrounding atmospheric conditions. Every time one wishes to decrease its altitude, the **output valve** is actuated, and a certain amount of hydrogen is released to the atmosphere.

- **Atmosphere subsystem** 🟡

  The fourth and last subsystem is the atmosphere itself. The balloon's movement will depend a lot on the outside conditions, especially the atmospheric pressure, temperature, and density that are registered at the altitude it is floating on.

The system is equipped with two actuation mechanisms:

1 - To provide lift, hydrogen is produced to increase the volume of the whole structure. A first solenoid valve **(input valve)** is actuated and used to control the amount of water entering the chemical reactor.

2 - To decrease lift, hydrogen is released to the atmosphere. A second solenoid valve **(output valve)** is actuated and used to control the amount of hydrogen that is being released.

To develop this prototype is a very complex task, as most of the variables and physical parameters that are involved are quite difficult to be determined without carrying out some experimental tests. A lot of the parameters are completely unknown. Examples of these are the spring stiffness, the syringe's dimensions, the reactor's physical dimensions, the balloon's elastic properties, etc...It seemed like a good idea to develop a computer model that would allow one to study the impact of changing each one of these parameters on the balloon's vertical movement. Being a project full of practical parameters that would require to be determined experimentally, it was the last goal of this master thesis to build a computer model able to describe the way the system behaves while working as a helpful tool for the future project generations. To accomplish this, this thesis focused on system's identification by using physical principles and curving parameterization methods. In addition to this, given the presence of the COVID-19 virus, by not being possible to access the laboratory as it would be during a normal year, most of the hours spent around this project were used on trying to find a suitable group of equations that would be able to describe an approximated way of the behaviour that the physical prototype would eventually display. Being a very specific project, especially because it involves the modelling of a chemical reaction, it was quite hard to find computational models that would fit for this project goals. Most of the computer models associated with hydrogen generation via a chemical reaction are the basis of very expensive and highly unreachable projects, thus meaning that most of the work here presented was developed without a lot of help.

1.6 Thesis outline

This thesis is divided in 5 different chapters.

Chapter 1 introduces the topic of stratospheric balloons. It performs an overview on the different types of balloons, different gas options for lift promoting and different high altitude control solutions. At the end of the chapter, it is presented the final solution.

Chapter 2 resumes all the theoretical principles and assumptions that considered for the modelling phase. In addition to this, the algorithms that were used in the simulation are also presented.

Chapter 3 contains the practical component. It presents the chemical reactor prototype that was built to perform the hydrolysis reactions and discusses the results that were obtained with its experiments.

Chapter 4 contains the practical aspects regarding the model's implementation. In this chapter, each subsystem is separately implemented from the others and, to validate them, their results are analysed.

Chapter 5 presents the final simulator and its respective results.

Chapter 6 resumes all the achievements and contributions, and proposes some future work ideas to further complement this work.

Chapter 2

Theoretical modelling of a latex balloon with a hydrogen generation system

This chapter focuses on the theoretical principles that were used during the entire modelling phase. The four subsystems that are presented in fig. 1.2 are explained in detail and simplified in what concerns their physical principles.

2.1 Syringe subsystem: modelling transient flow inside an experimental syringe

2.1.1 System schematics and physical introduction

The syringe subsystem is represented in a simplified way in fig. 2.1.

In what regards its input and output variables, these are presented next:

- **Input variables:**
  $\rightarrow$ input valve actuation period of time $\Delta t_{in,v}$
  $\rightarrow$ reactor's pressure p_R.
- **Output variables:**
  $\rightarrow$ water mass flow rate $\dot{m}_\omega$

The water flow inside a normal syringe may be modelled through the use of the well-known **Transient Bernoulli Equation**. By applying this equation to a streamline gathering points A and B (see figure 2.1), the *Bernoulli* equation with the transient component has the form:

$$p_A + \rho_\omega g z_A + \frac{1}{2}\rho_\omega u_A^2 = p_B + \rho_\omega g z_B + \frac{1}{2}\rho_\omega u_B^2 + \rho_\omega \int_{x_A}^{x_B} \frac{du(x)}{dt} dx + \int_{x_A}^{x_B} f \frac{1}{2} \frac{L_s}{\phi_s(x)} \rho_\omega u(x)^2 dx \quad (2.1)$$

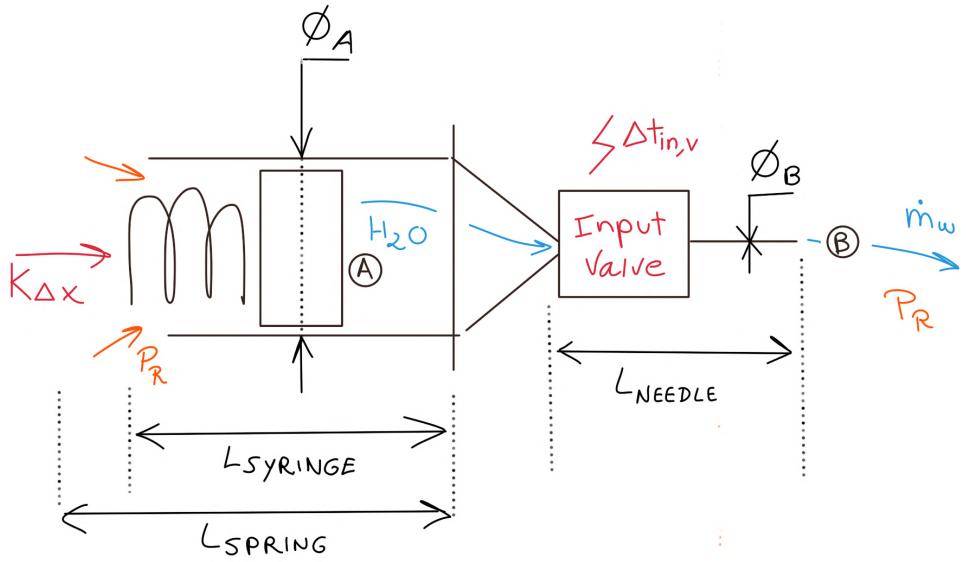

Figure 2.1: Syringe subsystem representation

where, x and z represent the fluid's longitudinal and vertical coordinates, respectively, u represents the fluid's longitudinal velocity along the syringe's streamline (being $x = 0$ the plunger's position for the situation at which the spring is at its most contracted position), p and ρ_ω represent the fluid's pressure and density, respectively, L_s represents the streamline's length (in this case, the syringe subsystem total length (from the beginning of the syringe to the needle's end)), g the acceleration of gravity, ϕ_s the syringe's subsystem diameter at a specific section, f the *Darcy* coefficient and $\rho_\omega \int_{x_A}^{x_B} \frac{du}{dt} dx$ represents the transient term of the equation.

2.1.2 Physical assumptions

This section explains all the physical approximations that one is dealing with when applying equation (2.1) and all the assumptions that were considered in order to simplify it.

- **Incompressible flow:**

  The *Bernoulli* equation can only be applied to incompressible flow situations, therefore it makes sense to evaluate if the *Bernoulli* principle is valid for these conditions. When dealing with general fluid motion (gases or liquids), one says a certain fluid displays an incompressible flow behaviour if its density is held constant throughout time and space. In order to know if this is the case, the *Mach* number M_a was analysed [30]. The *Mach* number is the ratio of the relative velocity of the fluid to the speed of sound inside that fluid. It is represented by:

  $$M_a = \frac{u_{fluid}}{u_{sound|fluid}} \tag{2.2}$$

  Basically, if $M_a < 1$, which occurs for subsonic low speed situations, the change in the fluid's density is so small it might be neglected and the flow may be considered as incompressible. For

the water case, sound is propagated faster than in air. In addition, if the spring stiffness constant k of the spring element is made adequately small, then the water moving from the syringe to the needle will move even slower, thus decreasing the *Mach* number.

In fact, the temperature of the fluid is also a factor to be considered. In stratosphere, temperatures are so low that water might rapidly start to freeze. Nevertheless, this problem must, of course, be solved, as no chemical reaction will occur at these conditions. Throughout the development of this thesis, it was assumed that the entire syringe subsystem was carefully isolated in order to guarantee that the water would remain in its liquid form. For liquid water, the effect of temperature is demonstrated in figure 2.2:

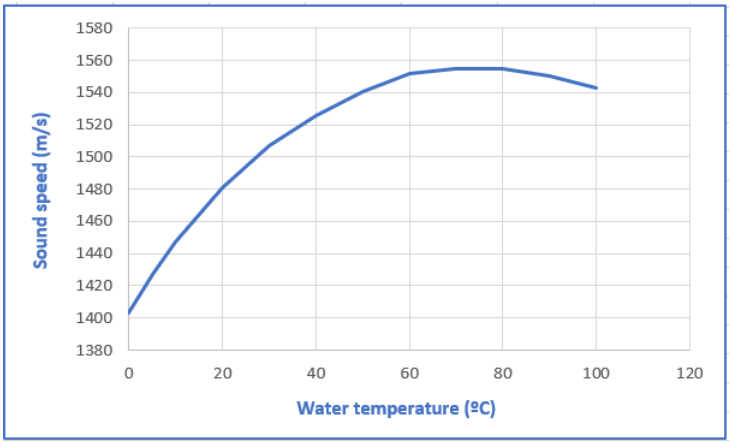

Figure 2.2: Sound speed [m/s] vs water temperature [ºC] [31]

By looking at fig. 2.2, the speed of sound increases from 1400 m/s when water is at 0ºC to 1560 m/s at 80ºC and starts to decrease for higher temperatures. But even within this range of temperatures, the sound speed is very high and the water flow might still be considered incompressible because of the resulting small number of *Mach*.

- **Continuity:**

  Regarding continuity, it was assumed that the water flow rate is constant throughout the entire syringe subsystem. This continuity criteria is expressed by:

$$Q_\omega = Q_A = Q_B = A_s(x)u(x) \tag{2.3}$$

  where Q_ω represents the water volumetric flow rate, $A_s(x)$ represents any syringe's subsystem sectional area and u represents the fluid's velocity in the same section.

- **Neglected inlet/outlet velocity terms:**

  When compared to the other terms of equation (2.1), the velocity terms corresponding to the velocities at points A and B are quite small. Given this, for the sake of simplicity, it was considered that $u_A \approx u_B \approx 0$.

- **Neglected gravity effect term:**

In addition to the previous assumptions, the gravity effect and change in altitude were also neglected. This corresponds to consider that $\rho_\omega g z_A \approx \rho_\omega g z_B$. In figure 2.1, the system was represented horizontally, however, in the physical prototype, the syringe subsystem would be placed vertically. When placed vertically, one might suggest that the plunger's and spring's masses will affect the fluid's vertical motion. However, given the presence of a very tiny needle, the surface tension forces acting at its tip are so strong, that the result is the same as neglecting gravity. This could also be observed at the laboratory, while running the water measurement experiments (section 3.3): while keeping the valve actuated, it was noticed that no water droplets would fall down, if no force was applied. Given this, it made sense to neglect this term, otherwise one would have to deal with a more complex equation.

- **Simplification of the transient term:**

  For an easier integration, the transient term was also simplified. The term $\frac{du(x)}{dt}$, which represents the change of water's velocity with time, might be considered bigger throughout the needle section comparing to the other circular sections of the syringe subsystem. With this assumption, the term adopts a new form:

$$\rho_\omega \int_{x_A}^{x_B} \frac{du(x)}{dt} dx \approx \rho_\omega \int_{needle} \frac{du(x)}{dt} dx \xrightarrow{continuity} \rho_\omega \frac{du_{needle}}{dt} L_{needle} \tag{2.4}$$

  where L_{needle} represents the needle's length and ρ_ω the water's density.

- **Neglected loss terms:**

  Throughout the different sections of the syringe subsystem, there are several regions where losses may easily occur. These losses are represented by the last term of equation (2.1), where the existence of localized loss coefficients is already neglected given the presence of very small velocities. This term is again represented by:

$$\text{Losses} = \int_{x_A}^{x_B} f \frac{1}{2} \frac{L_s}{\phi_s(x)} \rho_\omega u(x)^2 dx \tag{2.5}$$

  It is as bigger as higher becomes the term $u(x)^2$. By continuity, the velocity of the water in the needle section is higher when compared to the other sections, thus allowing this term to be neglected in other sections when compared to any needle's section. Having this in mind, the term might become even simpler and adopt the form represented by the following expression:

$$\int_{x_A}^{x_B} f \frac{1}{2} \frac{L_s}{\phi_s(x)} \rho_\omega u(x)^2 dx \approx f \frac{1}{2} \frac{L_{needle}}{\phi_B} \rho_\omega u_{needle}^2 \tag{2.6}$$

  where f is the so called loss coefficient or *Darcy* coefficient, which might be calculated in two different ways depending on the type of flow that is assumed: laminar or turbulent. The next

equation illustrates both cases [32]:

$$\begin{cases} Re_\phi \leq 2300 : f_{lam} = \frac{64}{Re_\phi} \\ Re_\phi > 2300 : \frac{1}{\sqrt{f_{turb}}} \approx 2\log(Re_\phi \sqrt{f_{turb}}) - 0.8 \end{cases} \tag{2.7}$$

where Re_ϕ is the **Flow Reynolds Number** defined by:

$$Re_\phi = \frac{u\phi}{\nu_\omega} \tag{2.8}$$

where u is the velocity, ϕ is the inner diameter of any circular section and ν_ω is the kinematic viscosity of water, which might be expressed in the following form:

$$\nu_\omega = \frac{\mu_\omega}{\rho_\omega} \tag{2.9}$$

being μ_ω the dynamic viscosity of the fluid.

- **Laminar flow:**
  In order to obtain the *Darcy* coefficient f and develop equation (2.6), laminar flow was assumed given the overall small velocities of the fluid throughout the entire syringe subsystem. By joining equations (2.6), (2.7), (2.8) and (2.9), the losses term adopts the form:

$$f_{needle} \frac{1}{2} \frac{L_{needle}}{\phi_B} \rho_\omega u_{needle}^2 = \frac{32 \mu_\omega L_{needle} u_{needle}}{{\phi_B}^2} \tag{2.10}$$

- **One dimensional flow**
  For the sake of simplicity, at the end, the flow was also assumed as being one-dimensional, therefore eliminating the possibility of vertical flow (having in mind the configuration represented in figure 2.1), which might in reality occur.

After making these simplifications, the last thing to do was to find the two expressions for p_A and p_B. To find these expressions, one needs to know, *a priori*, how the syringe and reactor subsystems are related, as the pressure applied in point A will depend a lot on the prototype's configuration (see figure 2.3):

- At point A, the pressure p_A is the sum of two different pressures directly applied on the plunger's left surface (see figure 2.1), the spring's pressure and the outside pressure:
  - On a first approach (fig. 2.3(a)), if the syringe is placed and fixed outside the reactor, the pressure applied on the plunger's left surface will be equal to the pressure defined for the environment around it. This brings a problem for the controlling approach, as the pressure may not be high enough to overcome the reactor's pressure, thus allowing for the water to back-flow.
  - On a second approach (fig. 2.3(b)), if one chooses to place the syringe inside the reactor, the outside pressure will be equal to the reactor's pressure p_R (as represented in fig. 2.1). If this

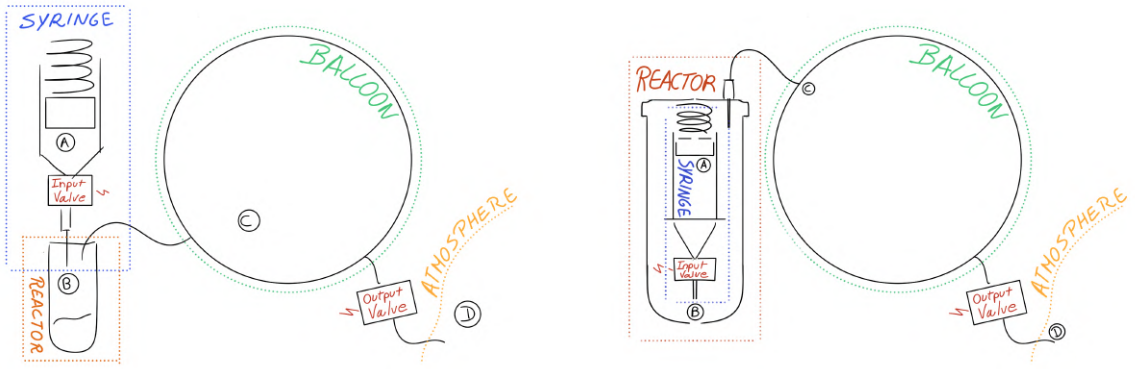

(a) Syringe placed outside the reactor

(b) Syringe placed inside the reactor

Figure 2.3: Prototype possible configurations

occurs, the pressure applied on the left side of the plunger will be the one defined by:

$$p_A = p_R + \frac{F_{spring}}{A_{plunger}} = p_R + \frac{4k(L_{spring} - x)}{\pi\phi_A^2} \tag{2.11}$$

where k represents the spring stiffness constant, L_{spring} the undistorted spring length, ϕ_A the plunger's diameter and x the plunger's position. It is important to notice once again that $x = 0$ refers to the position at which the spring is at its maximum compression state (maximum elastic force). Of course that this situation also brings a problem: the pressure and temperature generated inside the reactor might become so high that the system will require a proper thermal isolation, in order to prevent for the water to evaporate and thus being able to remain at its liquid state.

For the sake of simplification, the second case for the prototype's configuration was assumed, i.e., syringe is placed inside the reactor.

- At point B, the water exiting the syringe's subsystem will enter the chemical reactor in both configurations. As hydrogen is produced, pressure starts to increase and point B will be at the reactor's pressure, ($p_B = p_R$).

Finally, by substituting equations (2.11), (2.10) and (2.4) into equation (2.1) and by considering all of these assumptions, the simplified *Bernoulli* equation is:

$$p_R - p_R + \frac{4k(L_{spring} - x)}{\pi\phi_A^2} = \rho_\omega \frac{du_{needle}}{dt} L_{needle} + \frac{32\mu_\omega L_{needle} u_{needle}}{\phi_B^2} \tag{2.12}$$

where $p_R - p_R$ is represented just to make it easier to understand all the simplifications that were considered.

2.1.3 Solving for the water mass flow rate

In order to solve for the water's mass flow rate $\dot{m}_\omega$ (the subsystem's output), u_{needle} must be expressed by continuity in terms of the plunger's velocity $\dot{x}$. Since the flow rate is constant throughout the entire

water circuit, it is known that $\dot{x}A_{plunger} = u_{needle}A_{needle} \equiv \dot{x}\phi_A^2 = u_{needle}\phi_B^2$ and so therefore, u_{needle} might be expressed by:

$$u_{needle} = \dot{x}\frac{\phi_A^2}{\phi_B^2} \tag{2.13}$$

In addition to that, $\frac{du_{needle}}{dt} = \ddot{x}\frac{\phi_A^2}{\phi_B^2}$ and so therefore, equation (2.12) becomes equation (2.14):

$$\frac{4k(L_{spring} - x)}{\pi\phi_A^2} = \rho_\omega \ddot{x}\frac{\phi_A^2}{\phi_B^2}L_{needle} + \frac{32\mu_\omega L_{needle}\dot{x}\phi_A^2}{\phi_B^4} \tag{2.14}$$

From this, x is found as a function of $\dot{x}$ and $\ddot{x}$ and the water mass flow rate which is exiting the needle's section might be obtained by using:

$$\dot{m}_\omega = \rho_\omega(Au)_{needle} = \rho_\omega\frac{\dot{x}\pi\phi_A^2}{4} \tag{2.15}$$

For a specific valve actuation period $\Delta t_{in,v}$, the corresponding amount of water will enter the reactor and a certain volume of hydrogen will be produced through the hydrolysis reaction of calcium hydride. The next section explains what happens physically inside the chemical reactor when a small quantity of water is put together with a certain amount of calcium hydride, CaH_2.

2.2 Reactor subsystem: modelling the hydrolysis reaction inside an experimental glass reactor

2.2.1 System schematics and physical introduction

The reactor subsystem is represented in a simplified way in figure 2.4. For it to be easier to understand, the balloon subsystem is also partially represented and identified by the letter C. The syringe subsystem is not represented.

Regarding the system main input and output variables, these are the following:

- **Input variables:**
  → water mass flow rate $\dot{m}_\omega$
  → balloon's pressure p_b

- **Output variables:**
  → hydrogen input mass flow rate $\dot{m}_{H_2,R\rightarrow b}$ (from the reactor to the balloon)

When lifted up to the stratosphere, the balloon shall be provided with the total amount of hydride that is necessary to complete the desired flight duration. Since relatively small quantities of hydride yield, in theory, great amounts of hydrogen, it is assumed the reactor will contain the necessary amount of hydride necessary for the desired hydrogen production.

At the reactor, water molecules are mixed with calcium hydride CaH_2 to form calcium hydroxide

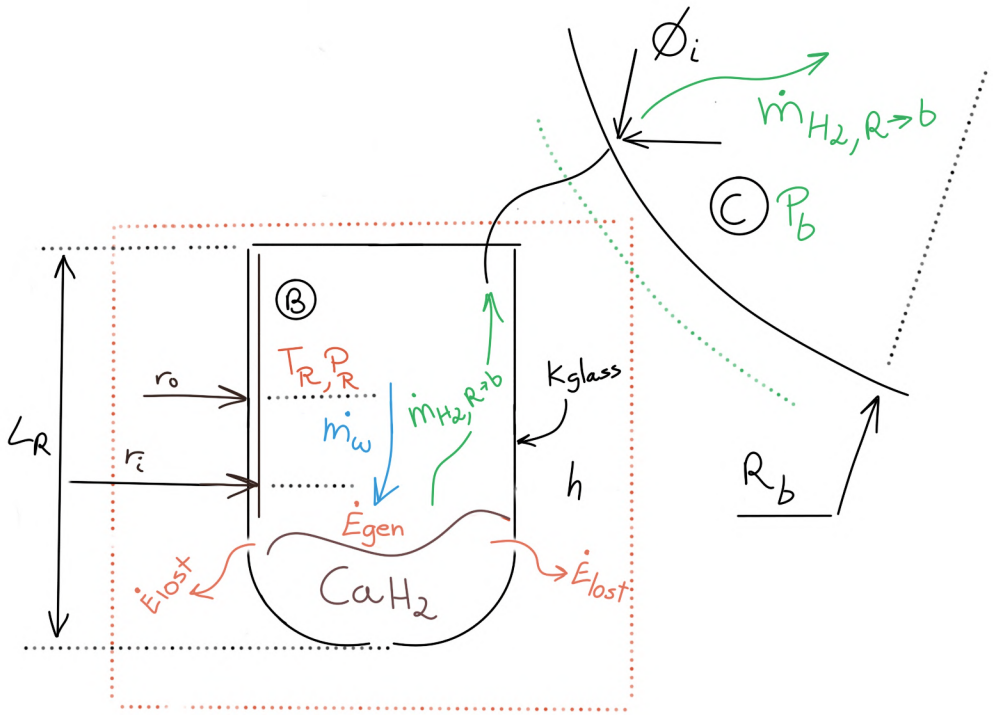

Figure 2.4: Reactor subsystem representation

$Ca(OH)_2$ and yield hydrogen H_2 according to:

$$CaH_2(s) + 2H_2O(l) \rightarrow Ca(OH)_2(aq) + 2H_2(g) + 183KJ \tag{2.16}$$

This equation represents a highly exothermic system, releasing great amounts of heat to its neighbouring environment. As for the case of the syringe subsystem, the reactor subsystem is quite complex to be modelled. The next section presents all the physical assumptions that were considered.

2.2.2 Physical assumptions

- **Constant reactant purity:**

  Calcium hydride is a highly pyrophoric substance, which means it can react spontaneously with the wet atmosphere that surrounds it. Due to this, it was assumed the reactor was already physically isolated from the atmosphere, thus making sure the purity of the reactant remained the same throughout the entire flight. At the laboratory, one was able to make some chemical tests which revealed a reactant purity of approximately 88.48% (see section 3.5).

- **Deviated stoichiometry:**

  Equation (2.16) represents the stoichiometric reaction, which, in theory, states that 1 mol of CaH_2 reacts with 2 mol of liquid H_2O to form approximately 1 litre of hydrogen. Unfortunately, things are not that simple and there are a lot of factors that might influence the way the reaction proceeds. As previously mentioned in section 1.3.1, this reaction yields hydrogen H_2 and calcium hydroxide $Ca(OH)_2$, which presents the very low solubility of 0.00173 grams in each cm^3 of water at room

temperature. During the reaction, a layer of this chemical compound starts to cover up the hydride, making it difficult for the reaction to proceed. The stoichiometric quantity of water might not even be enough to guarantee the production of the theoretical amount of hydrogen gas. After making several practical tests (see section 3.5), it was noticed that, for producing the desired amount of hydrogen, 4 to 5 times more water was necessary. This information was useful to define the initial mass of the two reactants, for the moment at which the flight begins.

- **Ideal gas approximation:**
  Regarding the substances placed and formed inside the reactor, the space occupied by the calcium hydride and the water droplets was assumed to be irrelevant. It was considered that hydrogen is the only element presented inside the reactor at each instant of time and that it behaves as an ideal gas. By considering this, one assumes the following equation is true:

$$p_R = \rho_{H_2,R} R_{g,H_2} T_R \tag{2.17}$$

  where p_R represents the reactor pressure (or reactor's hydrogen pressure), $\rho_{H_2,R}$ represents the hydrogen gas density inside the reactor, R_{g,H_2} the specific hydrogen universal gas constant $\left(= \frac{R_g}{M_{H_2}}\right)$ and T_R the temperature inside the reactor. This equation is only applied for incompressible fluids, which is not the case in consideration, as the density of the gas is always changing inside the reactor due to pressure building. Therefore, some errors are expected when comparing to the system's behaviour when subjected to real conditions. By considering equation (2.17), the reactor subsystem is approximated to a hydrogen volume which is capable of generating and releasing specific amounts of hydrogen depending on the amount of water that is entering inside the reactor and the pressure level generated inside it, respectively. By considering this, the next equation was used to describe the mass balance of the system:

$$\frac{d}{dt}(\rho_{H_2,R} V_R) = \dot{m}_{H_2,gen} (\approx f(\dot{m}_\omega)) - \rho_{H_2,R} \frac{\pi \phi_i^2}{4} v_i \tag{2.18}$$

  where V_R represents the reactor's fixed volume, $\dot{m}_{H_2,gen}$ represents the generated hydrogen mass flow rate (function of the water mass flow rate $\dot{m}_\omega$ (see section 4.2), ϕ_i represents the diameter of the tube connecting the balloon and the reactor and v_i represents the hydrogen inlet velocity.

- **Thermal approximation:**
  Last but not least, as for the practical experiments (section 3), a cylindrical glass reactor similar to a 15 cm-length test-tube was considered for the theoretical analysis. In what regards its **material**, ideally, one should have considered a metal reactor for the practical experiments (section 3), as it would allow to dissipate more energy and handle bigger differential pressures. Nevertheless, a glass reactor would allow one to visually observe the reaction. Here stands the reason behind the choice of a glass reactor: since it was the first time studying this chemical reaction, multiple errors could occur, which could hardly be identified if one was using a metal reactor. Regarding the external conditions, it was assumed an outside constant temperature T_{out} (to almost replicate

the laboratorial conditions (see section 3.4)). By taking into account all of this assumptions, an approximated thermal model was created to evaluate the reactor's inner temperature profile $T_R(t)$. For this specific case, the change in hydrogen temperature inside the reactor may be obtained by applying the well known **Lumped Capacitance Method**, which assumes that heat diffusion occurs fast enough in order to be possible to consider that temperature only varies with time. In this way, the spatial temperature gradients are neglected and the inner temperature derivative over time might be obtained by using the following expression [1]:

$$\rho_{H_2,R} Cp_{H_2} V_R \frac{d}{dt}(T_R) = \dot{E}_{gen} - \dot{E}_{lost} \tag{2.19}$$

where Cp_{H_2} represents the hydrogen's heat capacity and $\dot{E}_{gen}$ and $\dot{E}_{lost}$ represent the generated and released energy powers, respectively. In what concerns the hydrogen's heat capacity, one knows from theory that Cp is a function of temperature. By analysing table A4 in [1], one was able to conclude that the change in this value with temperature could be considered irrelevant, at least for the range of temperatures that one might have to deal with. Regarding the right terms, these were calculated in the following manner:

- **Generated power $\dot{E}_{gen}$:**

  From equation (2.16), it is known that, for each mol of CaH_2 that is consumed, 183 KJ are released in the form of heat. Since the laboratorial component was quite inconclusive regarding temperature measurement (see section 3.5), it was not possible to estimate the change in this value and so therefore, it was decided to consider the theoretical one. Then, by assuming the real stoichiometric ratios, if one knows hydrogen is being generated at γ mol/s, then CaH_2 is being consumed at a rate of $\frac{\gamma}{2}$ mol/s. Finally, $\dot{E}_{gen}$ may be calculated by:

$$\dot{E}_{gen} = 183000 \left(\frac{\gamma}{2}\right) \tag{2.20}$$

- **Released power $\dot{E}_{lost}$:**

  Regarding the loss term, this may be computed by:

$$\dot{E}_{lost} = \frac{T_R - T_{out}}{\Omega_T} L_R \tag{2.21}$$

  where T_{out} represents the outside temperature (assumed constant), L_R represents the reactor's length and Ω_T represents the total thermal resistance, which was calculated by considering the **equivalent thermal circuit** of this system (see figure 2.5).

  By taking this approach, the total thermal resistance Ω_T can be computed by:

$$\Omega_T = \frac{1}{2\pi r_o h} + \frac{ln\left(\frac{r_o}{r_i}\right)}{2\pi k_{glass}} \tag{2.22}$$

  where h represents the convection coefficient, k_{glass} the thermal conductivity of glass, r_o the external radius, and r_i the internal radius of the reactor.

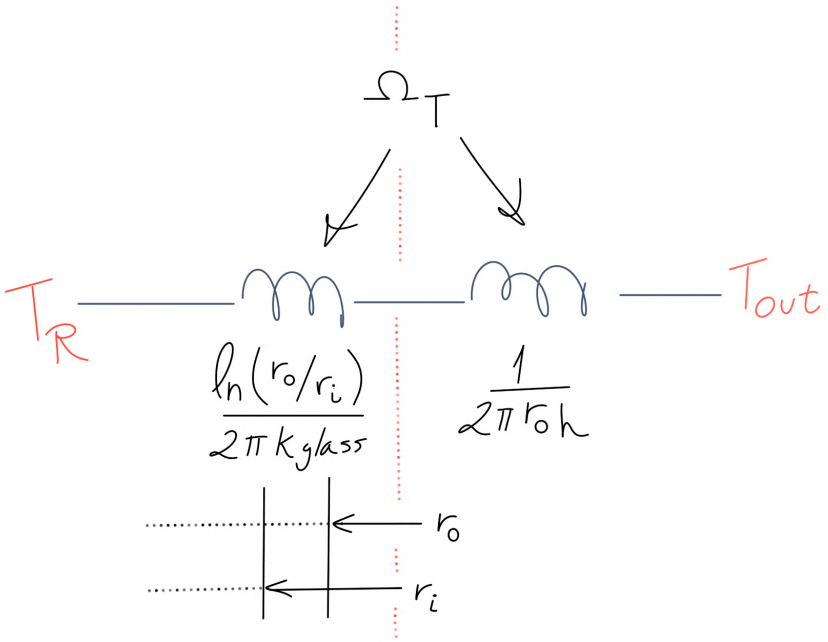

Figure 2.5: Equivalent thermal circuit for the reactor subsystem

2.2.3 Solving for the hydrogen input mass flow rate

Considering the previous approximations, the hydrogen flow rate may be computed by using once again the **Bernoulli equation** with the transient term (recall section 2.1), this time applied between points B and C (fig. 2.4):

$$p_B + \rho_{H_2,R} g z_B + \frac{1}{2}\rho_{H_2,R} v_B^2 = p_C + \rho_{H_2,R} g z_C + \frac{1}{2}\rho_{H_2} v_C^2 + \rho_{H_2,R} \int_{s_B}^{s_C} \frac{dv(s)}{dt} ds + f \frac{1}{2} \frac{\bar{BC}}{\phi_i} \rho_{H_2,R} v(s)^2 \quad (2.23)$$

where the letter s is used to represent a component aligned with the streamline gathering points B and C, v is the hydrogen velocity along the same streamline and the last terms represent the transient and loss terms. By analysing the streamline between points B and C, as in for the case of the syringe subsystem (review section 2.1), the transient change in velocity and respective losses will be greater in the tube comparing to the other regions, which means that the majority of the circuit may be neglected in terms of its losses and transient components. In addition, if the length of the connection tube (with diameter ϕ_i) is made really short ($\bar{BC} \approx 0$), then all of these terms may be completely neglected. Finally, by neglecting the gravity terms (to simplify), by assuming that the velocity at the tube is a lot greater than the velocity inside the reactor and by knowing that $p_B = p_R$ and $p_C = p_b$, equation (2.23) may be simplified to:

$$p_R = p_b + \frac{1}{2}\rho_{H_2,R} v_i^2 \quad (2.24)$$

where v_i represents the hydrogen's velocity through the connection tube with diameter ϕ_i (see fig. 2.4). Since the *Bernoulli* equation can only be applied to incompressible fluids, it is assumed the density of the gas does not change along this streamline.

The following algorithm was used to compute the reactor variables at each instant of time t:

1 - Initialize all the variables: $p_R(t)$, $p_b(t)$, $T_R(t)$, $v_i(t)$, $\rho_{H_2,R}(t)$.

2 - Compute the reactor's internal density derivative between time instants t and $t+\Delta t$, $\frac{d}{dt}(\rho_{H_2,R})|_{t\to t+\Delta t}$, using equation (2.18):

$$\frac{d}{dt}(\rho_{H_2,R})|_{t\to t+\Delta t} = \frac{\dot{m}_{H_2,gen}(t)}{V_R} - \rho_{H_2,R}(t)\frac{\pi\phi_i^2}{4V_R}v_i(t) \tag{2.25}$$

where $\dot{m}_{H_2,gen}(t)$ is a function of the water mass flow rate $\dot{m}_\omega$ (see section 4.2).

3 - Calculate the reactor's internal temperature derivative between time instants t and $t+\Delta t$, $\frac{d}{dt}(T_R)|_{t\to t+\Delta t}$, using equations (2.19), (2.20), (2.21) and (2.22):

$$\frac{d}{dt}(T_R)|_{t\to t+\Delta t} = \frac{\dot{E}_{gen}(t) - \dot{E}_{loss}(t)}{\rho_{H_2,R}(t)Cp_{H_2}V_R} \tag{2.26}$$

4 - Obtain the reactor's internal density at time instant $t+\Delta t$, $\rho_{H_2,R}(t+\Delta t)$:

$$\rho_{H_2,R}(t+\Delta t) = \rho_{H_2,R}(t) + \frac{d}{dt}(\rho_{H_2,R})|_{t\to t+\Delta t}\Delta t \tag{2.27}$$

5 - Obtain the reactor's internal temperature at time instant $t+\Delta t$, $T_R(t+\Delta t)$:

$$T_R(t+\Delta t) = T_R(t) + \frac{d}{dt}(T_R)|_{t\to t+\Delta t}\Delta t \tag{2.28}$$

6 - Compute the reactor's pressure at time instant $t+\Delta t$, $p_R(t+\Delta t)$, using equation (2.17):

$$p_R(t+\Delta t) = \rho_{H_2,R}(t+\Delta t)R_{g|H_2}T_R(t+\Delta t) \tag{2.29}$$

7 - Finally, compute the inlet velocity at time instant $t+\Delta t$, $v_i(t+\Delta t)$, using equation (2.24):

$$v_i(t+\Delta t) = \sqrt{\frac{2(p_R(t+\Delta t) - p_b(t+\Delta t))}{\rho_{H_2,R}(t+\Delta t)}} \tag{2.30}$$

Note: In order to use this equation, one needs to first obtain the value for the balloon pressure at the same instant of time. This is explained in the section 2.3.3.

The hydrogen input mass flow rate $\dot{m}_{H_2,R\to b}$ which is entering the balloon's subsystem (output of the reactor's subsystem) is finally computed for the same instant $t+\Delta t$ by:

$$\dot{m}_{H_2,R\to b}(t+\Delta t) = \rho_{H_2,R}(t+\Delta t)\frac{\pi\phi_i^2}{4}v_i(t+\Delta t) \tag{2.31}$$

2.3 Balloon subsystem: lift modelling of an experimental latex balloon

2.3.1 System schematics and physical introduction

The balloon subsystem is represented in a simplified way in figure 2.6. The reactor and atmospheric subsystems are also represented by the letters B and D, respectively.

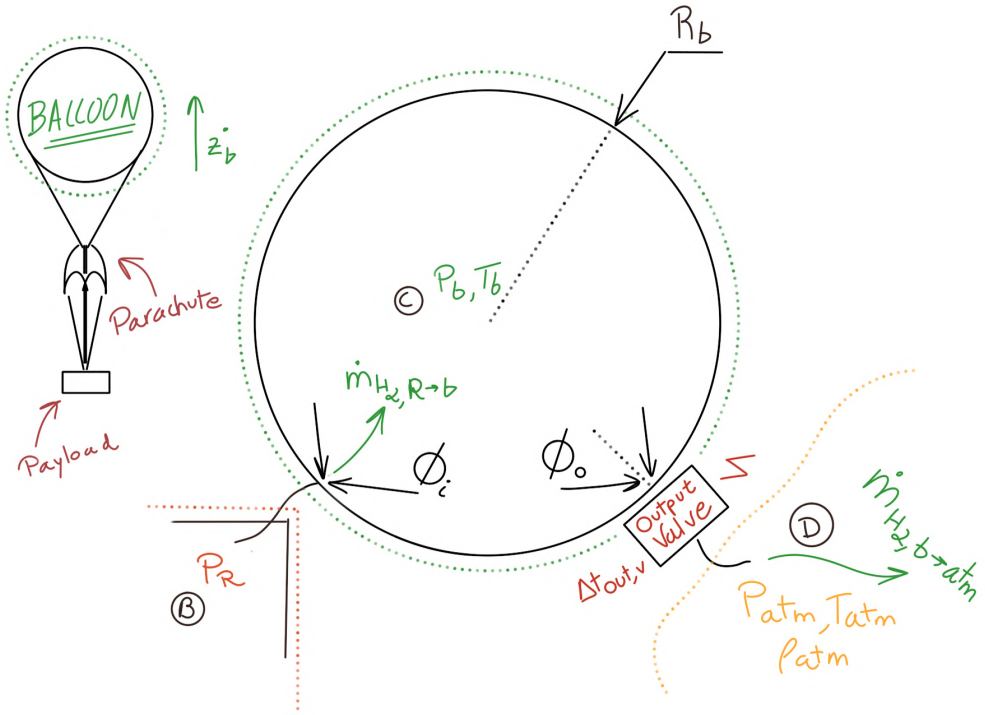

Figure 2.6: Balloon subsystem representation

The input and output variables of this subsystem are described next:

- **Input variables:**
  → hydrogen input mass flow rate $\dot{m}_{H_2,R\to b}$
  → output valve actuation period of time $\Delta t_{out,v}$
  → atmospheric properties $p_{atm}, T_{atm}, \rho_{atm}$.

- **Output variables:**
  → hydrogen output mass flow rate $\dot{m}_{H_2,b\to atm}$
  → altitude z_b
  → balloon's pressure p_b

As stated by the *Archimedes* principle, a body which is partially or fully immersed in a fluid will be actuated by a vertical force with intensity equal to the weight of the fluid's displaced volume. The same principle is applied to a latex balloon when moving through the earth's atmosphere. The balance of

forces acting on the balloon is represented by the following group of equations:

$$\sum F = m_{total}\frac{d\dot{z_b}}{dt} = \rho_{atm}V_b g - m_{total}g - \frac{1}{2}C_D A_b \rho_{atm}\frac{dz_b}{dt}\left|\frac{dz_b}{dt}\right| \tag{2.32}$$

$$m_{total} = m^0_{total} - m_{H_2,b\rightarrow atm} \tag{2.33}$$

$$m^0_{total} = m_{pch} + m_e + m_{rest} + m^0_\omega + m^0_{[CaH_2]} + \rho^0_{H_2,b}V^0_b \tag{2.34}$$

where C_D is the drag coefficient, $\frac{1}{2}C_D A_b \rho_{atm}\frac{dz_b}{dt}\left|\frac{dz_b}{dt}\right|$ is the term that represents the drag force, m_{total} represents the current total mass of he system (equations (2.33)), m^0_{total} represents the initial total mass (being m_{pch} the parachute's mass, m_e the envelope's mass, m_{rest} the mass of the tubes, supports, batteries and other components, m^0_ω the initial water mass, $m^0_{[CaH_2]}$ the initial hydride's mass and $\rho^0_{H_2,b}V^0_b$ the initial hydrogen's mass), $m_{H_2,b\rightarrow atm}$ represents the total mass of hydrogen that was already released, and $\rho_{atm}V_b g$ represents the buoyancy force. The buoyancy force only depends on the displaced volume, the density of the gas ρ_{H_2} only affects the overall balance of forces acting on the balloon and thus, its acceleration and vertical velocity. Having this in mind, if one wants to increase the balloon's altitude, the idea is to maximize $(\rho_{atm} - \rho_{H_2,b})V_b$ (the lift force), which means choosing a lighter gas than air (like hydrogen or helium) and increasing the volume of the displaced air (i.e., the volume of the balloon).

Regarding the thermal factor, in reality, temperature is not constant and can also affect the overall balance of forces acting on the balloon. By considering the energy exchanges (solar radiation) between the balloon and the outside environment, the temperature of the inner gas may be affected by the constant day-night shifts, which can result in its expansion or its contraction. Depending on the case, the volume of the balloon will be affected and a variation in the lift force will be noticed.

With the previous equations, it is possible to calculate the amount of lift gas that is required for the balloon to reach a certain desired altitude. Nevertheless, for the situations where the balloon can exchange not only energy but also mass with the exterior, solving for the lifting capacity becomes a more challenging task. If a certain mass of lift gas suddenly enters the balloon during a certain period of time, a transient phenomena needs to be solved, which may be done by including the mass balance equation of the system. In addition to this, by being latex type, the balloon will be deformed in a non-linear way. The solution for this problem is found by applying **hyper-elastic theory** to a normal latex balloon.

Studying the material laws which are capable of explaining the way hyper-elastic materials behave when subjected to an external force, is an extensive topic which goes beyond the scope of this master thesis. Since hyper-elasticity is a very large topic, the model that was used to describe the stretching behaviour of latex balloons was not studied in too much detail. Rubber and latex may be basically described as an incompressible type of material displaying a non-linear hyper-elastic behaviour. The stress-stretch relation of this material characterizes a typical **Mooney-Rivlin material** [2]. When applied to a rubber balloon, its inner-pressure/volume curve has the form represented by:

$$[p] = 2s_+\frac{t^0_e}{r^0_b}\left(\frac{r^0_b}{R_b} - \left(\frac{r^0_b}{R_b}\right)^7\right)\left(1 - \frac{s_-}{s_+}\left(\frac{R_b}{r^0_b}\right)^2\right) \tag{2.35}$$

where $[p]$ represents the difference between the internal and external pressures, $p_b - p_{atm}$, t_e^0 and r_b^0 represent the thickness and radius of the undeformed envelope, respectively, s_+ and s_- are elastic temperature linearly dependent constants and R_b is the current radius of the balloon. Regarding the previous elastic constants, they vary linearly with temperature and for a rubber material, at room temperature, their values are equal to $s_+ = 3$ bar and $s_- = -0.3$ bar. This equation describes a curve like the one represented in fig. 2.7.

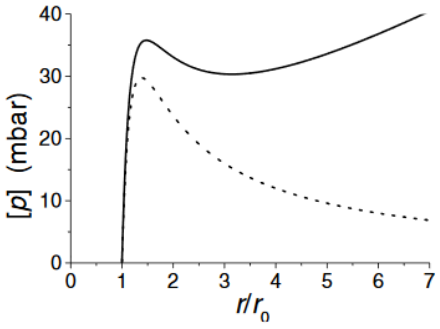

Figure 2.7: Pressure curve of a rubber balloon: Continuous curve - predicted by using the non-linear elasticity model of *Mooney-Rivlin* theory; Dashed curve - predicted by using the kinetic theory of rubber (not considered) [2]

The next section describes the physical assumptions that were considered in order to simplify the balloon's model.

2.3.2 Physical assumptions

- **Balloon's approximate shape:**
  Regarding its shape, the balloon was geometrically approximated to a sphere, in order to simplify volume and pressure calculations.

- **Neglected wind components:**
  In what concerns the wind, no horizontal or vertical components were considered. Forecasting the wind's direction and speed goes way beyond the scope of this master thesis. The main goal is to simulate a way of controlling the balloon's vertical motion, and since the vertical component of the wind is usually neglected, it has no effect on the vertical velocity. Regarding the horizontal components, it is really not important to which way the wind is circulating, what matters is one being capable of placing the balloon at different layers up on the atmosphere. Having considered this, no horizontal motion for the balloon was actually considered throughout the development of this thesis.

- **Neglected temperature transient phenomena:**
  Since balloons move slowly (around 5 m/s [33]) and atmospheric temperature varies slowly as well, it seemed valid to assume they are in constant thermal equilibrium with their neighbouring environment, thus allowing to eliminate the small transient part associated with this phenomena.

- **Perfect deflation:**

  Regarding the balloon's non-linear elasticity, it was assumed an equal pressure curve (like the continuous curve represented in figure 2.7) for the case when the balloon is being deflated. In addition to this, if a balloon is inflated several times, its associated pressure-volume curve will be different each time, as the envelope's material will start to lose its elastic properties, thus affecting the way the balloon deforms. Here, it was assumed the envelope's elastic properties remained constant throughout the entire flight.

- **Ideal gas approximation:**

  As for the case of the chemical reactor, hydrogen was assumed to behave as an ideal gas, thus respecting the ideal gas law represented by:

$$p_b = \rho_{H_2,b} R_{g,H_2} T_b \tag{2.36}$$

  where p_b and T_b represent the balloon's internal pressure and temperature, which is assumed to be equal to the outside temperature, T_{atm}.

Besides all of these approximations, it is known from section 2.2.3 that the hydrogen input mass flow rate is given by equation (2.31). With this being stated, by using equations (2.35) and (2.36), one is still not capable of solving for all the total system unknown variables ($\rho_{H_2,b}, p_b, R_b$) and therefore, a new equation must be found.

2.3.3 Solving for the balloon's altitude and hydrogen output mass flow rate

The balloon system is again represented in figure 2.8.

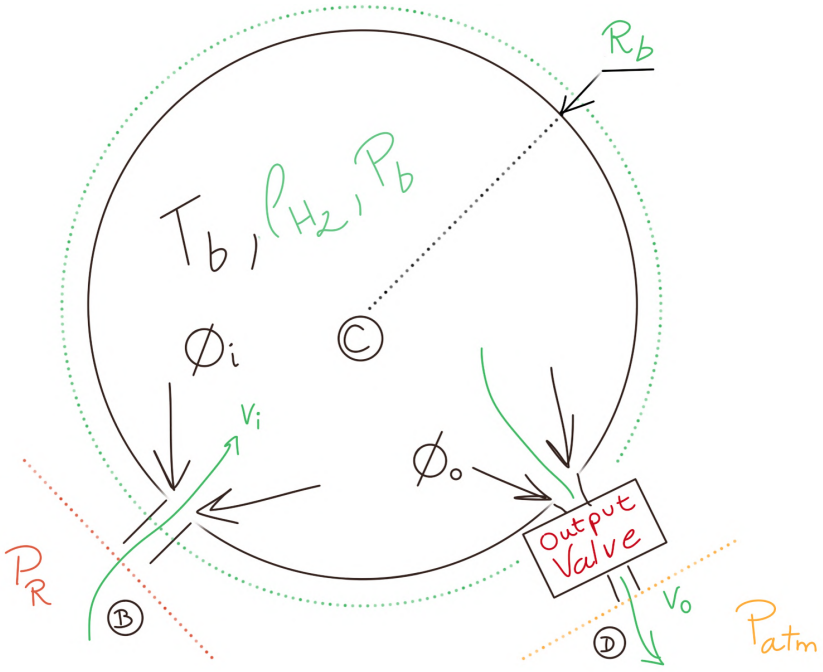

Figure 2.8: Balloon subsystem representation (detailed view)

To obtain the balloon's altitude z_b and the hydrogen output mass flow rate $\dot{m}_{H2,b\rightarrow atm}$, 5 unknown variables need to be discovered (the ones represented by the green color). For this, an additional expression is introduced (the mass balance of the balloon subsystem):

$$\frac{d}{dt}\left(\frac{4\pi R_b^3 \rho_{H_2,b}}{3}\right) = \dot{m}_{H_2,R\rightarrow b} - \rho_{H_2,b}\frac{\pi\phi_o^2}{4}v_o \tag{2.37}$$

where $\rho_{H_2,b}$ represents the density of the hydrogen placed inside the balloon, ϕ_o represents the diameter of the tube connecting the balloon to the atmosphere, v_o is the velocity of the gas exiting this tube and $\dot{m}_{H_2,R\rightarrow b}$ the hydrogen input mass flow rate.

The following algorithm was created to compute the balloon variables for any given instant of time t:

1 - Initialize all the unknown variables for $t = 0$ or start from their known values for time instant t: $\rho_{H_2,b}(t)$, $p_b(t)$, $R_b(t)$, $v_i(t)$, $T_b(t)$ and $v_o(t)$.

2 - Compute $\frac{d}{dt}(R_b^3\rho_{H_2,b})|_{t,t+\Delta t}$ by using equation (2.37):

$$\frac{d}{dt}(R_b^3\rho_{H_2,b})|_{t,t+\Delta t} = \frac{3\dot{m}_{H_2,R\rightarrow b}(t)}{4\pi} - \frac{3\rho_{H_2,b}(t)\frac{\pi\phi_o^2}{4}v_o(t)}{4\pi} \tag{2.38}$$

3 - Compute $R_b(t+\Delta t)^3\rho_{H_2,b}(t+\Delta t)$:

$$R_b(t+\Delta t)^3\rho_{H_2,b}(t+\Delta t) = R_b(t)^3\rho_{H_2,b}(t) + \frac{d}{dt}(R_b^3\rho_{H_2,b})|_{t,t+\Delta t}\Delta t = B(t+\Delta t) \tag{2.39}$$

$$\rho_{H_2,b}(t+\Delta t) = \frac{B(t+\Delta t)}{R_b(t+\Delta t)^3} \tag{2.40}$$

4 - Substitute the result from equation (2.40) into equation (2.36) in order to get an expression for $p_b(t+\Delta t)$:

$$p_b(t+\Delta t) = \frac{B(t+\Delta t)}{R_b(t+\Delta t)^3}R_{g,H_2}T_b(t) \tag{2.41}$$

Note: Unfortunately, $T_b(t+\Delta t) \approx T_{atm}(t+\Delta t)$ is only known after computing the radius of the balloon for the same instant of time. Since this value is still unknown at this point of the algorithm, $T_b(t) \approx T_{atm}(t)$ was used to compute this value. This approximation does not constitute however a huge approximation, as the balloon is assumed to move slowly and due to that, temperature may be assumed constant between two consecutive instants of time.

5 - Substitute $p_b(t+\Delta t)$ into equation (2.35) and solve for $R_b(t+\Delta t)$.

6 - Use equation (2.35) to calculate $p_b(t+\Delta t)$:

$$p_b(t+\Delta t) = p_{atm}(t) + 2s_+\frac{t_e^0}{r_b^0}\left(\frac{r_b^0}{R_b(t+\Delta t)} - \left(\frac{r_b^0}{R_b(t+\Delta t)}\right)^7\right)\left(1 - \frac{s_-}{s_+}\left(\frac{R_b(t+\Delta t)}{r_b^0}\right)^2\right) \tag{2.42}$$

7 - Compute $\rho_{H_2,b}(t+\Delta t)$, by using equation (2.40):

$$\rho_{H_2,b}(t+\Delta t) = \frac{B(t+\Delta t)}{R_b(t+\Delta t)^3} \tag{2.43}$$

8 - Check for the over-pressure $p_R - p_b$ and valve conditions:

- **Natural inflation:**

  If both input and output valves are closed and if $p_R(t) - p_b(t) > 0$, force $v_o(t + \Delta t)$ to be zero and compute the inlet gas velocity by using equation (2.44):

$$v_i(t + \Delta t) = \sqrt{\frac{2(p_R(t + \Delta t) - p_b(t + \Delta t)}{\rho_{H_2,R}(t + \Delta t)}} \tag{2.44}$$

  where $p_R(t + \Delta t)$ is obtained from the reactor subsystem previous equations (section 2.2.3).

- **Balloon's free behaviour:**

  If both input and output valves are closed and $p_R(t) - p_b(t) \leq 0$, force $v_o(t + \Delta t)$ and $v_i(t + \Delta t)$ to be zero.

- **Forced inflation:**

  If the input valve is opened and $p_R(t) - p_b(t) > 0$, force $v_o(t + \Delta t)$ to be zero and compute the inlet gas velocity by using once again equation (2.44).

- **Forced deflation:**

  If the output valve is opened, force $v_i(t + \Delta t)$ to be zero and compute the outlet gas velocity by using the same *Bernoulli* principle, this time applied to a streamline gathering points C and D and by assuming the same approximations that were assumed before:

$$v_o(t + \Delta t) = \sqrt{\frac{2(p_b(t + \Delta t) - p_{atm}(t)}{\rho_{H_2,b}(t + \Delta t)}} \tag{2.45}$$

  The hydrogen output mass flow rate is then compute by using:

$$\dot{m}_{H_2,b \to atm}(t + \Delta t) = \rho_{H_2,b}(t + \Delta t)\frac{\pi \phi_o^2}{4} v_o(t + \Delta t) \tag{2.46}$$

9 - Compute the altitude $z_b(t + \Delta t)$ by using equations (2.32), (2.33) and (2.34) and the new radius of the balloon $R_b(t + \Delta t)$.

When inflating the balloon voluntarily, it is assumed no hydrogen is being released to the atmosphere, which is the same as considering that the balloon is only in contact with the reactor. The same thing happens for the situation at which the balloon is being deflated, i.e., the input valve is automatically closed. Besides these two mechanisms, a third one is required to prevent back-flow of hydrogen towards the reactor. As soon as the pressure difference becomes zero $(p_R - p_b = 0)$, a third valve (or other type of mechanism) will automatically prevent for back-flowing to occur.

The main output of this subsystem, altitude z_b, will then be used as an input for the atmosphere subsystem. This subsystem is presented in the next section.

2.4 Atmosphere subsystem: modelling air pressure, temperature and density throughout the different layers of the atmosphere

2.4.1 Physical introduction

The fourth and last subsystem left to describe is the one related with the earth's atmosphere. Once the balloon is launched, it will reach different atmospheric layers. To obtain the values for the atmospheric pressure, density and temperature, the ISA (International Standard Atmospheric) model was used [34]. The model provides values of air pressure p_{atm} and atmospheric temperature T_{atm} for each specific altitude z_b according to the following equations:

- $z_b < 11000$m

$$\begin{cases} T_{atm} = 288.19 - 0.00649 z_b \\ p_{atm} = 101290 \left(\frac{T_{atm}}{288.08}\right)^{5.25577} \end{cases} \tag{2.47}$$

- $11000\text{m} \leq z_b \leq 25000\text{m}$

$$\begin{cases} T_{atm} = 216.69 \\ p_{atm} = 22650 e^{(1.73 - 0.000157 z_b)} \end{cases} \tag{2.48}$$

- $z_b \geq 25000$m

$$\begin{cases} T_{atm} = 141.94 + 0.00299 z_b \\ p_{atm} = 2488 \left(\frac{T_{atm}}{216.6}\right)^{-11.388} ; \end{cases} \tag{2.49}$$

Once temperature and pressure are known, density might be obtained by using the simple ideal gas law:

$$\rho_{atm} = \frac{p_{atm}}{R_{g,air} T_{atm}} \tag{2.50}$$

where $R_{g,air} = \frac{R_g}{M_{air}}$, being R_g the universal gas constant and M_{air} the approximated air molecular mass.

2.4.2 Physical assumptions

- **Neglected temperature daily variations:**
  This model assumes a constant average daily temperature value for each layer of the atmosphere. In reality, temperatures are higher during the day and lower during the night, nevertheless this fact would affect the complexity of the problem.
- **Constant thermal equilibrium with the balloon:**
  As already mentioned in the previous section, it was assumed that the balloon's temperature was always equal to the atmospheric temperature, which means that $T_b \approx T_{atm}$.

Now that it is almost everything set for the implementation phase, the second part of this thesis is related to its practical part. The next chapter explains all the practical experiments that were made with

the goal of better understanding the way CaH_2 reacts with water to yield great quantities of hydrogen gas. The results were used to improve the quality of the physical model that was developed in this chapter.

Chapter 3

Studying the hydrolysis reaction of calcium hydride

This chapter presents the laboratory experiments that were performed in order to study the hydrolysis reaction of calcium hydride CaH_2.

3.1 Chemical reactor prototype

To study the reaction, one had to find a way to obtain an easily controllable and measurable water flow rate. This would allow one to establish a correspondence between the amount of hydrogen produced and the mass of water added to reactor. The final prototype for the chemical reactor was the one represented in figure 3.1.

As it may be seen, a set composed of a glass syringe body, the input valve, its respective needle, and a fixed mass made of lead metal is responsible for pressuring down the water which is trapped inside the syringe (fig. 3.1(a)). Once actuated (order given by an *Arduino* code command), water droplets will enter the reactor and fall directly over the metal hydride (which is stored inside the chemical reactor) to form hydrogen gas (fig. 3.1(b)). Once formed, temperature and pressure will increase, and the gas will be released through the hydrogen tube (represented in blue in fig. 3.1(a) or in white in fig. 3.1(c)), towards the inverted beaker, in order to be measured (fig. 3.1(c)). A plastic beaker containing an inverted measuring tape was used, filled with water, and placed facing downwards as represented in fig. 3.1. This way, as hydrogen is produced, it will travel through the hydrogen tube, enter the beaker, and since hydrogen is lighter than water, water is forced to leave the tube. Hydrogen gas will settle at the top of the beaker and an equal volume of water will exit the beaker through its bottom towards the water container. For temperature, two thermocouples were placed as represented in fig. 3.1(b) and connected to an external multimeter. The first one was used to measure the core temperature of the reaction (placed inside the reactor, near its core) and the second one was used to measure the temperature of the reactor's surface, in order to find a relation between the two.

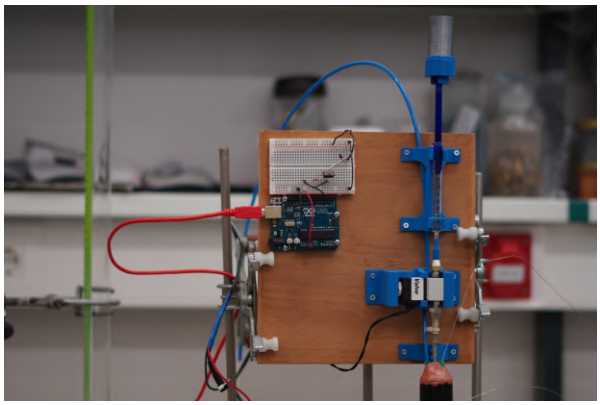

(a) Prototype front view

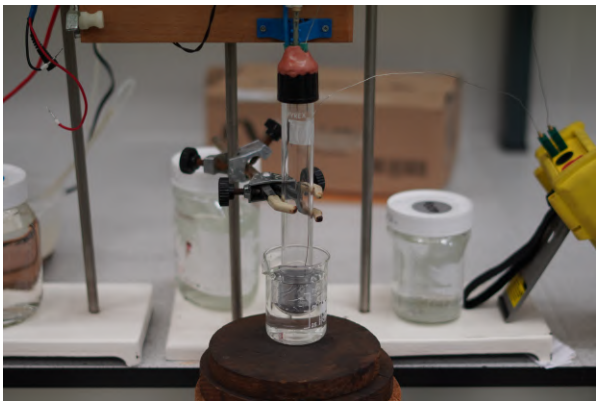

(b) Chemical reactor detailed view

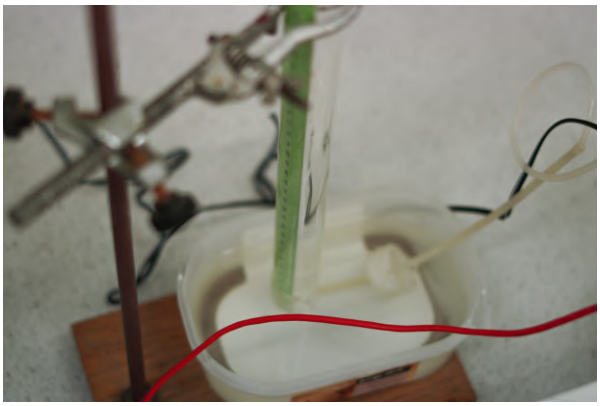

(c) Inverted beaker's entrance

(d) Work station

Figure 3.1: Chemical reactor's prototype

3.2 Prototype development

The prototype represented in fig. 3.1 had a few versions. Most of the time spent in the laboratory was used on trying to improve the installation. In order to reach better results, the following decisions were taken:

1 - **Ensure impermeability and leak-tightness:** To avoid water losses, as represented in fig. 3.2(a), all of the tubes and connections were strongly tightened to guarantee maximum impermeability. In addition to that, at the reactor's entrance (see fig. 3.2(b)), resin and glue were added together, in order to make sure hydrogen could not escape. In this way, one guarantees that, as soon as pressure starts building up, hydrogen may only follow one possible path, the hydrogen tube.

2 - **Ensure uprightness:** To ensure uprightness, the blue plastic parts were modelled, printed and nailed into the wood board represented in fig. 3.2(a) (indicated by the black arrows). Sometimes, to avoid unbalanced situations, a level tool was also used, in order to ensure that the droplets would fall vertically and centered over the hydride.

3 - **Avoid reactor breakage due to chemical heating:** As explained in section 1.3.1, the reaction is highly exothermic, therefore releasing a lot of heat to its surroundings. To prevent the glass from breaking, the reactor was placed inside a bigger beaker containing cold water, thus preventing

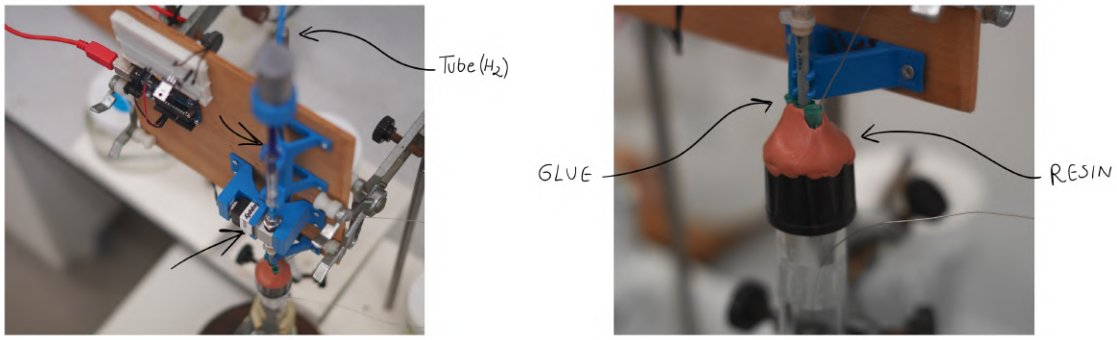

(a) Prototype top view

(b) Chemical reactor's lid

Figure 3.2: Mechanisms to ensure impermeability and leak-tightness

temperature and pressure from building up. Besides that, the reactor was involved with aluminum foil tape, in order to maximize energy losses (see fig. 3.3).

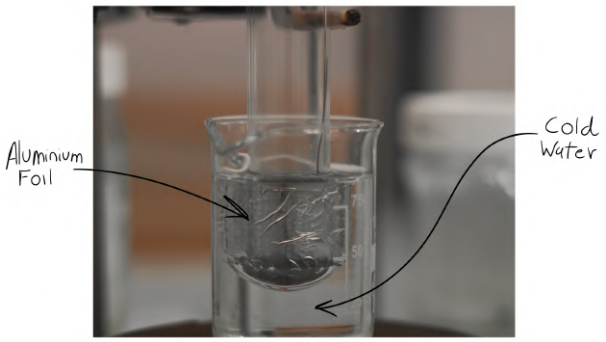

Figure 3.3: System used to avoid over-heating

4 - **Eliminate friction and variable mass problems:** To eliminate the friction factor, thus allowing for small pressures to exert the same effect, a glass syringe with a glass plunger was used to pressure the water towards the reactor. To do so, the system represented in fig. 3.4 was used. A certain lead mass was melted inside an iron mold and a plastic blue part was designed to work as its container. In this way, the vertical force is constant, balanced and enough to achieve a constant water mass flow rate, which is now only dependent on the period of time during which the input valve is being actuated.

3.3 Measuring the water mass flow rate

The system represented in figure 3.1(a) was built with the goal of achieving an easily measurable and controllable water mass flow rate. For this, an *Arduino* code was developed (fig. 3.5(b)) and uploaded to the board represented in fig. 3.5(a).

According to the code, the valve will be actuated and opened during a period of time set by the first

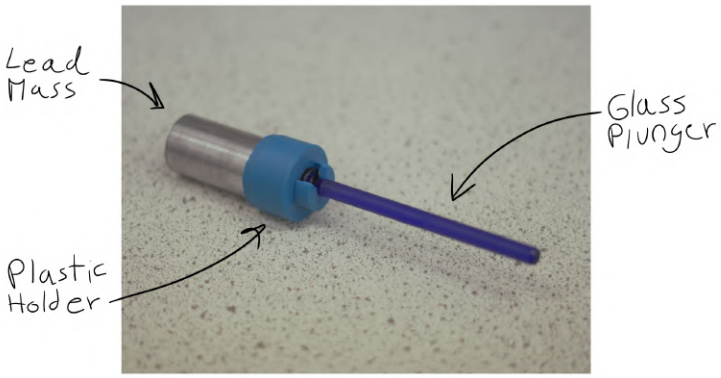

Figure 3.4: Lead mass pressure system

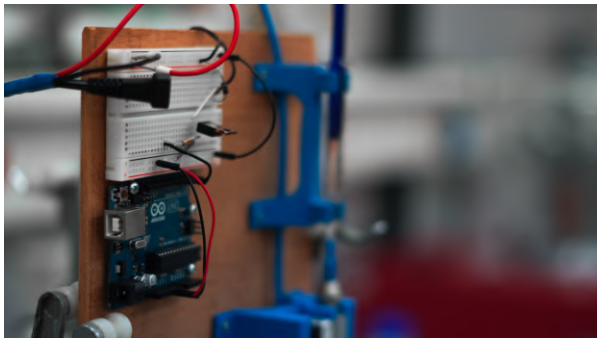

(a) Electrical circuit

```
int solenoidPin = 4;


void setup() {
  pinMode(solenoidPin, OUTPUT);     //Set pin as output
}


void loop() {
  digitalWrite(solenoidPin, HIGH); //Switch Solenoid ON
  delay(25);                       //Wait 25 miliSecond
  digitalWrite(solenoidPin, LOW);  //Switch Solenoid OFF
  delay(20000);                    //Wait 20 Seconds
}
```

(b) *Arduino* code

Figure 3.5: Input valve control

”delay” command (time is introduced in milliseconds). After that period, the valve will close and remain closed for a period of time set by the second ”delay” command. For this reaction, every droplet of water counts, which demanded a proper way to measure the mass of the water being released. For this, it was used a balance with a maximum precision of 0.001 grams (the one represented in figure 3.8). The valve was opened several times during different periods of time and the different mass quantities were read on the balance. Finally, in order to find a relation between the valve actuation time and the amount of water that is being released, the same test was performed multiple times (until the syringe was empty). Figure 3.6 presents the results for the different tests.

In each one of these tests, the glass syringe was filled to its maximum capacity and water was released within intervals of 20 seconds (each point in the curve represents a mass point, measured 20 seconds after the previous point). With these results, two conclusions were taken:

- The water mass flow rate is constant over time. For any of the experiments that were performed, the water mass measured on the balance varied linearly with time (not the actuation time). This allowed to confirm that the friction factor is equally constant for any section of the glass syringe that was selected. The result would certainly be different if one has decided to use a plastic syringe instead.

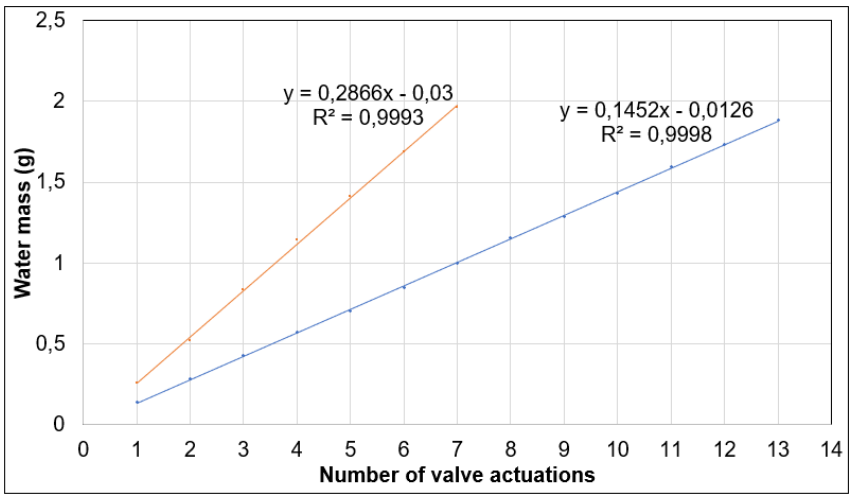

Figure 3.6: Water mass measured on the balance over time [g]: Orange curve ●: Actuation time of 190ms; Blue curve ●: Actuation time of 80ms

.

- The relation between the amount of water and its respective valve actuation time is not linear. By opening the valve during 80ms, an approximately constant mass of 0.145 grams of water was measured on the balance. To achieve the double of the mass (see figure 3.6), one would expect an opening time of 160ms (2 x 80ms). However, it was necessary to increase it to 190ms. Nevertheless, one is dealing with very small quantities of water. A droplet (for this specific needle) weights about 0.026 grams, which means that the difference in linearity was the same as having two or tree more droplets in the reactor than supposed. Still, despite believing this difference could be neglected, before every time a chemical reaction test was performed, first it was ensured that the flow rate was the desired one, by making one or two more tests like the previous two.

3.4 Experimental procedure

Once a viable system to control the amount of water entering the reactor was obtained, the hydrolysis reactions were tested. The experimental procedure was the one described in the following steps:

1 - Fill the inverted beaker with water, and use the clock glass represented in figure 3.7(a) to place the beaker faced downwards inside the water container. Be sure that the tip of the hydrogen tube is placed inside the water container, right underneath the inverted beaker (see figure 3.7(b)).

2 - To fill the syringe with water, remove the wood bases, the cold water beaker and unscrew the bottom part of the reactor (fig. 3.1(d)). Then, grab the cold water beaker, upload the program to the *Arduino* board (actuation time close to 3 seconds and infinite closed time) and while the valve is being actuated, grab the lead mass plastic holder and push the plunger up, in order to fill the syringe with water. After this, wait still in the position, until the valve is completely closed. The closing time is set to infinite in order to allow for the reaction to be prepared.

3 - Place the reactor as represented in figure 3.8 (check if the balance is calibrated and reset it to

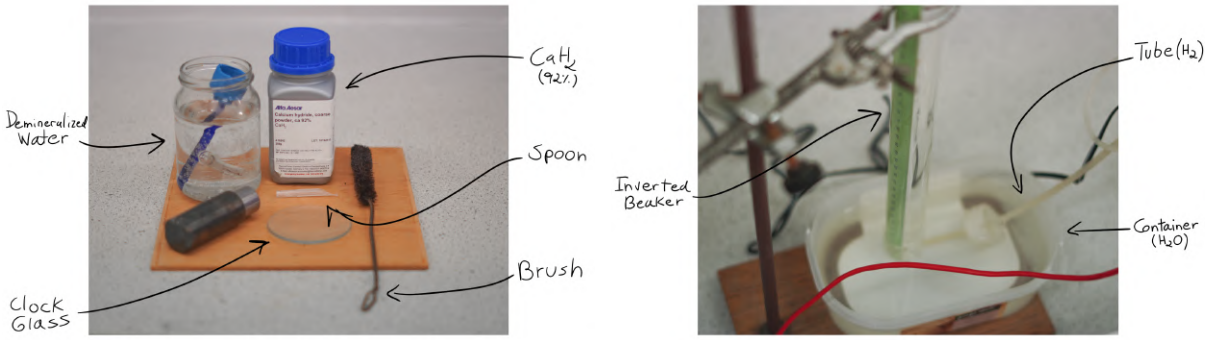

(a) Useful tools

(b) Inverted beaker and hydrogen tube representation

Figure 3.7: Useful tools and inverted beaker's entrance representation

zero), open the CaH_2 bottle (figure 3.7(a)) and pour the desired amount of reactant at the bottom of the reactor, by using the spoon represented in the same figure. Do it quickly and close the bottle, as the reactant is highly pyrophoric, which means it can start to react spontaneously with air, which will affect its purity. After doing this, screw the reactor and place it in a position as represented in figure 3.1(b). After this, fill the beaker once again with cold water (more or less with the same volume of water as before), and place it underneath the reactor together with the wood bases (fig. 3.1(d)).

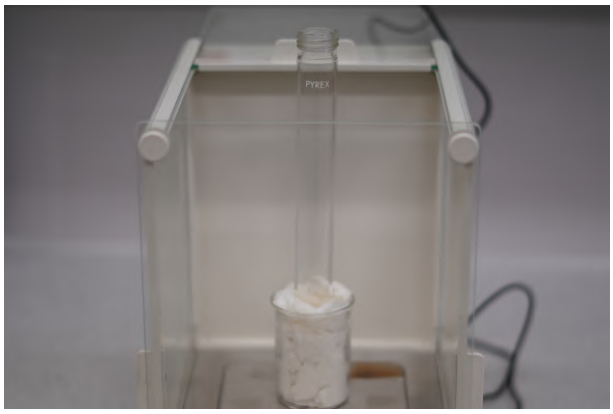

Figure 3.8: Calcium hydride mass measurement system

4 - To measure the temperature, plug in the thermocouples and turn on the multimeter. Before the reaction starts, prepare two cameras: one to record the hydrogen curve (camera pointing towards the inverted beaker) and a second one to record the multimeter screen (camera pointing towards the multimeter).

5 - Finally, to start with the hydrolysis reaction, start recording with both cameras, upload the program (fig. 3.5) to the *Arduino* board (modified to the desired test conditions) and wait until the production is completely finished.

6 - Once the chemical reaction ends, the reactor and its components are full of calcium hydroxide $Ca(OH)_2$, thus making it crucial to take some final precautions:

a - Depending on the amount of water which enters the reactor, the reaction may or may not be complete, thus meaning that a certain amount of CaH_2 might still exist inside the reactor. To avoid dangerous situations, open the valve and let the reaction proceed until no amount of CaH_2 is left to react. After this, remove and clean the reactor by using the test-tube brush represented in figure 3.7(a). Finally, dry it until being sure that no water droplet is left inside the tube, in order to avoid for unwanted chemical reactions to occur.

b - Clean the tips of the needles and thermocouples in order to avoid possible clogging situations for the next time a reaction is performed.

c - Empty the inverted beaker by releasing the hydrogen inside the laboratory exhauster. Despite the small quantities that might be formed, do it inside the laboratory exhauster, as one never knows if this quantity is enough to generate an accident.

d - In the case of leaving for the day, make sure the bottle of CaH_2 is tightly closed, be sure to remove the plunger from the syringe, and save it in a flask containing demineralized water (see figure 3.7(a)). This way of keeping the plunger is crucial to maintain the quality of its sensitive glass surface, as its contact with normal mineral water might ruin its friction-less properties.

3.5 Experimental results

When starting with the hydrolysis reactions, some trials were very useless, as a lot of tests displayed very inconsistent results. Either the system was not tightened enough or another problem was interfering with the repeatability of the process. Most of the time spent in the laboratory was used on trying to improve the prototype consistency and to achieve solid reaction conditions.

After several tries, a few days before the laboratory was closed (due to COVID-19 virus), it was finally possible to achieve some meaningful results. With the goal of quantifying the influence of each one of the reactants in the hydrolysis reaction, the same ideology of the well-known **Initial rates method** was considered: perform several tests in which only one of the initial reactants concentration is varied when compared to the conditions of the previous test. The initial rates method is excellent to assess the kinetic rate of reactions capable of reaching an equilibrium condition. However, for this specific case, it must not be applied, as the reaction does not reach an equilibrium condition and it does not make sense to study concentrations over time. Still, the method allows to extract some positive conclusions and therefore, a similar procedure was considered.

Table 3.1 presents the initial conditions for the first three tests that were performed, where $m^0_{CaH_2}$ corresponds to the initial mass placed inside the reactor and m^0_ω the mass of water added. Regarding $m^0_{[CaH_2]}$, the values are already including the reactant purity ($\approx 92\%$, according to the supplier).

First, the initial mass of CaH_2 was doubled while keeping the same amount of water inside the reactor (1º test $\rightarrow$ 2º test). Then, for an equal mass of calcium hydride, the water initial mass was duplicated (1º test $\rightarrow$ 3º test). The water quantities represented in table 3.1 were added to the reaction in one single shot. The results were the ones represented in figure 3.9.

Table 3.1: Laboratorial "single-shot" tests conditions

Test	$\Delta t_{in,v}$ [ms]	$m^0_{[CaH_2]}$ [g]	$m^0_{H_2O}$ [g]
1	80	0.232	≈ 0.1452
2	80	0.456	≈ 0.1452
3	190	0.225	≈ 0.2866

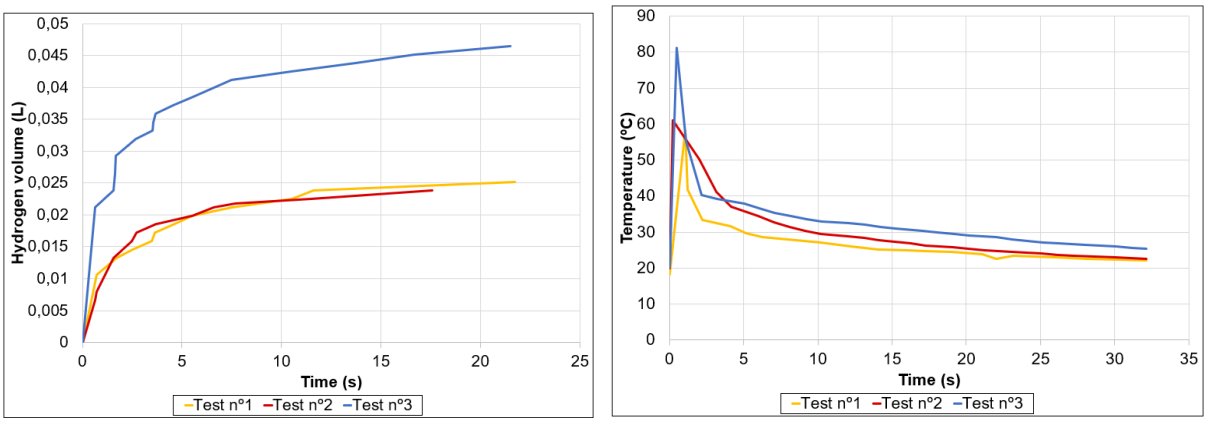

(a) Volume of hydrogen produced (L)

(b) Temperature response (ºC)

Figure 3.9: Hydrolysis results: Yellow curve ●: test nº1; Red curve ●: test nº2; Blue curve ●: test nº3

With these results, the following conclusions were taken:

- By comparing tests nº1 and nº2 (fig. 3.9(a)), one could suggest that the hydrogen curves are almost the same. By doubling the initial concentration of CaH_2 and maintaining the initial amount of water to react, no significant difference between the curves was noticed. This result was expected: since water is the limiting reactant, an increase in the mass of CaH_2 will produce an almost null effect.

- By comparing tests nº1 and nº3, a huge difference in the production of H_2 was noticed. By doubling the initial amount of water, the final hydrogen volume was also duplicated. Once again, this result came to confirm the water reactant as being the main reaction controller. Also, it allows to conclude that the amount of hydrogen produced varies linearly with initial amount of water.

- In what regards the temperature results (fig. 3.9(b)), these turned out to be inconclusive. In test nº3, a double amount of hydrogen was formed (when compared to test nº1 (see fig. 3.9(a))), therefore one was expecting a higher temperature pick. The difference that was noticed might be explained by the laboratory conditions and possible measurement procedures: the outside temperature is always changing; the amount of cold water placed inside the cold water beaker (used to cool down the glass reactor) might have been slightly different for the different reactions (as the beaker needs to be refilled every time a new reaction is about to begin), thus influencing the way heat is transferred to the outside. In addition to this, temperature was measured close but not exactly at the core of the reaction, which certainly affected the maximum temperature value that was registered. Finally, the multimeter might not have enough sampling resolution to capture the initial transient part of the temperature growth. All of these reasons combined with the high energy

dissipation could explain the non-variation observed during the transient regime of the different experiments.

- In addition to the previous conclusions, by looking at the time instants at which the reactions become stable, one might notice that the stoichiometric production ratio was never achieved in any of the three experiments. Take a look at test nº3: 0.225 grams of CaH_2 reacted with approximately 0.286 grams of water (water added in excess) to yield only about 0.05 liters of hydrogen, which represents more or less 25% of the volume that the reaction would theoretically be capable of producing. In addition, water was added in excess. Theoretically, 0.225 grams of CaH_2 require more or less 0.194 grams of water to produce 0.225 liters of hydrogen. To produce this hydrogen quantity, one would need 4 times more water than the amount that was added, which means 5 to 6 times more water than predicted. Despite representing a huge ratio, something like this could be expected, and the main reason for this to be observed could be explained by the bad dissolution properties displayed by the hydroxide that is being formed. As previously stated, $Ca(OH)_2$ presents the very low solubility of around 0.00173 grams in each cubic centimeter of water at 20ºC. Moreover, its solubility decreases for higher temperatures, which might be seen right now as a larger inconvenience, as the hydrolysis reaction is highly exothermic. Due to all of this, it is natural that, for producing the stoichiometric quantity of hydrogen, one will need more or less 5 times more water than theoretically stated. A part of that water is trying to dissolve the hydroxide and remove the protective layer that is being formed and covering the metal hydride.

In order to validate these conclusions, a fourth test was performed. This time, instead of a making a ”single-shot” test, water was added repeatedly on droplets form (like multiple sequential ”single-shot” tests). In the reactor, an initial mass of 0.125 grams of CaH_2 was poured on the test tube and within intervals of 20 seconds, a constant mass quantity of approximately 0.0263 grams of water was added to the mixture. The results were the ones represented in figure 3.10.

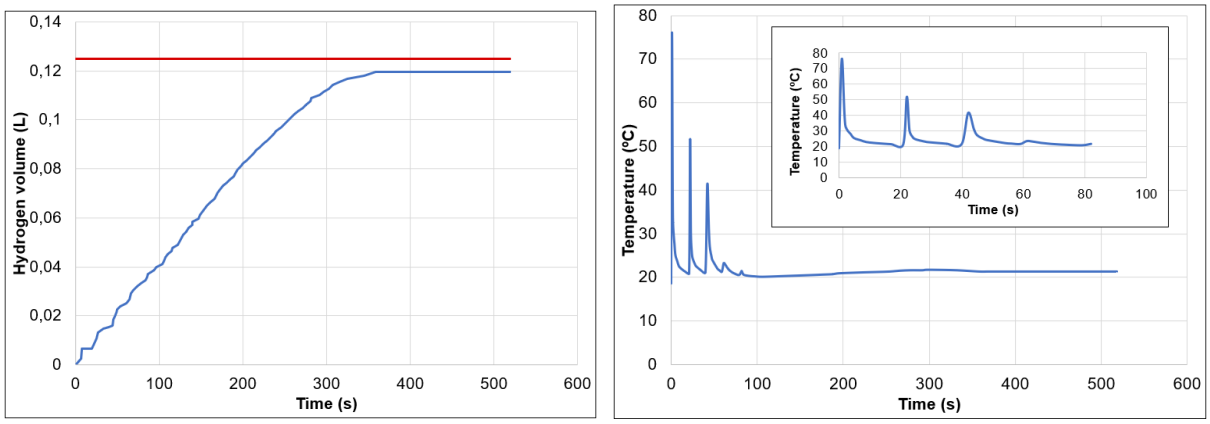

(a) Volume of hydrogen produced (L)

(b) Temperature response (ºC)

Figure 3.10: Hydrolysis results (final test): Red curve ●: theoretical limit for hydrogen production (according to equation (2.16)); Blue curve ●: actual volume of hydrogen produced

With these new results, new conclusions were taken:

- By looking at the results in figure 3.10(a), one was able to conclude that, 4 to 5 times more water was required to achieve the final hydrogen desired production. In this reaction, 0.125 grams of CaH_2 were poured inside the reactor, which theoretically, are capable of producing around 0.125 liters of hydrogen when put together with 0.1075 grams of liquid water. The reaction stabilized at the time instant t = 400s, thus meaning that around 400/20 x 0.0263g = 0.526g of water were necessary (more or less 4 times more water than predicted).

- Despite all of this, after 400 seconds of reaction, by adding more water, no more hydrogen was produced. This fact may be explained by the pyrophoric nature of the reactant and by its level of commercial purity. When pouring the desired amount of chemical hydride inside the chemical reactor, one needs to remove it from the CaH_2 bottle very quickly, in order to prevent irreversible reactions to occur. Nevertheless, as soon as the bottle is opened, CaH_2 will automatically start to react with the water vapor molecules that surround it and the top surface mass left inside the bottle will irreversibly display a lower level of purity for the next time the reactant is extracted. In addition to that, before the reaction starts, while setting the proper conditions for the reaction to occur, a considerable amount of reactant is also irreversibly lost due to the same pyrophoric nature. With these results, a new level of purity was estimated for the reactant (the one computed by using the results of figure 3.10(a)):

$$CaH_{2_{purity}}(\%) \approx \frac{0.11945}{0.125 \times 1.08} \approx 88.48\% \tag{3.1}$$

  where the value 0.11945 corresponds to the actual volume of hydrogen that was obtained and 0.125 x 1.08 corresponds to the hydrogen volume that the reaction would stoichiometrically be able to produce, in case the reactant had a purity of 100%.

- By noticing the temperature measurement graph (fig. 3.10(b)), one might say the results were once again very inconclusive. This is once again explained by the factors that were already mentioned: temperature was not read properly; the multimeter might not have enough sampling resolution to capture the initial temperature growth; laboratory conditions were different for each one of the reactions, etc...

Regarding all of these results, it is important to mention that the external temperature readings were neglected. Given the overall inconclusive temperature measurements, it became useless to record the outside temperature, as no possible relation could be established between the two.

For the implementation, ideally, the rate at which hydrogen is produced should depend on temperature and reactants concentrations, but since temperature was very hard to measure, the approach was different: to define a transfer function for relating the volume of hydrogen produced with the mass of water released, it was considered the curves corresponding to tests nº1 and nº3. Regarding temperature growth, since it was very difficult to estimate the amount of hydride that was actually consumed (because of the amount of hydroxide that was formed), the stoichiometric ratio was considered (equation (2.20)). Furthermore, it was assumed that the amount of water varied linearly with the valve actuation

time, and finally, given the results represented in fig. 3.9(a), the hydrogen volume was also assumed to vary linearly in time with the amount of water.

In the next chapter, a simulator for the entire system is developed and explained in detail.

Chapter 4

Simulator development and respective validation

The final simulator is a highly complex model: it is composed by four different models corresponding to each one of the different subsystems described in section 1.5. Having this in mind, before creating the final assembly, one had to develop computational models for each one of the four subsystems and perform their respective validation. This chapter focuses on the main aspects regarding their implementation. The different models were implemented in *Matlab/Simulink* R2018a. With the idea of using the final simulator as a possible tool for helping the future project generations, most of these subsystems were approximated to their versions of possible laboratory-scaled devices. For example, regarding the syringe subsystem, a syringe with a maximum volume of 10 ml was chosen; for the reactor, a test tube with a geometry similar to the one used in figure 3.1 was considered. When it comes to the balloon, since no practical experiment was performed in the laboratory (due the appearance of COVID-19 virus), a specific type of weather latex balloons was selected for the balloon's subsystem model implementation (introduced later in this chapter). Depending on the size and geometric properties that are considered for each one of the syringe and reactor subsystems, the final results may or may not be close to the reality: when selecting a weather balloon from the market, a maximum value for the payload mass is normally recommended. For this specific case, a percentage of that mass is necessarily saved for calcium hydride and water, and the higher their values, the more hydrogen is stored and available for lift promoting. It may not make sense to elevate a balloon to an altitude of 20 Km and bring reactant quantities which will only allow for really small altitude variations to occur. The problem is that, in the laboratory, the tests were performed inside a specific-sized reactor, and so therefore, for the implementation of the reactor's model, it made sense to assume the reactor would have the same size and geometric features as the ones of the reactor used during the practical experiments. In addition to this, due the appearance of the virus, there was not enough time to measure and estimate the mass of the rest of the payload components. Given these two main reasons, laboratory scaled-devices were considered for the implementation of the syringe and reactor models, but when it comes to the balloon, a balloon with maximum diameter of 3 m was selected for the implementation. Regarding the **sampling times** that were selected, as the

velocity at which a particular subsystem responds is greatly dependent on the parameters that are chosen (spring stiffness k, spring's natural length L_{spring}, reactor's dimensions, etc...), an iterative analysis for the sampling time convergence was performed every time the parameters were changed.

4.1 Syringe model

Figure 4.1 represents the simulator that was developed for the syringe subsystem.

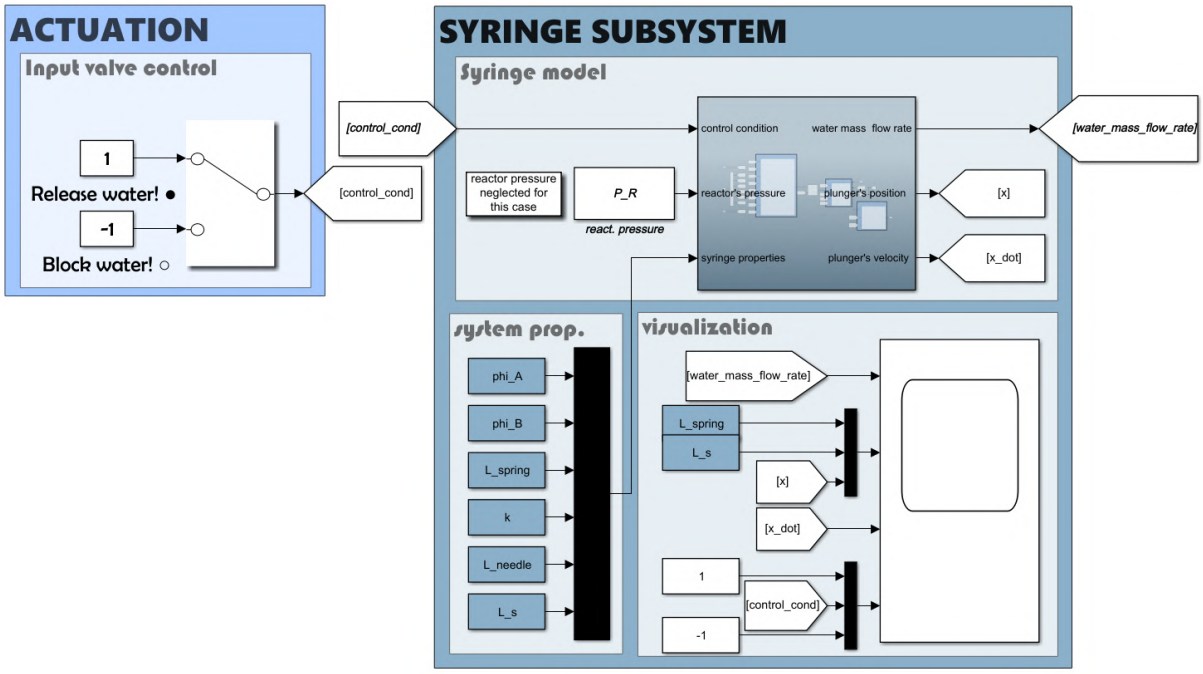

Figure 4.1: Syringe model implementation

This system outputs a certain amount of water per second $\dot{m}_\omega$ ("water_mass_flow_rate") as a function of the input valve signal condition it receives ("control_cond"). Besides that, the system also receives a set of constant parameters: these are represented in the block ("system prop.") and they correspond to the plunger's diameter ϕ_A ("phi_A"), the needle's diameter ϕ_B ("phi_B"), the spring's length L_{spring} ("L_spring"), the syringe's length $L_{syringe}$ ("L_s"), the needle's length L_{needle} ("L_needle"), and the spring's stiffness constant k ("k"). Depending on the type of syringe that is chosen, most of these parameters are known, but some of them remain to be determined. Finally, depending on the location of the syringe's subsystem (recall section 2.1.2), the amount of water exiting through the needle of the syringe might be strongly dependent on the value of the outside pressure (reactor's pressure) p_R ("P_R") therefore, this parameter was also considered as a model input (despite being neglected for the validation tests, which is the same as considering that the syringe subsystem is placed inside the reactor). The "Syringe model" block may be seen in more detail in figure 4.2.

Regarding the implementation of this subsystem, it was necessary to ensure that, as soon as the valve is closed or the plunger reaches its final position (delineated by the syringe's physical limits or the spring's elastic physical constraints), the plunger's velocity and acceleration are zero. To ensure this,

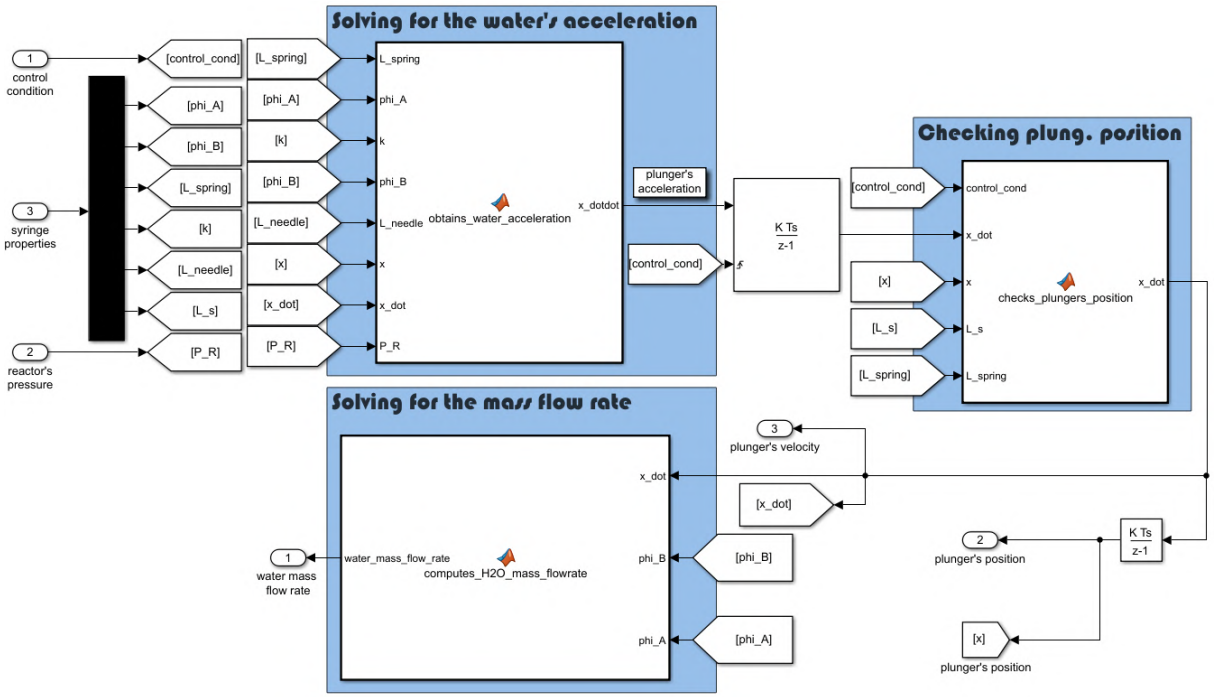

Figure 4.2: Syringe model block

the variable ”control_cond” was used to reset the first integrator's initial condition every time the same variable was increased (see fig.4.2). Regarding the three *Matlab* blocks that are presented, the first one, ”Solving for the water's acceleration” was created to solve the equation (2.14). The second one, ”Checking plung. position”, verifies if the plunger has reached or not the physical limit of the system. Finally, the last one, ”Solving for the mass flow rate”, computes the water mass flow rate $\dot{m}_\omega$ (the main output of the system) by applying continuity (equation (2.15)).

4.1.1 Special considerations regarding the syringe model implementation

In order to simplify and validate only the results corresponding to this particular subsystem, regarding the **reactor internal pressure** p_R (”P_R”), a random value was assumed and its effect was neglected which is the same as considering that the syringe is placed inside the reactor. In addition to this, for each one of the other constant simulation parameters, plausible prototype values were considered. Their values were chosen as if in the laboratory one would use a normal syringe with capacity up to 10 ml. This would later allow one to conclude about the validity of this model's behaviour by comparing it with the behaviour it would display at the laboratory.

For the **spring's stiffness constant** k, the value of 20 N/m was chosen. Nevertheless, this value should be obtained experimentally by making a simple tension test to the compressible spring element that would eventually be purchased and used for the real prototype. This situation represents one of the few examples where the model might work as a tool to determine its input parameters, as choosing a spring for the final prototype might not be a very intuitive task.

In what regards the **spring's length** L_{spring}, this value was varied multiple times in order to check

for the model's physical meaning. For the final simulator, the spring's natural length was assumed to be equal to the length of the syringe $L_{syringe}$.

Finally, for computing the water's mass flow rate and solving equation (2.14), one has considered a **dynamic viscosity** μ_ω equal to 10^{-3} Pa.s and a **water density** ρ_ω equal to 1000 Kg/m^3, defined inside their respective function blocks. All the parameters are resumed in table 4.1.

Table 4.1: Syringe model parameters

Geometric properties		**Fluid properties**		**System inputs**	
ϕ_A [m]:	0.0146	μ_ω [Pa.s]:	10^{-3}	p_R [Pa]:	101493
ϕ_B [m]:	0.0007	ρ_ω [Kg/m^3]:	1000		
L_{needle} [m]:	0.025				
$L_{syringe}$ [m]:	0.06				
k [N/m]:	20				

Regarding the sampling time, its value was reduced until its decrease would stop affecting the dynamics of the system's response. Of course that this response is greatly influenced by the constant parameters that are chosen, mainly the one associated with the spring, the stiffness constant k. For a fixed $k = 20$ N/m , the final **sampling time** for the isolated syringe subsystem model was $\delta_t = 0.001$s. Furthermore, it was noticed that the valve used in the prototype (already purchased at the beginning of the thesis) could not be actuated for periods smaller than this (due to mechanical restrictions). If a smaller sampling time was required, some restrictions would have to be applied to the variable "control_cond".

In the next section, the results are represented for each one of the validation tests that were performed.

4.1.2 Syringe model validation

The results for this subsystem's validation tests depend a lot on the parameters that were chosen for the model and to start the simulation. For each one of these, the values that were considered were the ones represented in table 4.1 and the only one that was changed was the one referring to the spring's length L_{spring}. Tab. 4.2 presents the values that were assumed for this variable.

Table 4.2: Syringe model test conditions

Test	L_{spring} [m]	$L_{syringe}$ [m]
1	0.1	0.06
2	0.04	0.06

- **Test 1:** $L_{spring} > L_{syringe}$

  When $L_{spring} > L_{syringe}$, the total amount of water that is placed inside the syringe will be completely released before the spring reaches its natural length L_{spring}. The plunger will reach its final position before the spring's elastic limit is achieved. As represented in figure 4.3, once the valve

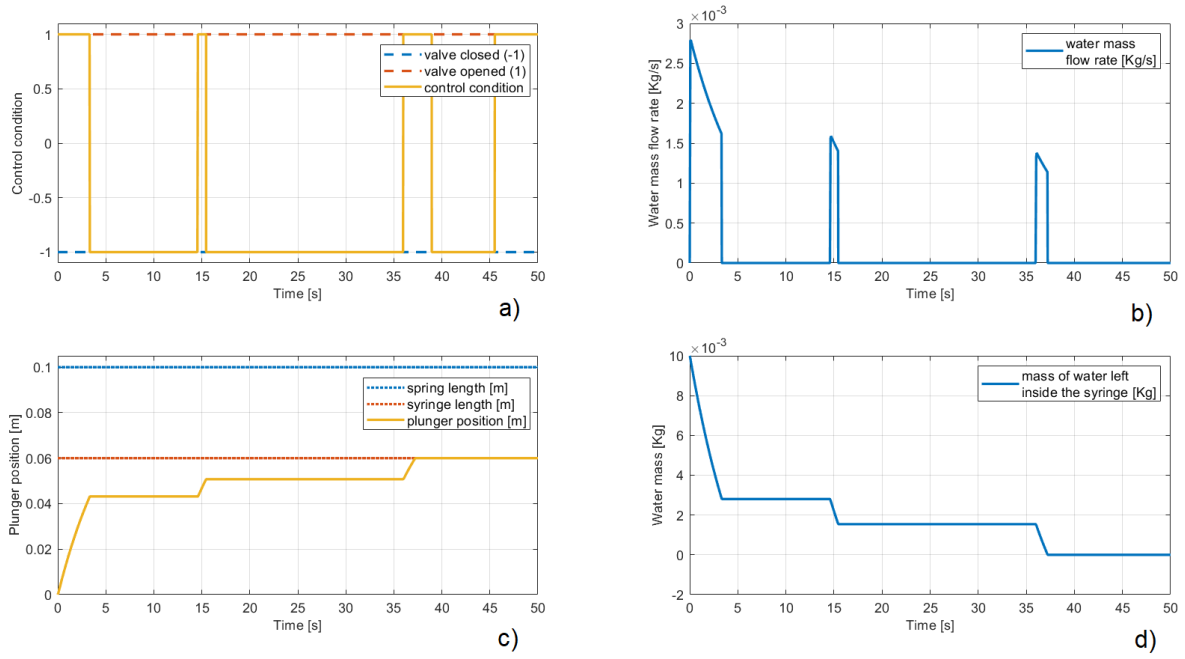

Figure 4.3: Syringe model validation (test nº1): a) control condition; b) water mass flow rate $\dot{m}_\omega$ [Kg/s]; c) plunger's position x [m]; d) mass of water left inside the syringe m_ω [Kg]

is actuated (fig. 4.3(a)), the water mass flow rate will increase from zero to a value dependent on the spring's remaining elastic force (fig. 4.3(b)). The results show that the water mass flow rate decreases with time, as every time the valve is actuated, less elastic force is exerted by the spring. As expected, the spring's elastic limit was never achieved: at t $\approx$ 36s, the valve was opened, and the water flow rate has increased once again, but only until the situation at which the syringe limit was reached. This may be observed in figure 4.3(c). Finally, as it may be seen in fig. 4.3(d), the initial 10 g of liquid water were totally released. The model did exactly what it was meant to do.

- **Test 2:** $L_{spring} < L_{syringe}$

  When $L_{spring} < L_{syringe}$, one expects the plunger to never reach the bottom of the syringe. The new final plunger's position will be determined by the spring's natural length. This may be observed in fig. 4.4(c). As it happened for the first test, during the actuation periods, the water flow rate also decreased over time (fig. 4.4(a) and fig. 4.4(b)). Finally, since the plunger did not reach the syringe's bottom, a certain mass was left inside it. This is demonstrated in fig. 4.4(d).

This system response depends a lot on the spring's elastic stiffness k and length L_{spring}. The higher the value of k, the faster the plunger will be moved. Regarding the value of L_{spring}, the higher this value, the less variation in the water flow rate will be noticed (for this syringe's case). With a higher length, one has the possibility to achieve a more constant water flow rate. Nevertheless, this comes with a cost, as larger springs will require more prototype space, thus ruining the total system's compactness.

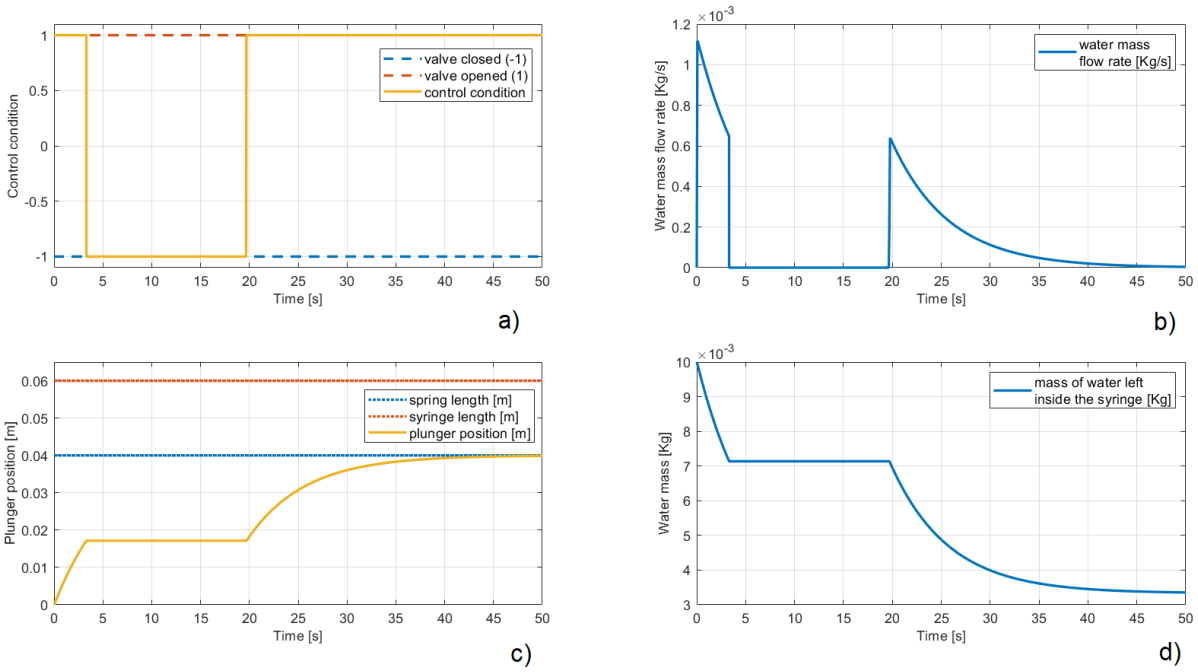

Figure 4.4: Syringe model validation (test n°2): a) control condition; b) water mass flow rate $\dot{m}_\omega$ [Kg/s]; c) plunger's position x [m]; d) mass of water left inside the syringe m_ω [Kg]

4.2 Chemical reaction parameterization

Before implementing the reactor's model, one had to find an expression to relate the amount of hydrogen that is being produced with the mass of water that is being added for a certain period of time. For this, the laboratorial curves that were obtained during the experimental part of this thesis were once again considered for this part of the analysis (see section 3.5).

By considering the experimental curves corresponding to the first three different hydrolise tests (see figure 3.9), one knows that these curves were obtained for a constant water mass flow rate rectangular pulse type of input signal. The difference obtained between the three different responses was just a direct and approximately linear consequence of the duration of the pulse.

Since the lead mass was constant for all the practical experiments (remember the system represented in figures 3.1 and 3.4), the pressure responsible for pushing the water into the reactor was also constant and thus its respective water mass flow rate. This means that, instead of representing unit step water mass responses, all of those curves describe the way the system behaves when subjected to a different type of input signals: water mass ramp signal inputs. The same curve (test n°3) was used to extract a proper transfer function, which would be able to describe a relation between the water mass flow rate $\dot{m}_\omega$ and the volume of hydrogen produced $V_{H_2,gen}$. By looking at the curve (again represented in figure 4.5), one could assume it represents a typical step response for a first order linear system, which in fact is not entirely true. While the valve is being actuated, the hydrogen's production time derivative, despite not possible to be captured (taking into account the laboratory conditions), will increase to a certain value and decrease right after the valve is closed, which means that the system will be of second order or higher. To find an accurate higher order approximation for this part of the implementation,

the matlab systems identification toolbox *"ident"* was used for the task. Basically, the laboratorial curve corresponding to the test nº3 was imported into the software's workspace along with its respective input signal and multiple combinations of transfer functions with different number of poles and zeros were experimented. The best results were found to be the ones for the case of a fourth order system containing 4 poles and 3 zeros (see figure 4.5). The transfer function for this system is represented in equation (4.1).

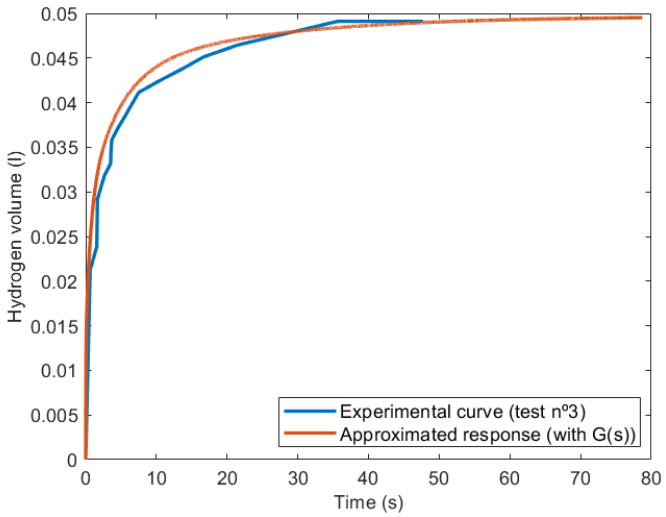

Figure 4.5: Volume of hydrogen produced $V_{H_2,gen}$ for a rectangular pulse input with an amplitude of 1.7875 g/s of water and a pulse duration of 160ms: Blue curve ●: volume of hydrogen produced in test nº3 (fig. 3.9(a)); Orange curve ●: volume of hydrogen produced by the system with a transfer function defined by G(s)

$$G(s) = \frac{50.1218s^3 + 115.6012s^2 + 24.7381s + 0.6803}{s^4 + 1.0931s^3 + 0.1636s^2 + 0.0039s} \tag{4.1}$$

After doing this, it was built the simulink model represented in figure 4.6, in order to simulate the laboratory conditions and compute the volume of hydrogen produced $V_{H_2,gen}$.

In figure 4.6, the block "lead mass system model" replicates the laboratorial conditions corresponding to the test nº3. Fig. 4.7 presents the block in more detail. In test nº3, 0.286g of water fell into the reactor during an actuation period of 0.160s. Since pressure was always the same (given the lead-mass system), as already explained, the water mass flow rate was constant and approximately equal to 1.7875 $\times 10^{-3}$ Kg/s (fig. 4.7). By running the model as represented in figure 4.6, the results were the ones represented in figure 4.8. Regarding the **sampling time**, the same value was used as for the previous case ($\delta_t = 0.001$s).

The results show that the model is well implemented. As expected, a total mass of 0.286g of water were released until the valve was closed (t = 0.160ms) (fig. 4.8(a)), and the final volume of hydrogen produced inside the reactor was 0.05 liters (fig. 4.8(b)), which is the same amount that was produced in test nº3.

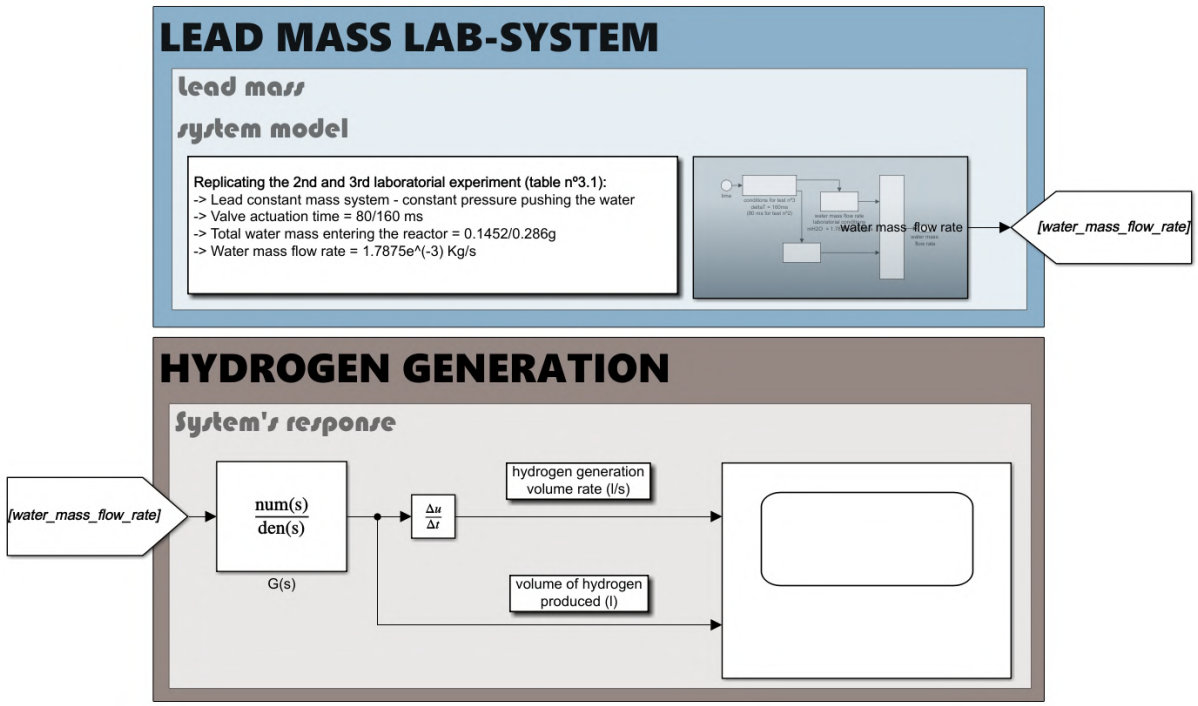

Figure 4.6: Model developed to simulate the hydrolysis tests

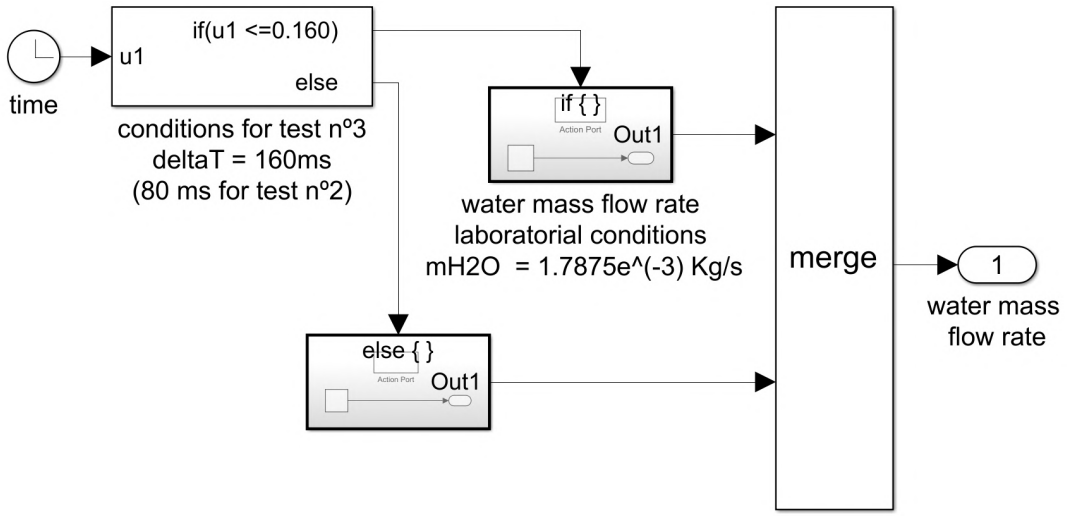

Figure 4.7: Lead mass system model block

4.3 Reactor model

Figure 4.9 represents the simulator for the reactor subsystem.

The reactor subsystem will output a certain hydrogen mass flow rate $\dot{m}_{H_2,R\rightarrow b}$ (”m_dot_H2_R_b”) and the mass of hydride that is left to react m_{CaH_2} (”m_CaH2”) as a function of the hydrogen volume generation rate $\dot{V}_{H_2,gen}$ (”hydrogen_gen_vol_rate”), the balloon’s pressure p_b (”p_b”), the input valve condition (”control_cond”) and a set of constant parameters (as for the case of the syringe subsystem): the thermal conductivity k_{glass} and thickness of the glass wall t_{glass} (”k_material” and ”t_material”), the outside mean temperature T_{out} (”T_outside”), the convection coefficient h (”h”), the internal radius r_i and length of the

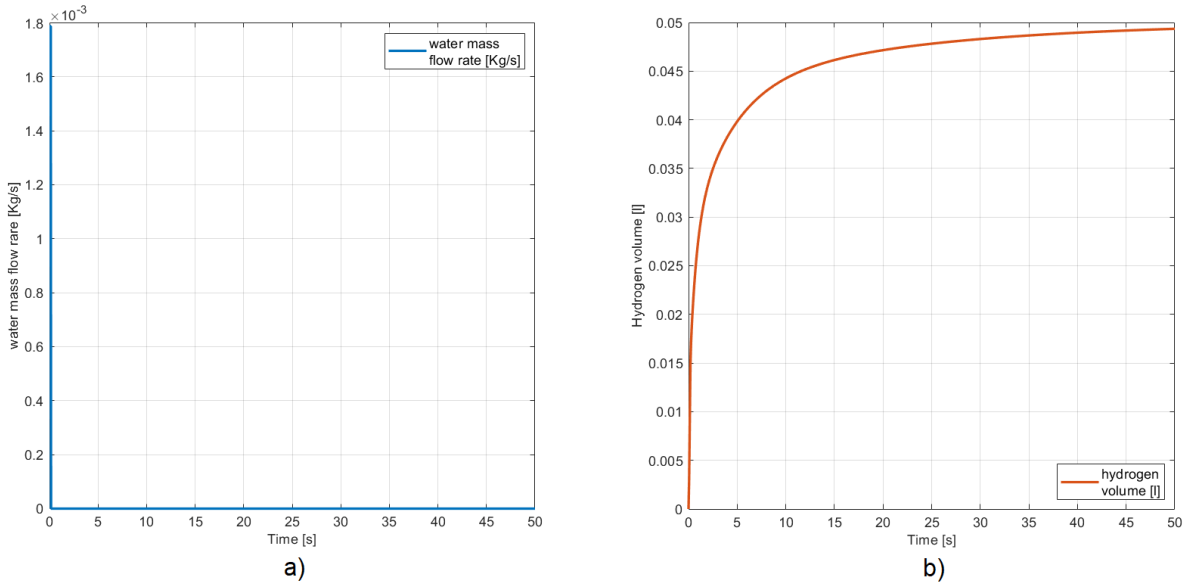

Figure 4.8: Replication of test nº3 (section 3.5): a) water mass flow rate $\dot{m}_\omega$ [Kg/s]; b) volume of hydrogen produced $V_{H_2,gen}$ [L]

.

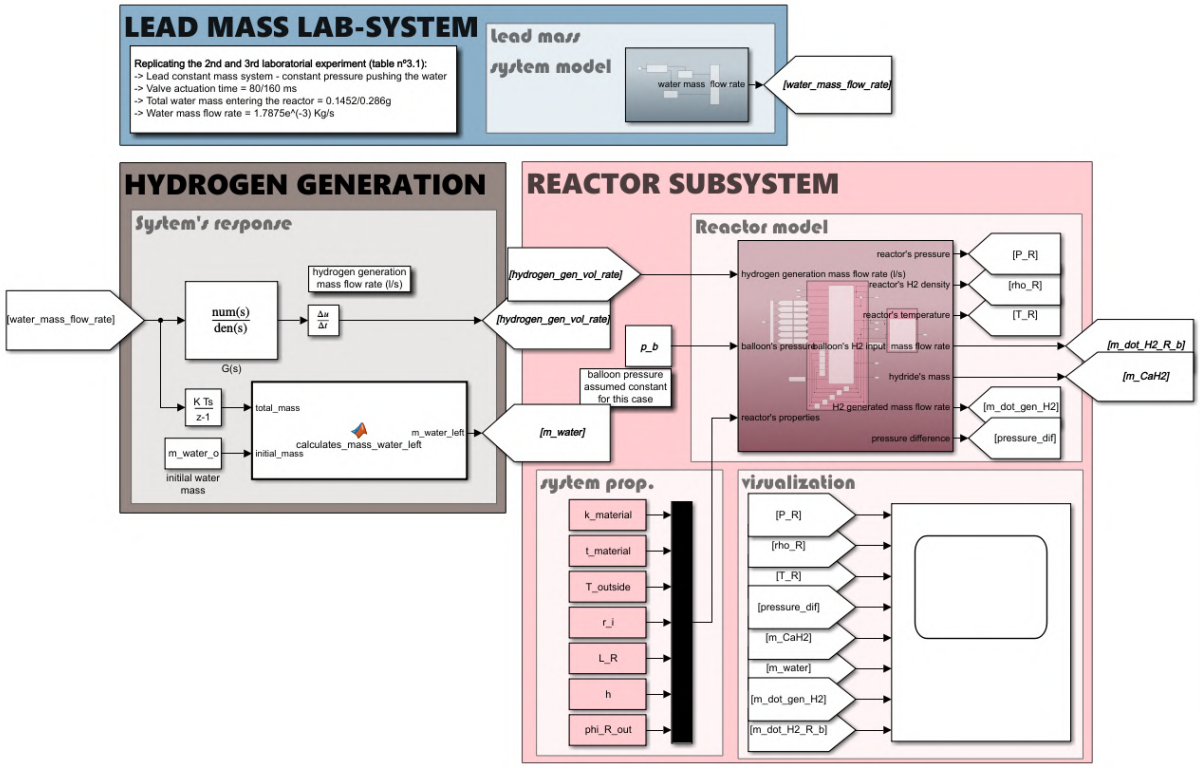

Figure 4.9: Reactor model implementation

reactor L_R (”r_i” and ”L_R”) and the diameter of the connection tube between the balloon and the reactor ϕ_i (”phi_R_out”). Regarding hydrogen generation, the previous model was changed in order to account for the change of water's mass inside the syringe m_ω (”m_water”) (block ”System's response”, function ”calculates mass water left”). The ”Reactor model” block may be seen in more detail in figure 4.10.

The block represented on the left, ”Solving for the reactor variables”, was built to run the algorithm

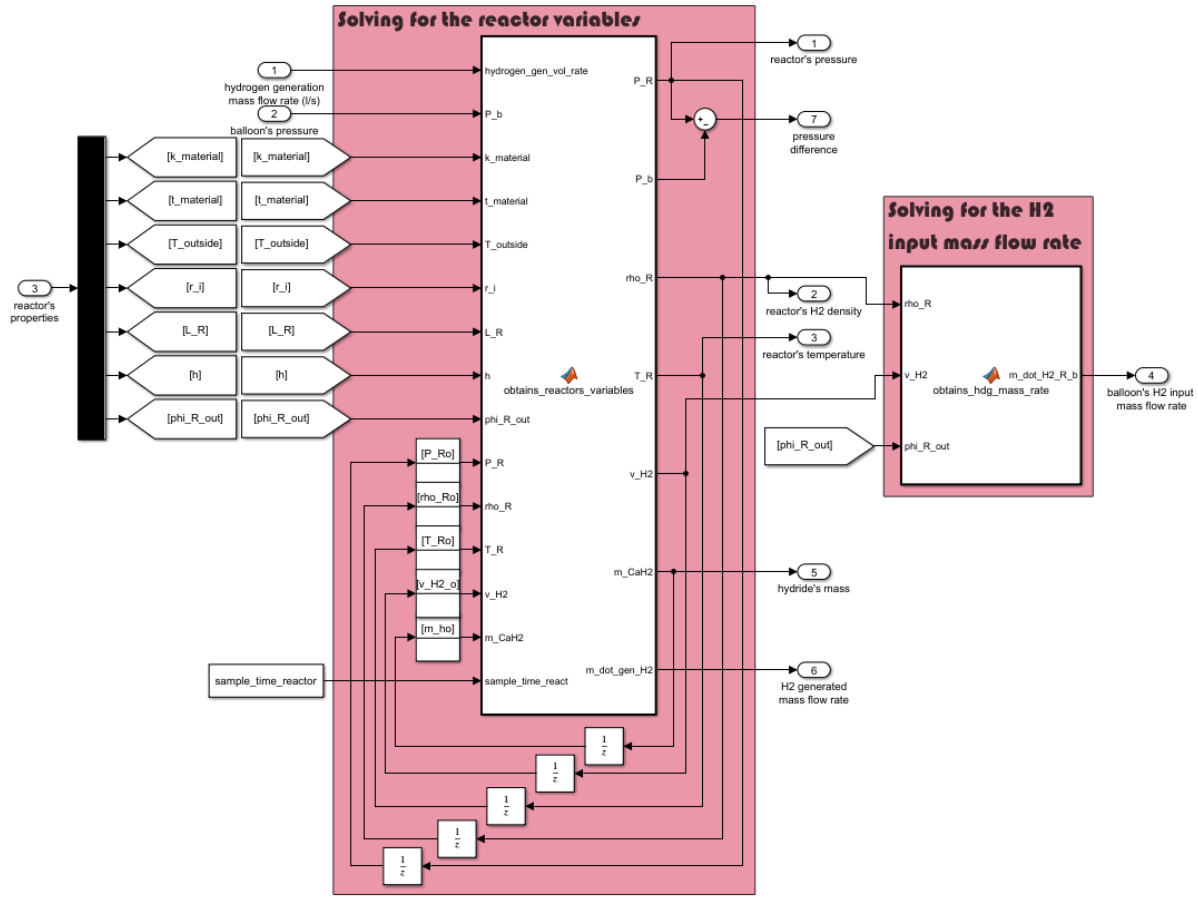

Figure 4.10: Reactor model block

represented in section 2.2.3. The block represented on the right serves to compute the main output of the system (the hydrogen input mass flow rate, $\dot{m}_{H_2,R\rightarrow b}$).

4.3.1 Special considerations regarding the reactor model implementation

Regarding its multiple inputs, in order to only evaluate and validate the behaviour of this subsystem in particular, some variables were considered constant and other assumptions were made.

In what concerns the **balloon's pressure** p_b, this value was considered constant and equal to the atmospheric pressure at sea level ($p_b = 101493$ Pa), according to the ISA model. Regarding its physical properties, a **thermal conductivity** k_{glass} for the glass wall of 0.67 W/(m.K) was considered. For the convection part, a **convection coefficient** h of 100 W/(m^{2}K) was adopted (liquid water environment) and the **outside temperature** T_{out} was assumed to be constant and equal to 288.19 K. In what concerns the reactor geometrical properties, the reactor was considered to have a cylindrical shape with a **wall thickness** t_{glass} equal to 2 mm, an **internal radius** r_i of 0.015 m, a cylindrical **length** L_R of 15 cm, and a hole for the connection tube located between the balloon and the reactor with an **internal tube diameter** ϕ_i of 1 mm. Regarding other parameters, these were assumed to be fixed and defined inside their respective *Matlab* functions: for the **hydrogen's heat capacity** Cp_{H_2}, as explained in section 2.2.2, the value of 14.5 J/(Kg.K) was considered; on what concerns the **entalphy of reaction** H_R, this value

was assumed to be known and equal to its theoretical value, 183 KJ/(mol$_{[CaH_2]}$) and finally, for the volume-mass conversions, a **molar volume** V_M of 22.4 dm^3/mol was considered for the calculations (this is a significant approximation, as this value is only approximately true for normal pressure and temperature conditions [PTN]). The parameters are resumed in table 4.3.

Table 4.3: Reactor model parameters

System inputs		**Physical properties**		**Geometric properties**		**Other parameters**	
p_b [Pa]:	101493	k_{glass} [W/(m.K)]:	0.67	r_i [m]:	0.015	Cp_{H_2} [J/(Kg.K)]:	14.5
		h [W/(m^2.K)]:	100	L_R [m]:	0.15	H_R [KJ/mol$_{[CaH_2]}$]:	183
		T_{out} [K]:	288.19	ϕ_i [m]:	0.001	V_M [dm^3/mol]:	22.4
				t_{glass} [m]:	0.002		

In what concerns the **sampling time**, after making several tests, it was noticed that the system's truthful dynamics could only be totally captured when using a sample time $\delta_t = 0.00001$s. Despite being extremely small, this value is justified by the fact that the reactor's subsystem displays a really fast response, which was also noticed during the multiple laboratory experiments (recall section 3.5).

4.3.2 Reactor model validation

Test nº3 was simulated to validate this system (see section 3.5). Table 4.4 presents the initial conditions for the simulation, where T_R^0, p_R^0, ρ_R^0, v_i^0, m_ω^0 and $m_{[CaH_2]}^0$ are the initial reactor's temperature, pressure and hydrogen density, initial hydrogen input velocity and initial hydride's and liquid water masses, respectively. The results are represented in figure 4.11.

Table 4.4: Reactor test initial conditions

Reactor test initial conditions	
T_R^0 [K]:	288.19
p_R^0 [Pa]:	101493
$\rho_{H_2,R}^0$ [Kg/m^3]:	0.0847
v_i^0 [m/s]:	0
m_ω^0 [Kg]:	0.01
$m_{[CaH_2]}^0$ [Kg]:	0.0025

The results show the model is well implemented (having in mind the approximations that were considered). Regarding the initial conditions (table 4.4), by assuming an initial reactor's density $\rho_{H_2,R}^0$ equal to 0.0847 Kg/m^3 (fig. 4.11(d)), one is considering that, at the beginning of the simulation, a certain amount of hydrogen is already stored inside the reactor. Until the valve is actuated, this mass of hydrogen gas will remain inside the reactor at normal temperature and pressure conditions, as the reactor and balloon pressures are equal, thus not allowing for this initial amount to escape. The model represented in figure 4.9 was designed to start with a valve actuation period of 0.160s (to replicate the conditions of test nº3). During this period, approximately 0.286 g of water were mixed with an initial mass of 2.5 g of CaH_2, in order to start with the hydrolysis reaction. As soon as the water is released, pressure will increase,

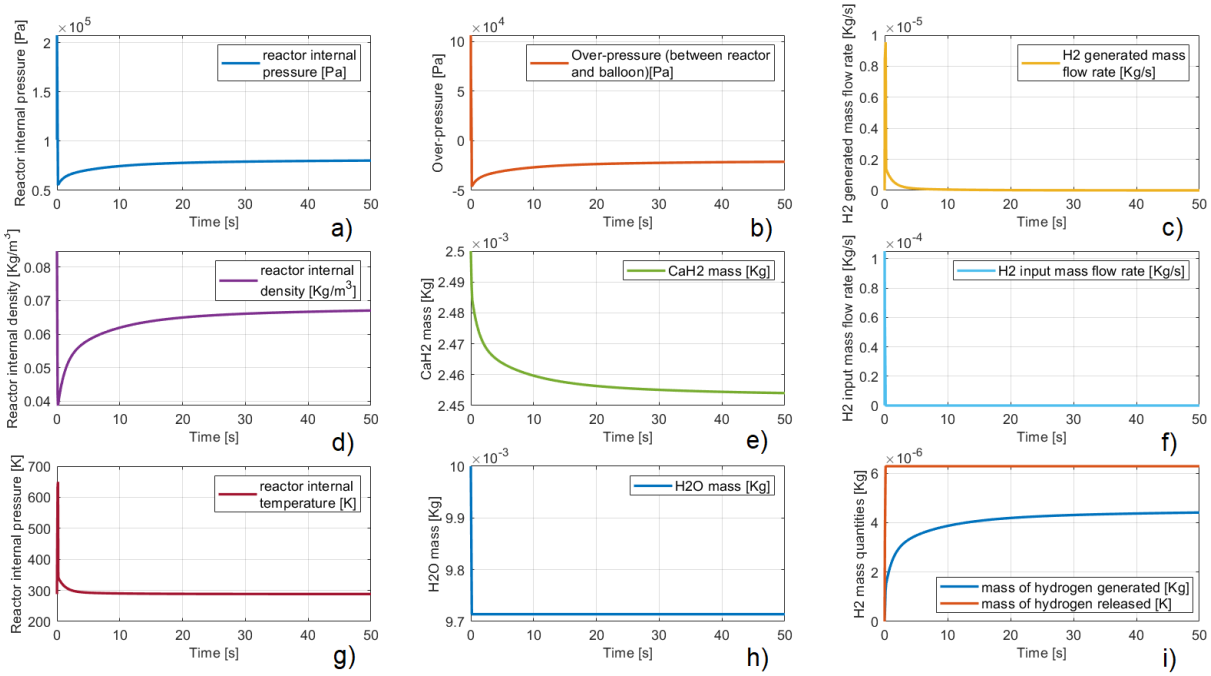

Figure 4.11: Reactor model validation (replication of test n°3): a) reactor's internal pressure p_R [Pa]; b) over-pressure $p_R - p_b$ [Pa]; c) hydrogen generated mass flow rate $\dot{m}_{H_2,gen}$ [Kg/s]; d) reactor's internal density $\rho_{H_2,R}$ [Kg/m^3]; e) mass of hydride inside the reactor $m_{[CaH_2]}$ [Kg]; f) hydrogen input mass flow rate $\dot{m}_{H_2,R\rightarrow b}$ [Kg/s]; g) reactor's internal temperature T_R [K]; h) mass of water left inside the syringe m_ω [Kg]; i) hydrogen generated and released mass quantities $m_{H_2,gen}$ and $m_{H_2,R\rightarrow b}$ [Kg]

and since the reactor already contains an initial amount of hydrogen gas, density will drop abruptly, thus causing pressure to decrease (fig. 4.11(a)). At the same time, temperature has increased to 650 K (an increase of approximately 350°C). One would say this value is extremely high when compared to the one obtained for the laboratorial tests, however, one must consider all the measuring errors that were committed and the sampling resolutions of all the instruments that were used in the laboratory: temperature was not measured at the core of the reaction; the multimeter used to record the temperature values had a shorter sampling resolution than desired. All of these factors combined with the approximations that were assumed (recall equation (2.20)) make the comparison between the simulation and laboratory results more challenging. This abrupt change in the reactor's temperature may actually be high, however, one would need different laboratory conditions to assess its validity. Regarding the mass of the reactants, 0.286g of water were used (fig. 4.11(h)) but only 0.05 g of CaH_2 were consumed (fig. 4.11(e)), which represents approximately 5 to 6 times less mass than theoretically stated (stoichiometrically, 1 gram of water reacts with 1 gram of CaH_2, approximately). This result is explained by the approximations that were considered (recall equation (2.20) and section 2.2.2). Finally, as explained in section 2.2.2, as long as the pressure in the reactor is kept higher than the pressure in the balloon, hydrogen will escape from the reactor. This might be observed in figures 4.11(c) and 4.11(f): despite hydrogen is still being produced, because of the nonexistent or negative differential pressure (fig. 4.11(b)), only a small portion of hydrogen gas enters the balloon. Fig. 4.11(i) presents the mass of hydrogen generated and the mass of hydrogen that was released to the balloon. The amount of hydrogen that was kept inside the reactor at the beginning of the simulation ($\rho^0_{H_2,R}V_R$) plus the amount which was generated

($m_{H_2,gen}$ at t = 50s) must be equal to the amount that was left inside the reactor ($\rho_{H_2,R}V_R$ at t = 50s) plus the amount of hydrogen released ($m_{H_2,R\rightarrow b}$ at t = 50s). Figures 4.11(d) and 4.11(i) confirm this result. At the beginning and end of the simulation, the reactor had a hydrogen mass of 0.009 g and 0.007g, respectively and approximately. Regarding the other quantities, it may be seen in fig. 4.11(i), that the masses that were generated and released to the balloon were 0.0042 g and 0.0062 g, approximately. With this results, one may confirm the model was well implemented, as 0.009 + 0.0042 = 0.007 + 0.0062. With the goal of exploring the balloon's behaviour, the improvement of this model was left for the future project generations.

4.4 Balloon model

The simulator for the balloon subsystem is represented in figure 4.12.

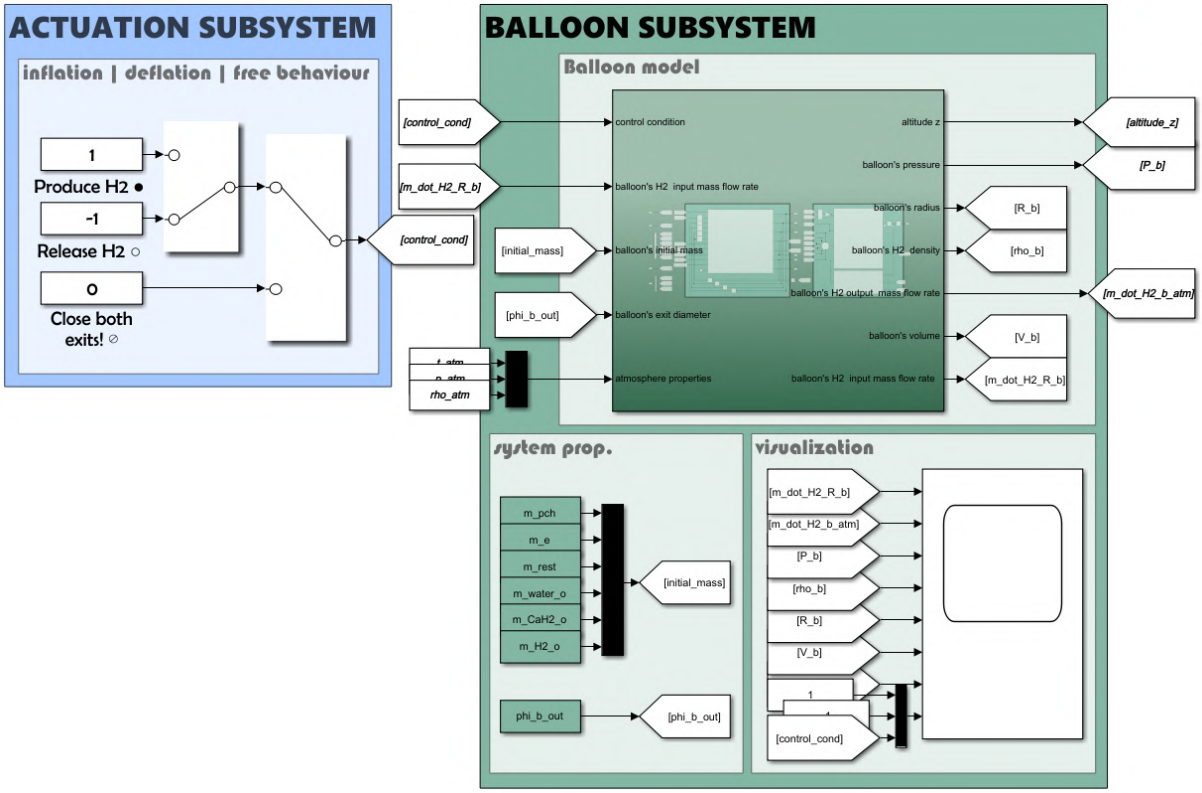

Figure 4.12: Balloon model implementation

The balloon will achieve a certain altitude z_b ("altitude_z") with a certain internal pressure p_b ("P_b") as a function of the hydrogen mass it receives $\dot{m}_{H_2,R\rightarrow b}$ ("m_dot_H2_R_b") or releases to the atmosphere that surrounds it $\dot{m}_{H_2,b\rightarrow atm}$ ("m_dot_H2_b_atm") (depends on the output valve condition for each instant of time ("control_cond")). Furthermore, the system receives the atmospheric properties T_{atm}, p_{atm} and ρ_{atm} ("t_atm", "p_atm" and "rho_atm"), which will influence the way the balloon deforms upon the different atmospheric layers. In addition to this, in order to work, the system will also receive its initial total mass m^0_{total} ("initial_mass"), composed by the parachute's mass m_{pch}, the balloon's envelope mass m_e, the mass of the unknown components m_{rest} (supports, tubes, reactor, syringe, batteries, etc...), the initial

mass of water m_{ω}^{0}, the initial mass of calcium hydride $m_{[CaH_2]}^{0}$ and the initial mass of hydrogen $\rho_{H_2,b}^{0} V_b^{0}$ ("m_pch", "m_e", "m_rest", "m_water_o", "m_CaH2_o" and "m_H2_o", respectively). Finally, to compute the mass of hydrogen that is being released to the atmosphere, the system also need its outlet tube geometric properties ϕ_o ("phi_b_out"). The "Balloon model" block details are depicted in the simulink model represented in figure 4.13.

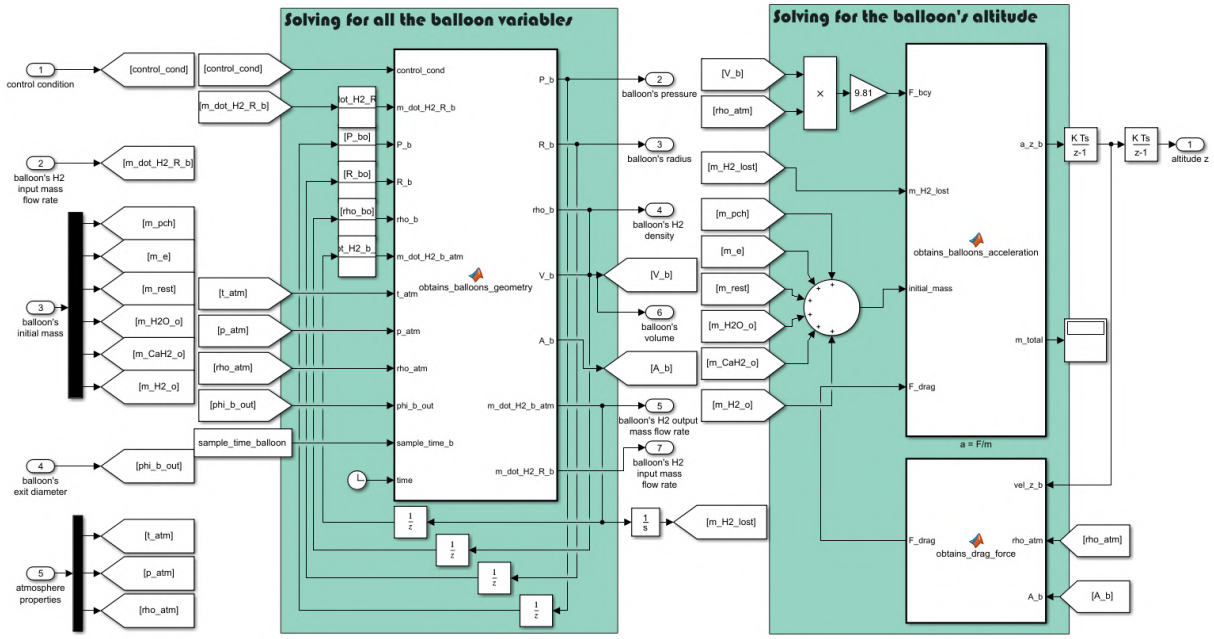

Figure 4.13: Balloon model block

These two blocks were built to solve the algorithm described in section 2.3.3. The block "Solving for all the balloon variables" computes the pressure p_b and the radius of the balloon R_b for each instant of time (algorithm presented in section 2.3.3) and the block "Solving for the balloon's altitude" is the block at which the *Newton's* second law is applied in order to solve for the balloon's vertical acceleration (equations (2.32), (2.33) and (2.34)), where "m_H2_lost" represents the total mass of hydrogen gas that was already lost and released to the atmosphere, $m_{H_2,b \rightarrow atm}$.

4.4.1 Special considerations regarding the balloon model implementation

The balloon's behaviour depends a lot on the **hydrogen input mass flow rate** $\dot{m}_{H_2,R \rightarrow b}$, which is determined by the difference between the reactor and balloon respective internal pressures. The generation of hydrogen inside the reactor might not even be enough to build the required pressure for pumping the gas towards the balloon. One might need to change the reactor's geometry in order to guarantee the pressure will be enough, but this analysis must be done for the case where these two subsystems are studied simultaneously, which is something to be addressed in the next chapter. Here, for the sake of simplification and validation goals, this variable was assumed to be constant and already known (not a function of the reactor characteristics). An arbitrary value of 3.72×10^{-4} Kg/s was considered.

In what regards the size of the balloon, several types of weather balloons are available in the market. Nevertheless, this choice is conditioned by the total mass it will have to carry. With the impossibility of

measuring the mass of the components (batteries or solar panels, sensors, syringe and needles, spring and reactor, etc...), one had to estimate their mass. By using a 10 ml syringe, it is estimated that the **total amount of water** m_{ω}^{0} placed inside the syringe at the beginning of the flight will be approximately equal to 10 g of liquid water. Regarding the **hydride's initial and total mass** $m_{[CaH_2]}^{0}$, with the results obtained in section 3.5, one may recall that for each 1 g of liquid water, approximately just 0.25 g of calcium hydride are consumed for hydrogen production. With those conclusions, one has assumed an initial hydride's mass of 2.5 g. These two values, m_{ω}^{0} and $m_{[CaH_2]}^{0}$, were only considered for the initial part of the simulation: since an arbitrary value for $\dot{m}_{H_2,R\rightarrow b}$ was assumed and no reaction was included, these values were kept constant throughout the simulation. This means that, when producing hydrogen at a constant flow rate of 3.72×10^{-4} Kg/s (figure 4.12), for this simulation in particular, one is not consuming chemical reactants. This was assumed only for this simulation in particular, as the main goal is to check if the balloon behaves as desired in terms of its elastic properties. In addition to these, as expressed in equations (2.32), (2.33) and (2.34), the initial total mass of the system is composed by four more components: the **mass of the remaining components** m_{rest} (batteries or solar panels, sensors, syringe and needles, spring and reactor); the **envelope's mass** m_e, the **parachute's mass** m_{pch} and finally, the **mass of hydrogen held inside the envelope** $\rho_{H_2,b}^{0}V_b^{0}$. For m_{rest}, it was assumed a total components mass of 0.2 Kg. This value should later be measured in the laboratory and replaced by its correct value. Regarding the other mass parameters, these are dependent on the size and type of balloon. The balloon size was selected from within the different types of balloons that are presented in [35]. The document presents two types of balloons that are normally used: TA type (natural latex) and TX type (special latex compound). In order to save costs and to account for the mass of the previous components, the TA 200 model was selected. According to its specifications, the balloon weights about 200 g (m_e = 0.2 Kg) and can elevate a maximum payload mass of 250 g. Furthermore, when released, is is recommended for the balloon to have a initial radius R_b^0 of 0.558 m [35]. This means that the initial mass of hydrogen $\rho_{H_2,b}^{0}V_b^{0}$ will be more or less 63 g . In addition to this, for the mass of the parachute m_{pch}, a value of 70 g was considered [35].

On what concerns the balloon's **geometrical properties**, the balloon's neck was assumed to have a diameter of 3 cm [35]. Finally, in what regards the **atmospheric properties**, these were considered constant, but only for this model in particular. As previously done for the case of the syringe and reactor subsystems, other constant variables were defined inside their respective function blocks: the **envelope's thickness** t_e^0, the balloon's **barely inflated radius** r_b^0, the *Mooney-Rivlin* equation **elastic parameters** s_+ and s_- and finally, the balloon's **drag coefficient** C_D. In [35], the balloon is recommended to be released with an initial radius of 0.558 m. However, in order to apply the *Mooney-Rivlin* theory (equation (2.35)), it is also required to know the thickness of the balloon's envelope t_e^0 and its barely inflated radius r_b^0. In what concerns the last one, the document clearly indicates a value of 0.275m, nevertheless, regarding its thickness, no information was found. In addition to this, the pressure curve represented in figure 2.7 and described by equation (2.35) is defined for a typical ratio t_e^0/r_b^0 of 0.008 [2], which suggests that the balloon will have an undeformed thickness t_e^0 equal to 0.002 m (a small value for a typical weather balloon). Nevertheless, in [2], it is not clear if the equation is valid for other ratios and

so therefore, a thickness of 0.002 m was assumed for the model. In what regards the same equation elastic parameters, values of 3 bar and -0.3 bar were considered [2]. For the drag coefficient C_D, a value of 0.47 was used. Table 4.5 resumes this parameters.

Table 4.5: Balloon model parameters

System inputs		**Total mass**		**Geometric prop.**		**Other param**	
$\dot{m}_{H_2,R\rightarrow b}$ [Kg/s]:	3.72×10^{-4}	m_{pch} [Kg]:	0.07	ϕ_o [m]:	0.03	t_e^0/r_b^0:	0.008
T_{atm} [K]:	288.19	m_e [Kg]:	0.2			r_b^0 [m]:	0.275
p_{atm} [Pa]:	101493	m_{rest} [Kg]:	0.2			s_+ [bar]:	3
ρ_{atm} [Kg/m^3]:	1.2271	m_ω^0 [Kg]:	0.01			s_- [bar]:	-0.3
		$m_{[CaH_2]}^0$ [Kg]:	0.0025			C_D	0.47
		$\rho_{H_2,b}^0 V_b^0$ [Kg][1]:	0.063				

Finally, regarding the **sampling time**, after several experiments, the value of $\delta_t = 0.001$s was chosen. With this sampling time, one was able to capture the correct system dynamics. Of course that this value is also dependent on the parameters that are chosen.

4.4.2 Balloon model validation

Despite the entire mass of the system being defined in the previous section, here, it was assumed to be zero to check for the *Mooney-Rivlin* curve, as the balloon is not capable of elevating its components when released with radius close to its barely inflated radius r_b^0. For this simulation, the conditions were the ones represented in table 4.6, where T_b^0, p_b^0, $\rho_{H_2,b}^0$, R_b^0 and z_b^0 are the initial balloon's internal temperature, pressure, hydrogen density, internal radius and altitude, respectively. Figure 4.14 presents the results.

Table 4.6: Balloon test initial conditions

Balloon test initial conditions	
T_b^0 [K]:	288.19
p_b^0 [Pa]:	101493
$\rho_{H_2,b}^0$ [Kg/m^3]:	0.0847
R_b^0 [m]:	0.275 [35]
z_b^0 [m]:	0

By looking at the results, one shall see the balloon behaves as desired. At t $\approx$ 520s, the valve was opened and a constant hydrogen mass flow rate entered the balloon (fig. 4.14(c)). From t $\approx$ 520s to t $\approx$ 3625s, the balloon was inflated and its radius was increased from 0.275 m (the barely inflated radius) to 1.47 m (close to burst radius [35]). During this period, the *Mooney-Rivlin* pressure-radius curve may clearly be seen, thus confirming the model was well implemented: for a constant atmospheric pressure (which was the case for the simulation of this model), since it was used the equation corresponding to the pressure curve of figure 2.7, at its maximum peak, the difference between the internal and external

[1] for a R_b^0 equal to 0.558 m, the launch radius

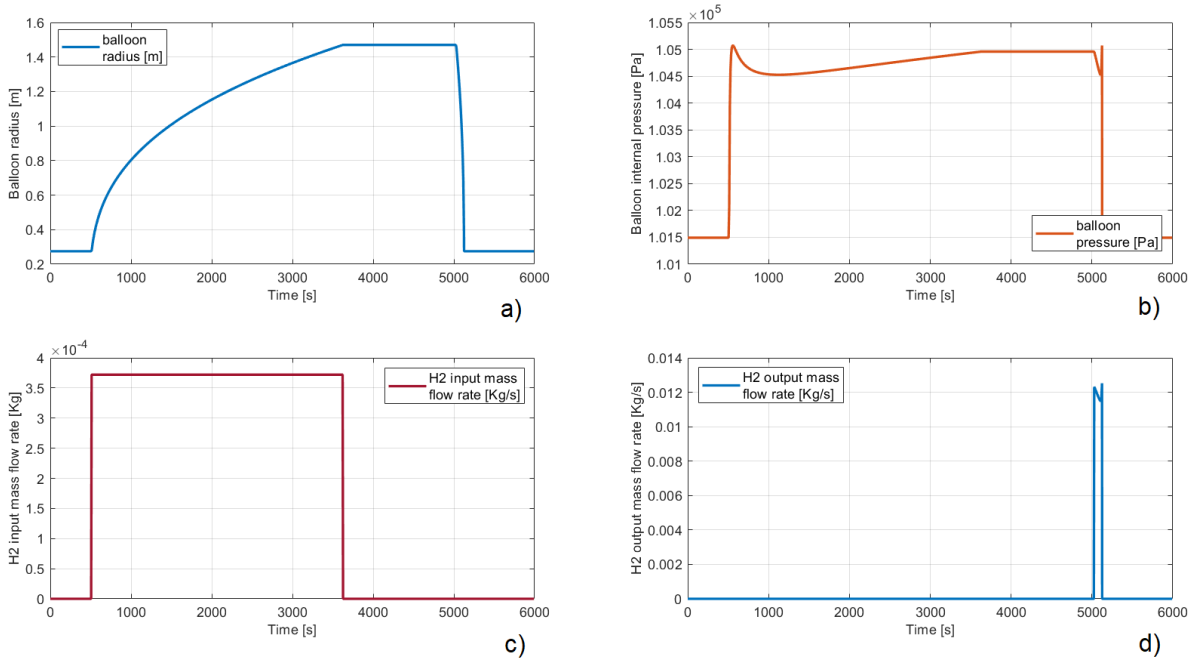

Figure 4.14: Balloon model validation: a) balloon internal radius R_b [m]; b) balloon's internal pressure p_b [Pa]; c) hydrogen input mass flow rate $\dot{m}_{H_2,R\rightarrow b}$ [Kg/s]; d) hydrogen output mass flow rate $\dot{m}_{H_2,b\rightarrow atm}$ [Kg/s]

pressures should not overpass 35 mbar. As represented in fig. 4.14(b), a maximum pressure difference of 35 mbar is observed (recall that the ambient pressure is constant and equal to 101493 Pa (table 4.5)). In addition to this, according to the *Mooney-Rivlin* pressure-radius curve (figure 2.7), the pressure peak will occur for a typical balloon's radius ratio R_b/r_b^0 close to 1.5. By comparing the figures 4.14(a) and 4.14(b) at the pressure peak instant (t $\approx$ 560 s), one might confirm it occurs for the same balloon's radius ratio (at t $\approx$ 560s, R_b is equal to 0.413 m). At t $\approx$ 3625s, the valve was closed (fig. 4.14(c)). From t $\approx$ 3625s to t $\approx$ 5030s, since the atmospheric properties are constant (only for this model) and since no hydrogen was produced or released, the balloon properties remained constant. At t $\approx$ 5030s, the output valve was actuated (fig. 4.14(d)) to deflate the balloon. At t $\approx$ 5030s, the balloon had a diameter of 3 m (fig. 4.14(a)), approximately. It took around 90s to deflate it, which, for a neck diameter ϕ_o of 3 cm, seems very realistic. Furthermore, the hydrogen output mass flow rate $\dot{m}_{H_2,b\rightarrow atm}$ is a function of the difference between the balloon's internal pressure and outside pressure. Since the balloon is deformed in a non-linear way, it is also expected to achieve a non-linear neither constant hydrogen output mass flow rate variation. This is demonstrated in fig.4.14(d). Until now, the model behaves exactly as pretended. Now, it is only required to account for the system's total mass and the change in atmospheric conditions. The effects of these parameters are analysed in the next section.

4.5 Atmosphere model

To simulate the atmospheric subsystem, the model represented by the yellow color in figure 4.15 was built. The function "gives_atm_air_properties" computes all the subsystem outputs, ρ_{atm}, p_{atm} and T_{atm}

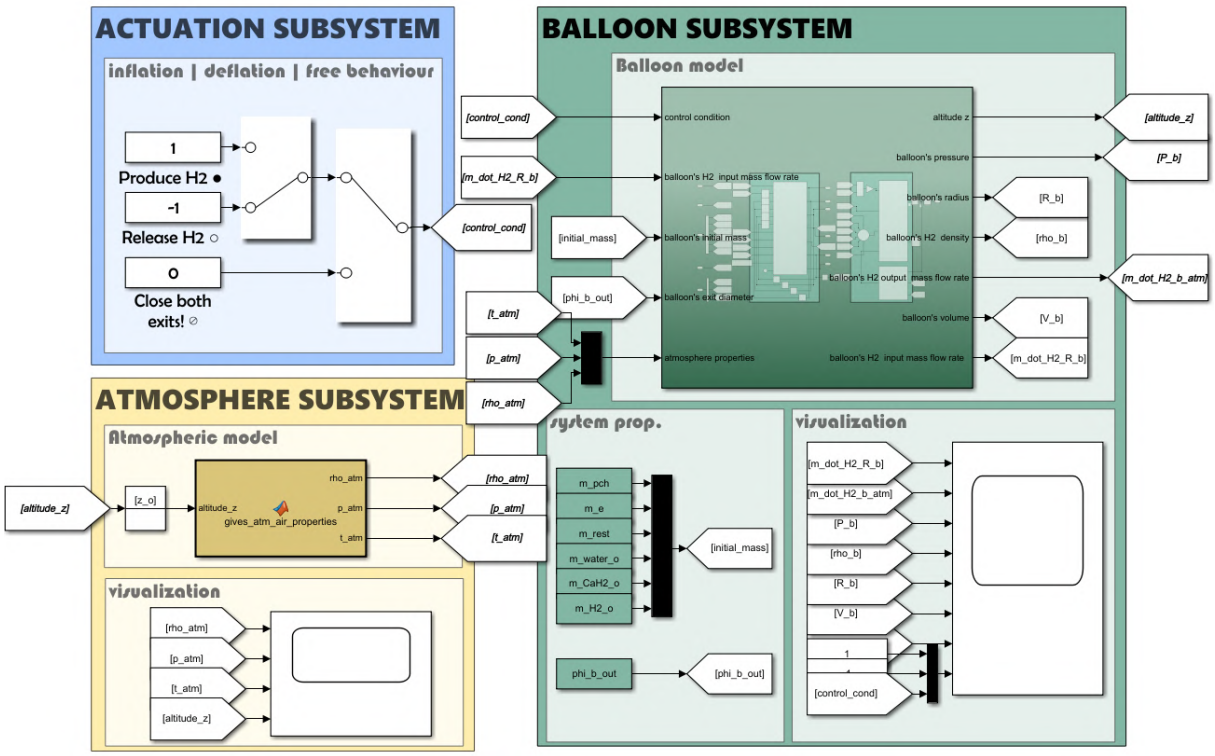

Figure 4.15: Atmosphere model implementation

("rho_atm", "p_atm" and "t_atm") receiving its single input, the altitude z_b ("altitude_z") and using the equations presented in section 2.4.1. In figure 4.15, the atmospheric model simulator was represented together with the balloon's model, because its validation includes checking the influence of the atmospheric properties in the balloon's movement and elastic deformation. When launching the balloon with a certain initial volume inside the earth's atmosphere, it is expected the balloon will start to expand with the goal of trying to equalize the balloon's internal and external pressures. In addition to this, as the model does not consider the slightly permeable properties of latex, once all outlets are closed, hydrogen gas will never be lost to its surroundings, and so therefore the balloon will reach a certain altitude and will remain in there until some action takes place. In the real world, latex envelopes are porous, thus allowing for the gradual escape of lift gas. For the sake of simplification, the model did not consider this change of mass, and if no action is taken, the balloon will hover at a specific altitude, which will happen when the resultant force acting on the balloon becomes zero. This is expressed by the next equation, the hovering condition:

$$\rho_{atm} V_b g = m_{total} g \tag{4.2}$$

where ρ_{atm}, V_b and m_{total} represent the atmospheric density, the balloon's current volume and the total mass of the system, respectively.

4.5.1 Atmosphere model validation

As explained in the previous chapter, for the type of balloon that was chosen (TA 200 [35]), the balloon is expected to burst at an altitude of 21200 m with a diameter of 300 cm (R_b equal to 1.5 m). Given

this, with this simulation, it is expected for the balloon to behave the same way. Regarding the model parameters, these were the same as the ones presented in table 4.5 but with one exception: it was allowed for the atmospheric conditions to change with altitude. Finally, it was considered a balloon's initial radius R_b^0 of 0.558 m [35] and, in what regards the total mass of the system, in contrary to what was made in the previous section, its value was totally considered. Table 4.5 also presents the values for its mass. The rest of the initial conditions are represented in table 4.7, where T_b^0, p_b^0, $\rho_{H_2,b}^0$, R_b^0, z_b^0 T_{atm}^0, p_{atm}^0 and ρ_{atm}^0 are the initial internal temperature, pressure, hydrogen density, internal radius and altitude for the balloon's subsystem, and temperature, pressure and air density for the atmospheric subsystem, respectively. By closing all the valves during the entire simulation and by including the atmosphere's respective model, the results were the ones represented in figure 4.16.

Table 4.7: Atmosphere and balloon test initial conditions

Atmosphere and balloon test initial conditions	
T_b^0, T_{atm}^0 [K]:	288.19
p_{atm}^0 [Pa]:	101493
p_b^0 [Pa]:	104785
$\rho_{H_2,b}^0$ [Kg/m^3]:	0.0875
R_b^0 [m]:	0.558
ρ_{atm}^0 [Kg/m^3]:	1.227
z_b^0 [m]:	0

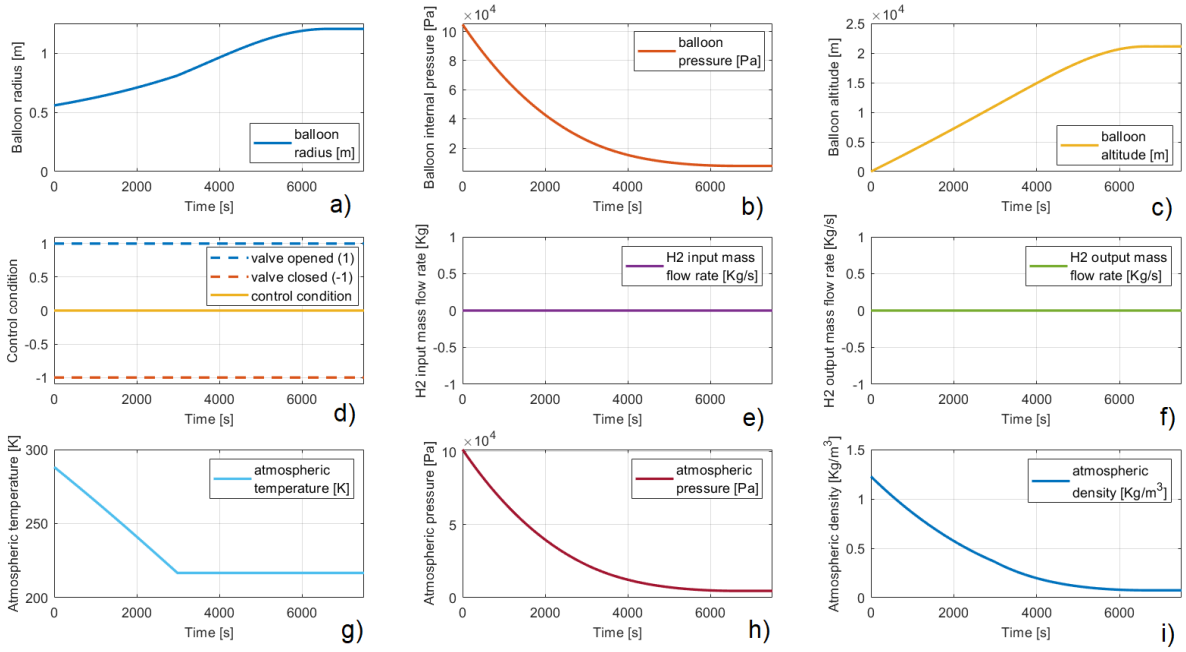

Figure 4.16: Atmospheric model validation: a) balloon's internal radius R_b [m]; b) balloon's internal pressure p_b [Pa]; c) balloon's altitude z_b [m]; d) control condition; e) hydrogen input mass flow rate $\dot{m}_{H_2,R\to b}$ [Kg/s]; f) hydrogen output mass flow rate $\dot{m}_{H_2,b\to atm}$ [Kg/s]; g) atmospheric temperature T_{atm} [K]; h) atmospheric pressure p_{atm} [Pa]; i) atmospheric density ρ_{atm} [Kg/m^3]

As it can be seen, the balloon actually starts to expand because of the existing over-pressure. In-

stead of reaching 21000 m with a radius of 1.5 m , the balloon reached this altitude with a radius of 1.2 m (approximately), which represents less 30 cm than expected (figures 4.16(a) and 4.16(c)). Nevertheless, if one takes into account all the approximations and assumptions that were considered, this result may actually be really good: hydrogen was assumed to behave as an ideal gas; the elastic parameters defined in equation (2.35) vary linearly with temperature but their values were kept constant (no information regarding the change of these values was found); the atmosphere was modelled according to the ISA model; a value of 0.002 m was considered for the balloon's thickness and its value was kept constant throughout the entire the simulation (in reality, as the balloon is deformed, this value should also change); finally, the specifications that are presented in [35], one is assuming they are based on helium balloon type of experiments. All of these assumptions and considerations had probably affected the final result, but nevertheless the results were very promising. Figures 4.16(g), 4.16(h) and 4.16(i) present the atmospheric conditions for the altitude at which the balloon is floating on. With these results, one may conclude the ISA model was correctly implemented. In addition to this, one may see that, despite the radius increased (fig. 4.16(a)), pressure decreased (fig. 4.16(b)). This happened because, in contrary to the simulation of the previous section, the atmospheric properties are changing. Since pressure is changing, its impact in equation (2.35) will be considerably higher, thus affecting the way the balloon's internal pressure varies. In addition to this, the results displayed in figure 4.16(c) prove that the model is well implemented, as the balloon was able to reach an equilibrium condition with the atmosphere that surrounds it. Finally, figures 4.16(d), 4.16(e) and 4.16(f) confirm that no hydrogen mass was produced or released. The balloon reached an hovering condition without exchanging mass with the exterior.

Chapter 5

Latex balloon with a hydrogen generation system: final simulator

This chapter presents the final simulator. It is represented in figure 5.1.

5.1 Special considerations regarding the final implementation

For the final simulator, the balloon and reactor models were merged together, in order to make sure their variables would always be computed at the same time. This way, the algorithms described in sections 2.2.3 and 2.3.3 are solved simultaneously. The models are exactly the same as represented before, the only difference lies inside the block ”Balloon + Reactor”. This block is represented in figure 5.2.

As represented in figure 5.2, the final simulator accounts for the mass variations of each one of the chemical reactants. All the reactor and balloon subsystems respective variables are computed inside the block represented on the left. The functions represented on the right are exactly the same as before. The next section presents the final results for the final simulator.

5.2 Final simulator results

Obtaining results with this simulator turned out to be very challenging. Given the really small sampling time that was previously selected for the reactor subsystem, δ_t = 0.00001s, the simulator became very slow, thus making it harder to extract results for simulations with more than 15 minutes. Given this, in order to be sure that the final model was well implemented (same blocks, same equations, same parameters, etc...), it was performed an equal test like the one that was performed in section 4.5.1, but with a sampling time for the reactor subsystem equal to 0.001s. This approximation is valid for this test in particular because no chemical reaction is occurring, which would cause the physical parameters within the reactor to vary sharply in time. The main objective was to check if the balloon would reach the same vertical altitude with a similar radius (recall figures 4.16(a) and 4.16(c)). The initial conditions for the simulation (test nº1) are represented in table 5.1, where T_b^0, T_{atm}^0, p_b^0, p_R^0, p_{atm}^0, $\rho_{H_2,b}^0$, $\rho_{H_2,R}^0$, ρ_{atm}^0, R_b^0,

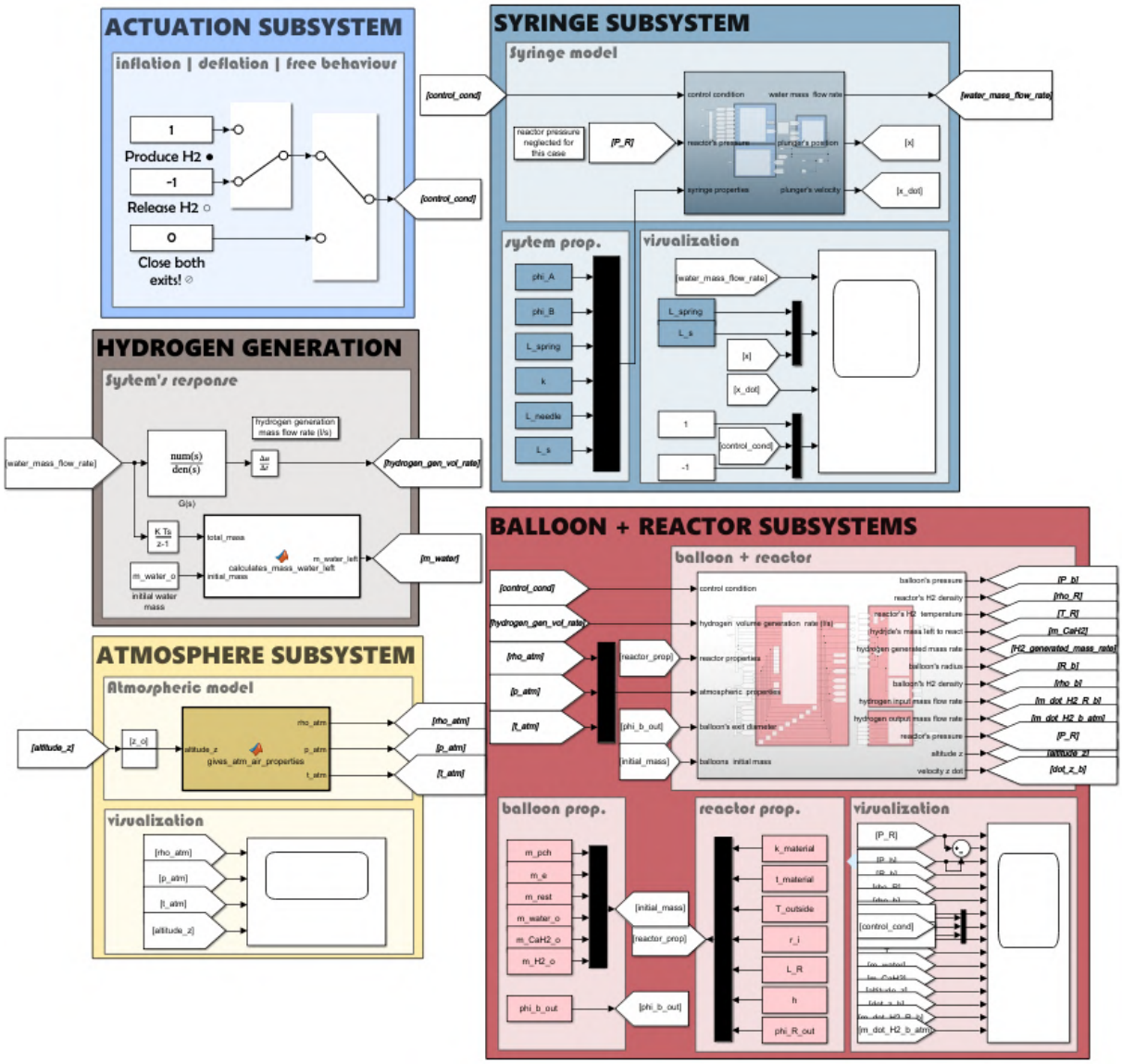

Figure 5.1: Final simulator for the latex balloon with a hydrogen generation system

$m^0_{[CaH_2]}$, m^0_ω, $\dot{z}^0_b$, z^0_b, v^0_i and v^0_o represent the initial balloon's temperature, initial atmospheric temperature, initial balloon's internal pressure, initial reactor's internal pressure, initial atmospheric pressure, initial balloon's hydrogen density, initial reactor's hydrogen density, initial atmospheric density, initial balloon radius, initial mass of calcium hydride, initial mass of liquid water, initial balloon's ascent rate, initial altitude and initial inlet and outlet gas velocities, respectively. Figure 5.3 presents the results.

As it may be seen, due to the way the model is implemented, the reactor variables varied over time: at the beginning of the simulation, the pressure inside the balloon is higher than the reactor's internal pressure (tab. 5.1 and fig. 5.3(d)). After being launched, pressure in the balloon decreases (fig. 5.3(b)) and this difference approaches zero: as soon the internal pressure of the balloon approaches the reactor's internal pressure, the over-pressure will not be kept exactly at zero. Smaller pressure variations will allow for the gradual escape of the gas held inside the reactor. This may be observed in fig. 5.3(i): during the entire simulation, for certain periods, the pressure in the reactor will be slightly

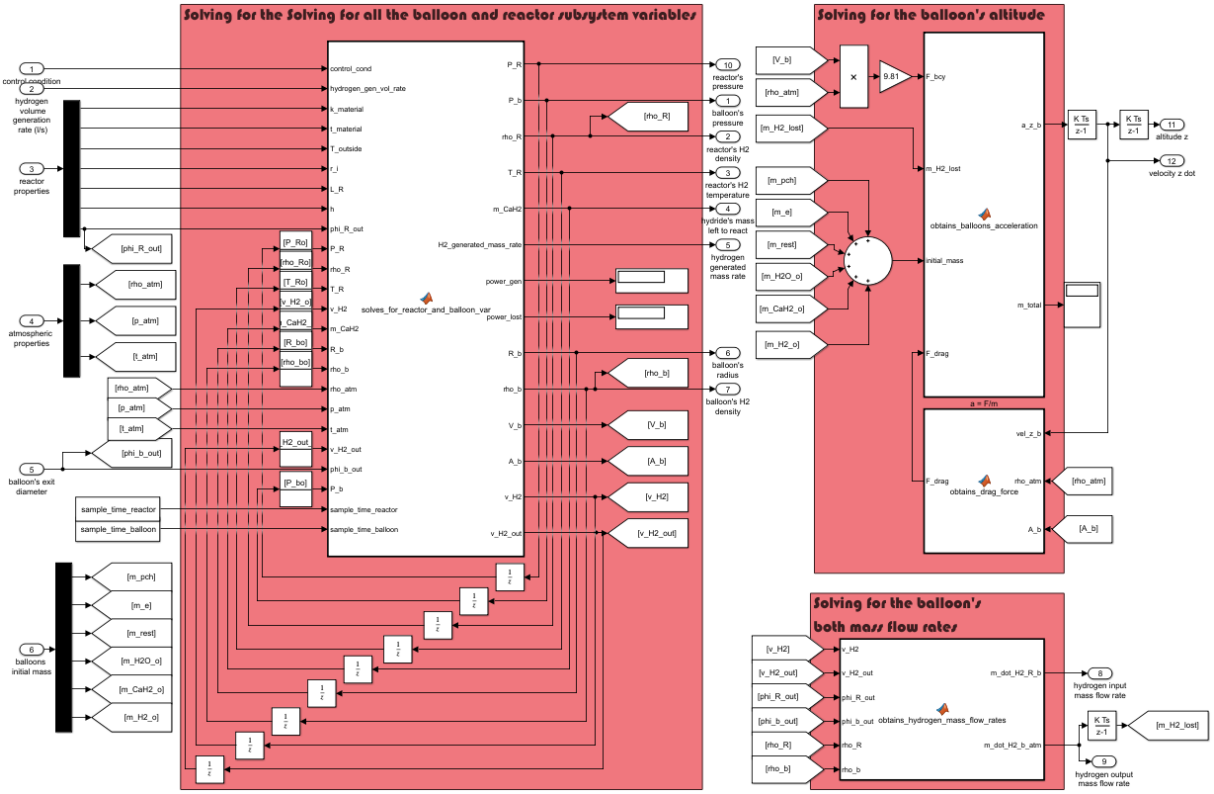

Figure 5.2: Balloon + reactor model

Table 5.1: Final simulator initial conditions (test n°1)

Final simulator initial conditions (test n°1)	
T_b^0, T_{atm}^0 [K]:	288.19
p_R^0, p_{atm}^0 [Pa]:	101493
p_b^0 [Pa]:	104785
$\rho_{H_2,R}^0$ [Kg/m^3]:	0.0847
$\rho_{H_2,b}^0$ [Kg/m^3]:	0.0875
R_b^0 [m]:	0.558
ρ_{atm}^0 [Kg/m^3]:	1.227
$m_{[CaH_2]}^0$ [Kg]:	0.0025
$m_{[H_2O]}^0$ [Kg]:	0.01
v_i^0 [m/s]:	0
v_o^0 [m/s]:	0
$\dot{z}_b^0$ [m/s]:	0
z_b^0 [m]:	0

higher than the pressure in the balloon, and because of this, during those periods, a certain hydrogen mass will enter the balloon, and since no hydrogen is being produced (fig. 5.3(h)), pressure and density will decrease (figures 5.3(e) and 5.3(f), respectively). Nevertheless, the mass of hydrogen that is initially inside the reactor is really small: only about 0.009 g ($\rho_{H_2,R}^0 V_R$) (the balloon itself contains an initial amount of 63 g (tab. 4.5)), which is much higher). In addition to this, the density inside the reactor is not fully eliminated (fig. 5.3(f)), which means that only a mass quantity lower than 0.009 g was actually

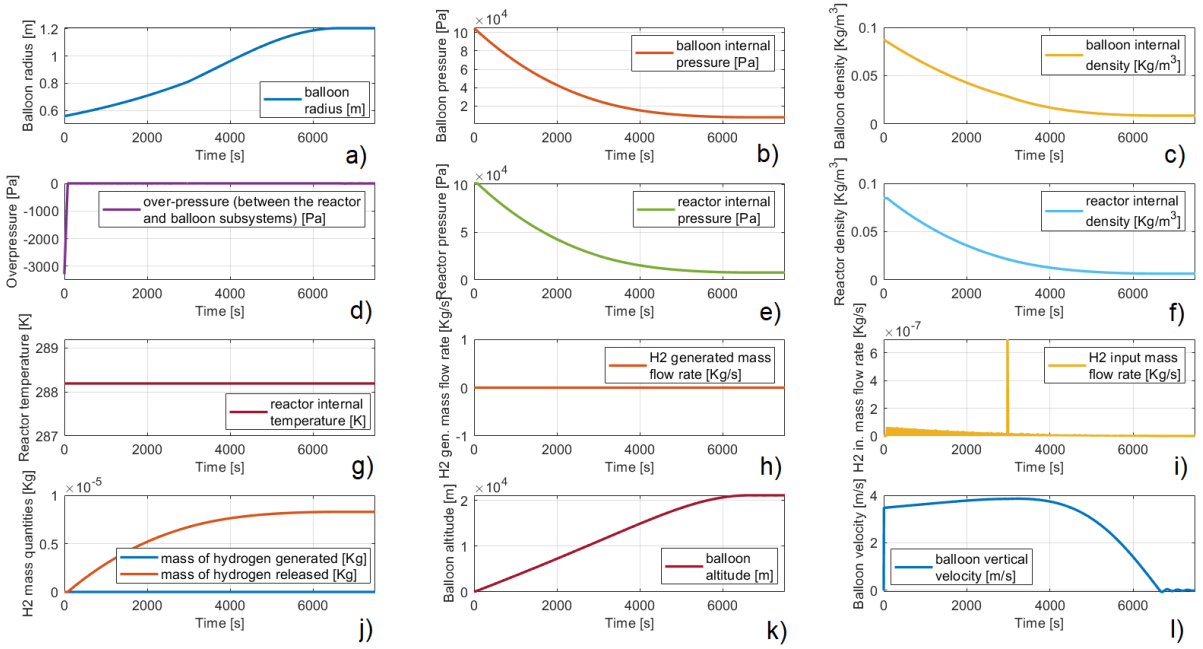

Figure 5.3: Final simulator results (test nº1): a) balloon's internal radius R_b [m]; b) balloon's internal pressure p_b [Pa]; c) balloon's internal density $\rho_{H_2,b}$ [Kg/m^3]; d) over-pressure $p_R - p_b$ [Pa]; e) reactor's internal pressure p_R [Pa]; f) reactor's internal density $\rho_{H_2,R}$ [Kg/m^3]; g) reactor's internal temperature T_R [K]; h) hydrogen generated mass flow rate $\dot{m}_{H_2,gen}$ [Kg/s]; i) hydrogen input mass flow rate $\dot{m}_{H_2,R\rightarrow b}$ [Kg/s]; j) hydrogen generated and released mass quantities $m_{H_2,gen}$ and $m_{H_2,R\rightarrow b}$ [Kg]; k) balloon's altitude z_b [m]; l) balloon's vertical velocity $\dot{z}_b$ [m/s]

released to the balloon (fig. 5.3(j) confirms this). This amount is so small that it really did not affect the balloon's movement that much. The results were equal to the ones displayed in figure 4.16: the balloon radius has increased from 0.558 m to around 1.2 m (fig. 5.3(a)), and it took around 6500 s for the balloon to achieve an altitude close to 21000 m (figures 5.3(k) and 5.3(l)). These results confirm that the equations were implemented in the same manner as in the previous models.

In order to check for the final simulator results, a final test was performed. Nevertheless, before presenting its results, it is important to remind the reader about the scale factors and physical dimensions that were once again considered. The balloon carries 10 g of liquid water, which according to the experimental results, will produce an hydrogen volume close to 1.8 liters, i.e., 0.150 g (a really small value). If totally released to the balloon, it is expected for the balloon's internal radius to vary only a little. For the simulation, it will be assumed the balloon is already hovering at an altitude close to 21000 m (the final conditions of the previous simulation). For this altitude, if 0.150 g of hydrogen enter the balloon, the altitude variation will be really small, as this amount of hydrogen is not enough to produce a considerable change in the balloon's internal radius. Nevertheless, as already explained several times throughout the development of this thesis, all the practical tests were performed at the laboratorial scale, where a reactor similar to the one represented in figure 3.1(b) was used for the tests. Since the model was assembled in a way to use the practical responses that were obtained, it seemed correct to assume the implemented reactor would have the same size. In addition, due to the pandemic, it was impossible to estimate the other important components mass (sensors, batteries, supports, cables, etc), and the more accurate their value, the more space is left for the chemical reactants (and consequently, a higher

hydrogen storage). In reality, if the balloon is released from sea level and no hydrogen is produced between its release and the altitude of 21 km, at this altitude, the balloon should be carrying a higher quantity of chemical reactants that would allow it to produce a hydrogen quantity greater than 0.150 g. Still, given all of the reasons previously presented, less unrealistic quantities were considered for the model. Regarding this final test, since the reactor model displays a huge role in the total system's response, it was required once again to change its sampling time from 0.001s to 0.00001s (now, a certain quantity of hydrogen will be generated), otherwise some simulation errors would appear. Table 5.2 presents the initial conditions for the final test (final conditions of the previous simulation). The results are represented in figure 5.4.

Table 5.2: Final simulator initial conditions (test nº2)

Final simulator initial conditions (test nº2)	
T_b^0, T_{atm}^0 [K]:	216.69
p_b^0 [Pa]:	$\approx$ 7842
p_R^0 [Pa]:	$\approx$ 7840
p_{atm}^0 [Pa]:	$\approx$ 4644
$\rho_{H_2,b}^0$ [Kg/m^3]:	$\approx$ 0.0087
$\rho_{H_2,R}^0$ [Kg/m^3]:	$\approx$ 0.0065
R_b^0 [m]:	$\approx$ 1.2041
ρ_{atm}^0 [Kg/m^3]:	$\approx$ 0.0747
$m_{[CaH_2]}^0$ [Kg]:	0.0025
$m_{[H_2O]}^0$ [Kg]:	0.01
v_i^0 [m/s]:	0
v_o^0 [m/s]:	0
$\dot{z}_b^0$ [m/s]:	$\approx$ 0.0074
z_b^0 [m]:	$\approx$ 21111

The results show the model is well implemented. At t $\approx$ 70s, the input valve was actuated (fig. 5.4(g)) and the total amount of water was released (fig. 5.4(h)): approximately 10 g of water entered the chemical reactor and, as expected, approximately 0.150 g of hydrogen were generated (fig. 5.4(i)). Temperature has increased to 800 K (a change of approximately 500ºC) and the pressure that was generated was enough to pump the total mass of hydrogen towards the balloon: fig. 5.4(i) demonstrates that the entire mass that was generated was released to the balloon. During the period of actuation, more or less 50s (fig.5.4(g)), the over-pressure was above zero, thus allowing for the gas to escape (fig. 5.4(c)). In addition to this, by looking at figures 5.4(e) and 5.4(i), one might confirm a correct hydrogen mass balance: the mass of hydrogen held inside the reactor at the beginning of the simulation ($\rho_{H_2,R}^0 V_R$) plus the amount of hydrogen that was generated ($m_{H_2,gen}$ at t = 850s) was equal to the amount that was released ($m_{H_2,R\rightarrow b}$ at t = 850s) plus the amount that was kept inside the reactor at the end of the simulation ($\rho_{H_2,R} V_R$ at t = 850s). At t $\approx$ 70s, due to the mass of hydrogen that entered the balloon, the balloon's radius and velocity increased (figures 5.4(a) and 5.4(k)), and with an additional quantity of 0.150g, the balloon's altitude varied about 35 m (from 21111 m to 21145 m, approximately (fig. 5.4(l))). At t $\approx$ 270s, the balloon reach the altitude at which it would stabilize (the new hovering condition). From

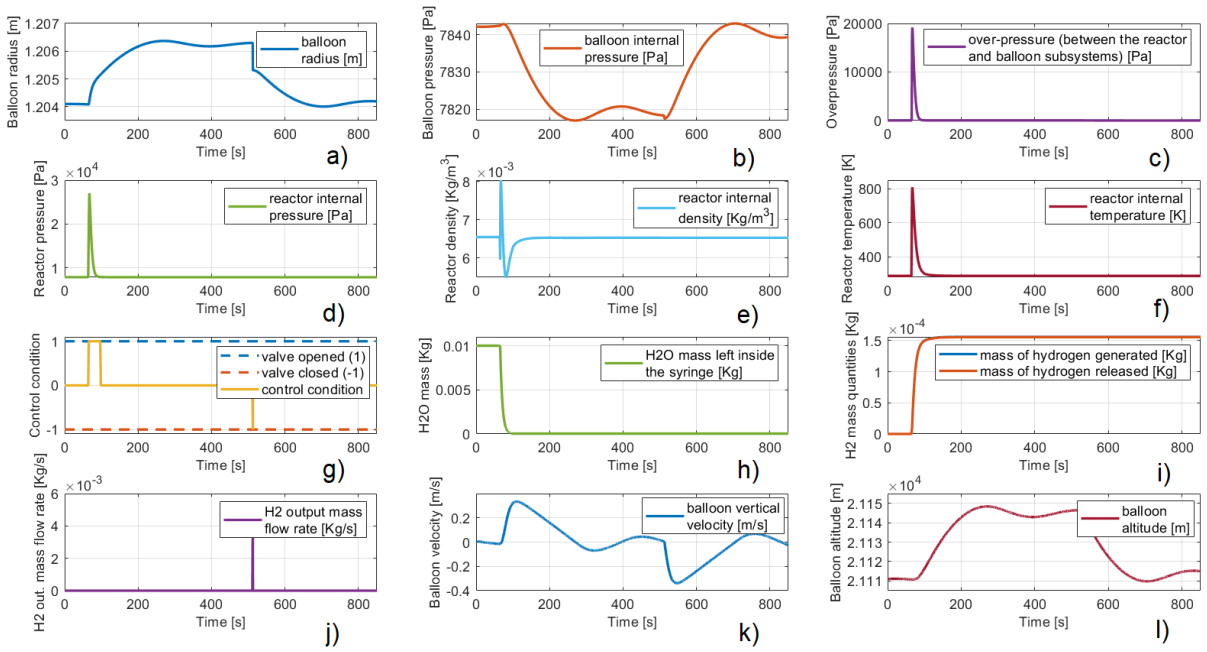

Figure 5.4: Final simulator results (test n°2): a) balloon's internal radius R_b [m]; b) balloon's internal pressure p_b [Pa]; c) over-pressure $p_R - p_b$ [Pa]; d) reactor's internal pressure p_R [Pa]; e) reactor's internal density $\rho_{H_2,R}$ [Kg/m^3]; f) reactor's internal temperature T_R [K]; g) control condition; h) mass of water left inside the syringe m_ω [Kg]; i) hydrogen generated and released mass quantities $m_{H_2,gen}$ and $m_{H_2,R\rightarrow b}$ [Kg]; j) hydrogen output mass flow rate $\dot{m}_{H_2,b\rightarrow atm}$ [Kg/s]; k) balloon's vertical velocity $\dot{z}_b$ [m/s]; l) balloon's altitude z_b [m]

t = 0s to t $\approx$ 700s, the mass of the total system was kept constant. At t $\approx$ 700s, the output valve was actuated (fig.5.4(g)) and a certain amount of hydrogen was released to the atmosphere (fig.5.4(j)). Nevertheless, the mass that was released was very small: the balloon returned to its initial position (slightly higher altitude (fig. 5.4(l))) with the same initial radius (fig. 5.4(a)).

For other type of parameters, the results would be very different. However, as the different sampling times were changed in order to capture the full system dynamics and its values were found specifically for the parameters defined in chapter 4, these were left unchanged. In order to get other type of results, such as higher altitude variations, one would need a bigger reactor and a bigger syringe. However, as the hydrolysis results were obtained for a small reactor, no other parameters were tested.

Chapter 6

Conclusions

This project has changed a lot since the day it started. The first objective was to develop a physical prototype in the laboratory and try to control the latex balloon by managing the amount of lift gas that is held inside it. This would be done by using the hydrolysis reaction of CaH_2 (to produce hydrogen and increase the altitude) and by simply releasing lift gas (to decrease the altitude). The first practical experiments were performed with this target in mind, and a chemical reactor prototype was built with the goal of studying the hydrolysis reaction of CaH_2. As soon as the reaction tests would be done, the final prototype (including the latex balloon) would start to be assembled.

Unfortunately, due to the pandemic, the objectives of this thesis were changed given the impossibility of staying in the laboratory. At the end, its main goal was to develop a simulator in order to predict the system's behaviour.

6.1 Achievements

The final target was successfully achieved: it was developed a simulator for a latex balloon with a hydrogen generation system. The simulator allows to predict and to study the way the physical prototype will behave. It saves time and money for the future project generations, by helping them to predict the effect of changing each one of parameters and physical dimensions that are involved. Even if the future project doesn't fit for its main purpose (which is to control the altitude of the balloon and increase its flight duration), this model would help to predict that unfortunate outcome, thus allowing for other solutions to be explored and implemented. During the practical component of this project, buying the material and predict the outcome of using that material (springs, reactors, tubes) was a lot challenging. This simulator prevents useless costs to occur, as it allows one to make multiple experiments and get an approximated response of the practical system before trying to buy and assemble its components. In the laboratory, in the event of a balloon being connected to the installation, without this simulator, one would not have the guaranty that the test-tube that was selected to perform the hydrolysis reactions would serve its purpose, meaning that all the installation would have to be rebuilt and all the time spent on the reactions would be needlessly wasted. Another example of this is related with the spring element: at the beginning of the

project, a spring was purchased, and its stiffness was randomly selected because of the previous lack of knowledge about the system. With this simulator results, one may develop an idea regarding the final prototype's response and the effect of changing any of its parameters in that response.

Regarding the final results (section 5.2), despite the theoretical assumptions that were considered, one believes this model is quite close to reality. With the idea of one being capable to experiment all sorts of weather balloons, *Mooney-Rivlin* theory was applied and implemented to simulate the way a weather balloon is deformed. The results were very promising, as for the balloon that was selected, it was noticed it was capable of reaching its bursting altitude with a diameter close to its bursting diameter (a difference of 30 cm was noticed (fig. 4.16)). Furthermore, with the additional hydrogen quantity of 0.150g that was produced, the balloon's altitude increased about 35m (fig. 5.4). Nevertheless, the amount of hydrogen generated was highly affected by the reactant available quantities and by the results obtained with the hydrolysis reaction. Regarding the reaction (section 3.5), in the laboratory, it was possible to verify that its rate is highly affected by the hydroxide's poor solubility. Practically, in all the experiments that were performed, 5 to 6 times more water was necessary to achieve the stoichiometric hydrogen production. The chemical prototype that was developed suited to achieve consistent constant water mass flow rates, but for the reaction, a lot of things should be improved.

6.2 Future Work

For future work, it is proposed to study the hydrolysis reactions more carefully. The hydrolysis of CaH_2 is the most sensitive aspect of this thesis, and unfortunately, due to the pandemic, it was the subject that most fell far short of expectations. Regarding the chemical reactor prototype, it is suggested to replace the glass reactor by a metal reactor: when compared to glass, metal allows to dissipate energy faster and can support higher differential pressures (even when subjected to really high temperatures). Furthermore, by using a metal reactor, one is able to run the experiments at a higher scale, as more water may be released inside the reactor without the concern of possibly breaking it. Finally, it is suggested to find another way for measuring temperature. The temperature curves that were obtained with this chemical reactor were very inconclusive, but nevertheless, it was quite hard to find a proper way for doing it. By being afraid of ruining the chemical reaction, the tip of the thermocouple was not placed exactly at the core of the reaction, as the water droplets coming from the syringe would probably fall directly above the cables, and thus interfere with the reaction rate. As the quantities of reactants were, in general, very small, if the thermocouple was placed between the syringe and the hydride, a lot of the water mass would collide with the thermocouple, thus not reacting with the metal hydride, or at least, not reacting so fast. Having this in mind, it is suggested to place the thermocouple tip exactly at the core of the reaction but without interfering with it. This could probably be repeated during the development of this thesis, but due to the pandemic, there was simply not enough time. Furthermore, in the event of not being possible to place the tip at the core of the reaction, it is recommended to use another type of multimeter, as the sampling resolution of the one that was used was not high enough to capture the transient part of the temperature's response. Capturing temperature is fundamental, as

the way the reaction proceeds depends a lot on the temperature registered at the moment. According to *Arrhenius*, the rate of reaction is greatly depend on its core temperature. Since it was not possible to accurately measure the temperature growth, the model that was created did not consider its effect. In the model, temperature was a consequence of the hydrogen production rate, but nevertheless, both variables should depend on each other. In the future, the chemical reaction should be modelled in terms of its rate, which is a function of the reaction temperature. Still with regard to the reaction, it is proposed to explore different reactants or different ways in order to improve its rate. As discussed in section 1.3.1, there are a lot of metal hydrides which might serve the final purpose. Nevertheless, despite not achieving very satisfactory results, not enough research was devoted to CaH_2, and so therefore, it is recommend to improve its reaction, in order to assess its possible benefits: in terms of stoichiometry, to achieve the theoretical volume of hydrogen, one would need 4 to 6 times more water than expected, and the main reason for this to occur is related to the hydroxide's dissolution properties. The poor dissolution of calcium hydroxide clearly affects the hydrogen production. Even worse, its solubility decreases for higher temperatures, which is now seen as a major disadvantage of using this chemical compound. For the future, it is recommended to explore and use different types of chemical catalysts, in order to improve the chemical reaction rate. With the results that were obtained, one estimated that 10 g of water would be capable of producing 0.150 g of hydrogen, which is a really small quantity. Let's consider the perfect situation, where hydrogen is produced according to the stoichiometric ratio: with 10 g of water, the mass of hydrogen that would be generated would be something close to 1 g ($\approx$ 11 liters). Furthermore, if the available payload space would allow for greater reactant quantities, this mass would be even higher, which would greatly influence the duration of the balloon's flight, as more hydrogen could be stored in powder form. Regarding other important aspects, since the practical temperature responses were very inconclusive, and since not enough theory regarding the hydrolysis of CaH_2 was found, temperature was assumed to vary differently. With the model results, one is not quite sure about the validity of the temperature values that were obtained, as no other results were found for a possible comparison. In addition to this, the pressure generated inside the reactor was an estimation based on the temperature values. However, the model does not consider the sensitive properties of glass, and for the differential pressures that are being generated, glass may or may not break. The only way to find out, is by including the sensitive properties of glass in the model. By doing this, one may reach new conclusions regarding the feasibility of the project. If a metal reactor is used, higher differential pressures might be handled, but nevertheless, since the model lacked precision in computing the pressure generated inside it, it is not guaranteed that this solution might work. Furthermore, regarding control requirements, it might be desired to pump hydrogen at a certain velocity, and the pressure generated might not be enough to guarantee that result. Regarding this problem, a compressor might help to solve it, but nevertheless, it will increase the cost and complexity of the project, making it non-feasible.

In what concerns the parameters that were chosen for the different systems, one must remember the fact that the practical experiments were performed in a laboratorial scale. The parameters that were chosen were selected in order to be consistent with the size of the instruments that were used in the lab. This will of course affect the results that are demonstrated. The greater the amounts of water

and calcium hydride, the longer will be the balloon's flight, as more hydrogen may be produced and released. The problem is that not all the components were able to be weighted during the practical part. Examples of these are the electrical components, the syringe, the reactor test-tube, the batteries, etc. All of this components greatly influence the way the balloon moves, and the more accurate is their mass inside the simulator, the more space is left for the mass of the chemical reactants. Nevertheless, due to the pandemic, there was not enough time to weight all of this components, and so therefore, their mass was estimated. Given its inaccuracy, before using the simulator, it is suggested to weight all of the components, or at least a great part of them, and then input their mass values in the simulation, in order to check for the validity of the model.

Regarding the final simulator, it is recommended to experiment another type of software. *Matlab* lacked memory to export the results for simulations with more than 15 minutes. Given the sampling times, the simulator turned out to be extremely slow. In addition to this, *Matlab* requires a very expensive license in order to be used, which might decrease the simulator's accessibility.

Bibliography

[1] T. L. B. Frank P. Incropera, David P. Dewitt and A. S. Lavine. *Fundamentals of Heat and Mass Transfer*. John Wiley & Sons, 6th edition, 2007. ISBN: 978-0-471-45728-2.

[2] I. Muller and P. Strehlow. *Rubber and Rubber Balloons*. Springer, 2004. ISBN 3-540-20244-7. URL https://d-nb.info/972144528/34.

[3] H. Du, M. Lv, J. Li, W. Zhu, L. Zhang, and Y. Wu. Station-keeping performance analysis for high altitude balloon with altitude control system. *Aerospace Science and Technology*, 92:644–652, 2019.

[4] Hindenberg. URL https://www.britannica.com/topic/Hindenburg.

[5] M. Greshko. *We Discovered Helium 150 Years Ago. Are We Running Out?* National Geographic, 2018. URL https://www.nationalgeographic.com/science/2018/08/news-helium-mri-superconducting-markets-reserve-technology.

[6] Hydrogen resources. URL https://www.energy.gov/eere/fuelcells/hydrogen-resources.

[7] E. Aribaş and E. Dağlarli. High altitude smart monitoring system integration by using a helium powered mechanical balloon. In *2017 8th International Conference on Recent Advances in Space Technologies (RAST)*, pages 167–170. IEEE, 2017.

[8] Fuel cells. URL https://www.eesi.org/files/FactSheet_Fuel_Cells_110515.pdf.

[9] T. Agrawal, R. Ajitkumar, R. Prakash, and G. Nandan. Sodium silicide as a hydrogen source for portable energy devices: a review. *Materials Today: Proceedings*, 5(2):3563–3570, 2018.

[10] Helium cost concerns. URL https://www.peakscientific.com/discover/news/helium-cost-concerns.

[11] T. Hiraki, S. Hiroi, T. Akashi, N. Okinaka, and T. Akiyama. Chemical equilibrium analysis for hydrolysis of magnesium hydride to generate hydrogen. *International journal of hydrogen energy*, 37(17): 12114–12119, 2012.

[12] C. M. G. ARAÚJO. *Hydrogen Storage Materials*. Acta Universitatis Upsaliensis Uppsala, 2008. ISBN:978-91-554-7129-3.

[13] J. Andersson and S. Grönkvist. Large-scale storage of hydrogen. *International journal of hydrogen energy*, 44(23):11901–11919, 2019.

[14] Sodium hydroxide, . URL https://en.wikipedia.org/wiki/Sodium_hydroxide.

[15] Sodium hydride. URL https://onlinelibrary.wiley.com/doi/abs/10.1002/047084289X.rs073.pub2.

[16] G. K. Pitcher. Solid lithium hydride as a hydrogen source for fuel cells. In *Proceedings of Symposium on Autonomous Underwater Vehicle Technology*, pages 455–460. IEEE, 1996.

[17] Lithium hydroxide, . URL https://en.wikipedia.org/wiki/Lithium_hydroxide.

[18] Lithium hydride, . URL https://en.wikipedia.org/wiki/Lithium_hydride.

[19] Magnesium hydroxide, . URL https://en.wikipedia.org/wiki/Magnesium_hydroxide.

[20] C. H. Chao and T. C. Jen. Reaction of magnesium hydride with water to produce hydrogen. In *Applied Mechanics and Materials*, volume 302, pages 151–157. Trans Tech Publ, 2013.

[21] A. Figen and K. Taşçı. Hydrolysis characteristics of calcium hydride (cah2) powder in the presence of ethylene glycol, methanol, and ethanol for controllable hydrogen production. *Energy Sources, Part A: Recovery, Utilization, and Environmental Effects*, 38(1):37–42, 2016.

[22] Calcium hydroxide, . URL https://en.wikipedia.org/wiki/Calcium_hydroxide.

[23] Calcium hydride, . URL https://en.wikipedia.org/wiki/Calcium_hydride.

[24] Types of balloons. https://www.nasa.gov/scientific-balloons/types-of-balloons, . Accessed: 2017-08-05.

[25] A. Sushko, A. Tedjarati, J. Creus-Costa, S. Maldonado, K. Marshland, and M. Pavone. Low cost, high endurance, altitude-controlled latex balloon for near-space research (valbal). In *2017 IEEE Aerospace Conference*, pages 1–9. IEEE, 2017.

[26] Super pressure balloon design approach. https://sites.wff.nasa.gov/code820/spb_design_approach.html, .

[27] S. Saleh and H. Weiliang. New design simulation for a high-altitude dual-balloon system to extend lifetime and improve floating performance. *Chinese Journal of Aeronautics*, 31(5):1109–1118, 2018.

[28] Loon project definition. https://loon.com, .

[29] Google patented project loon. https://www.youtube.com/watch?time_continue=1&v=jjSV_UAaO4I, .

[30] Mach number: Role in compressible flows. https://www.grc.nasa.gov/WWW/BGH/machrole.html. Accessed: 2014-06-12.

[31] Velocity of sound in water. URL https://www.engineeringtoolbox.com/sound-speed-water-d_598.html.

[32] L. A. Oliveira and A. G. Lopes. *Mecânica de Fluídos*. Lidel, 5th edition, 2016. ISBN: 978-989-752-221-5.

[33] Students send balloons to the stratosphere. https://www.nasa.gov/centers/glenn/technology/explorers_balloons.html. Accessed: 2017-08-07.

[34] Atmosphere model. https://www.grc.nasa.gov/www/k-12/airplane/atmosmet.html. Accessed: 2015-05-15.

[35] Weather balloons and accessories. http://www.myhoskin.com/newsletters/PDF/WeatherBalloonsandAccessories.pdf.